frontiers in Physics

REVIEW
published: 09 May 2018
doi: 10.3389/fphy.2018.00040

Lepton Number Violation: Seesaw Models and Their Collider Tests

Yi Cai[1], *Tao Han*[2,3], *Tong Li*[4,5]* *and Richard Ruiz*[6]

[1] School of Physics, Sun Yat-sen University, Guangzhou, China, [2] Department of Physics and Astronomy, University of Pittsburgh, Pittsburgh, PA, United States, [3] Department of Physics, Tsinghua University, and Collaborative Innovation Center of Quantum Matter, Beijing, China, [4] School of Physics, Nankai University, Tianjin, China, [5] ARC Centre of Excellence for Particle Physics at the Terascale, School of Physics and Astronomy, Monash University, Melbourne, VIC, Australia, [6] Department of Physics, Institute for Particle Physics Phenomenology, Durham University, Durham, United Kingdom

The Majorana nature of neutrinos is strongly motivated from the theoretical and phenomenological point of view. A plethora of neutrino mass models, known collectively as Seesaw models, exist that could generate both a viable neutrino mass spectrum and mixing pattern. They can also lead to rich, new phenomenology, including lepton number non-conservation as well as new particles, that may be observable at collider experiments. It is therefore vital to search for such new phenomena and the mass scale associated with neutrino mass generation at high energy colliders. In this review, we consider a number of representative Seesaw scenarios as phenomenological benchmarks, including the characteristic Type I, II, and III Seesaw mechanisms, their extensions and hybridizations, as well as radiative constructions. We present new and updated predictions for analyses featuring lepton number violation and expected coverage in the theory parameter space at current and future colliders. We emphasize new production and decay channels, their phenomenological relevance and treatment across different facilities in e^+e^-, e^-p, and pp collisions, as well as the available Monte Carlo tools available for studying Seesaw partners in collider environments.

Keywords: lepton number violation, neutrino mass models, collider physics, seesaw mechanisms, Majorana neutrinos
ARXIV EPRINT: 1711.02180

OPEN ACCESS

Edited by:
Frank Franz Deppisch, University College London, United Kingdom

Reviewed by:
Oliver Fischer, Karlsruher Institut für Technologie, Germany
Miha Nemevsek, Jožef Stefan Institute (IJS), Slovenia

***Correspondence:**
Tong Li
nklitong@hotmail.com

Specialty section:
This article was submitted to High-Energy and Astroparticle Physics, a section of the journal Frontiers in Physics

Received: *20 November 2017*
Accepted: *16 April 2018*
Published: *09 May 2018*

Citation:
Cai Y, Han T, Li T and Ruiz R (2018) Lepton Number Violation: Seesaw Models and Their Collider Tests. Front. Phys. 6:40. doi: 10.3389/fphy.2018.00040

1. INTRODUCTION

Neutrino flavor oscillation experiments from astrophysical and terrestrial sources provide overwhelming evidence that neutrinos have small but nonzero masses. Current observations paint a picture consistent with a mixing structure parameterized by the 3×3 Pontecorvo-Maki-Nakagawa-Sakata (PMNS) matrix [1–3] with at least two massive neutrinos. This is contrary to the Standard Model of particle physics (SM) [4], which allows three massless neutrinos and hence no flavor oscillations. Consequently, to accommodate these observations, the SM must [5] be extended to a more complete theory by new degrees of freedom.

One could of course introduce right-handed (RH) neutrino states (ν_R) and construct Dirac mass terms, $m_D \overline{\nu_L} \nu_R$, in the same fashion as for all the other elementary fermions in the SM. However, in this minimal construction, the new states do not carry any SM gauge charges, and thus these "sterile neutrinos" have the capacity to be Majorana fermions [6]. The most significant consequence of this would be the existence of the RH Majorana mass term $M_R \overline{(\nu_R)^c} \nu_R$ and the explicit violation of lepton number (L). In light of this prospect, a grand frontier opens for theoretical model-building with rich and new

phenomenology at the collider energy scales, which we will review in this article.

Generically, if we integrate out the new states, presumably much heavier than the electroweak (EW) scale, the new physics may be parameterized at leading order through the dimension-5 lepton number violating operator [7], the so-called "Weinberg operator,"

$$\mathcal{L}_5 = \frac{\alpha}{\Lambda}\,(LH)(LH) \xrightarrow{\text{EWSB}} \mathcal{L}_5 \ni \frac{\alpha v_0^2}{2\Lambda}\,\overline{(\nu_L)^c}\,\nu_L, \tag{1.1}$$

where L and H are, respectively, the SM left-handed (LH) lepton doublet and Higgs doublet, with vacuum expectation value (vev) $v_0 \approx 246$ GeV. After electroweak (EW) symmetry breaking (EWSB), $\mathcal{L}_5$ generates a Majorana mass term for neutrinos. One significance of Equation (1.1) is the fact that its ultraviolet (UV) completions are severely restricted. For example: extending the SM field content minimally, i.e., by only a single SM multiplet, permits only three [5] tree-level completions of Equation (1.1), a set of constructions famously known as the Type I [8–14], Type II [14–18], and Type III [19] Seesaw mechanisms. These minimal mechanisms can be summarized with the following:

Minimal Type I Seesaw [8–14]: In the minimal Type I Seesaw, one hypothesizes the existence of a right-handed (RH) neutrino ν_R, which transforms as a singlet, i.e., $(1, 1, 0)$, under the SM gauge group $\mathrm{SU}(3)_c \otimes \mathrm{SU}(2)_L \otimes \mathrm{U}(1)_Y$, that possesses a RH Majorana mass M_{ν_R} and interacts with a single generation of SM leptons through a Yukawa coupling y_ν. After mass mixing and assuming $M_{\nu_R} \gg y_\nu v_0$, the light neutrino mass eigenvalue m_ν is given by $m_\nu \sim y_\nu^2 v_0^2 / M_{\nu_R}$, If $y_\nu \simeq 1$, to obtain a light neutrino mass of order an eV, M_{ν_R} is required to be of order $10^{14} - 10^{15}$ GeV. M_{ν_R} can be made much lower though by balancing against a correspondingly lower y_ν.

Minimal Type II Seesaw [14–18]: The minimal Type II Seesaw features the introduction of a Higgs field Δ with mass M_Δ in a triplet representation of $\mathrm{SU}(2)_L$ and transforms as $(1, 3, 2)$ under the SM gauge group. In this mechanism, light neutrino masses are given by LH Majorana masses $m_\nu \approx Y_\nu v_\Delta$, where v_Δ is the vev of the neutral component of the new scalar triplet and Y_ν is the corresponding Yukawa coupling. Due to mixing between the SM Higgs doublet and the new scalar triplet via a dimensionful parameter μ, EWSB leads to a relation $v_\Delta \sim \mu v_0^2 / M_\Delta^2$. In this case the new scale Λ is replaced by M_Δ^2/μ. With $Y_\nu \approx 1$ and $\mu \sim M_\Delta$, the scale is also $10^{14} - 10^{15}$ GeV. Again, M_Δ can be of TeV scale if Y_ν is small or $\mu \ll M_\Delta$. It is noteworthy that in the Type II Seesaw, no RH neutrinos are needed to explain the observed neutrino masses and mixing.

Minimal Type III Seesaw [19]: The minimal Type III Seesaw is similar to the other two cases in that one introduces the fermionic multiplet Σ_L that is a triplet (adjoint representation) under $\mathrm{SU}(2)_L$ and transforms as $(1, 3, 0)$ under the SM gauge group. The resulting mass matrix for neutrinos has the same form as in Type I Seesaw, but in addition features heavy leptons that are electrically charged. The new physics scale Λ in Equation (1.1) is replaced by the mass of the leptons Σ_L, which can also be as low as a TeV if balanced with a small Yukawa coupling.

However, to fully reproduce oscillation data, at least two of the three known neutrinos need nonzero masses. This requires a nontrivial Yukawa coupling matrix for neutrinos if appealing to any of the aforementioned Seesaws mechanisms, and, if invoking the Type I or III Seesaws, extending the SM by at least two generations of multiplets [20], which need not be in the same SM gauge representation. In light of this, one sees that Weinberg's assumption of a high-scale Seesaw [7] is not necessary to generate tiny neutrino masses in connection with lepton (L) number violation. For example: the so-called Inverse [21–24] or Linear [25, 26] variants of the Type I and III Seesaw models, their generic extensions as well as hybridizations, i.e., the combination of two or more Seesaw mechanisms, can naturally lead to mass scales associated with neutrino mass-generation accessible at present-day experiments, and in particular, collider experiments. A qualitative feature of these low-scale Seesaws is that light neutrino masses are proportional to the scale of L violation, as opposed to inversely related as in high-scale Seesaws [27].

The Weinberg operator in Equation (1.1) is the lowest order and simplest parameterization of neutrino mass generation using only the SM particle spectrum and its gauge symmetries. Beyond its tree-level realizations, however, neutrino Majorana masses may alternatively be generated radiatively. Suppression by loop factors may provide a partial explanation for the smallness of neutrino masses and again allow much lower mass scales associated with neutrino mass-generation. The first of such models was proposed at one-loop in Zee [28] and Hall and Suzuki [29], at two-loop order in Cheng and Li [16], Zee [30], and Babu [31], and at three-loop order in Krauss et al. [32]. A key feature of radiative neutrino mass models is the absence of tree-level contributions to neutrino masses either because there the necessary particles, such as SM singlet fermion as in Type I Seesaw, are not present or because relevant couplings are forbidden by additional symmetries. Consequently, it is necessary that the new field multiplets run in the loops that generate neutrino masses.

As observing lepton number violation would imply the existence of Majorana masses for neutrinos [33–35], confirming the existence of this new mass scale would, in addition, verify the presence of a Seesaw mechanism. To this end, there have been on-going efforts in several directions, most notably the neutrinoless double beta ($0\nu\beta\beta$)-decay experiments, both current [36–39] and upcoming [40–42], as well as proposed general purpose fixed-target facilities [43, 44]. Complementary to this are on-going searches for lepton number violating processes at collider experiments, which focus broadly on rare meson decays [45–47], heavy neutral fermions in Type I-like models [48–52], heavy bosons in Type II-like models [53–55], heavy charged leptons in Type III-like models [56–58], and lepton number violating contact interactions [59, 60]. Furthermore, accurate measurements of the PMNS matrix elements and stringent limits on the neutrino masses themselves provide crucial information and knowledge of lepton flavor mixing that could shed light on the construction of Seesaw models.

In this context, we present a review of searches for lepton number violation at current and future collider experiments. Along with the current bounds from the experiments at LEP, Belle, LHCb and ATLAS/CMS at 8 and 13 TeV, we present

studies for the 13 and 14 TeV LHC. Where available, we also include results for a future 100 TeV hadron collider, an *ep* collider (LHeC), and a future high-energy e^+e^- collider. We consider a number of tree- and loop-level Seesaw models, including, as phenomenological benchmarks, the canonical Type I, II, and III Seesaw mechanisms, their extensions and hybridizations, and radiative Seesaw formulations in *pp*, *ep*, and *ee* collisions. We note that the classification of collider signatures based on the canonical Seesaws is actually highly suitable, as the same underlying extended and hybrid Seesaw mechanism can be molded to produce wildly varying collider predictions.

We do not attempt to cover the full aspects of UV-complete models for each type. This review is only limited to a selective, but representative, presentation of tests of Seesaw models at collider experiments. For complementary reviews, we refer readers to Gluza [61], Barger et al. [62], Mohapatra and Smirnov [63], Rodejohann [64], Chen and Huang [65], Atre et al. [66], Deppisch et al. [67] and references therein.

This review is organized according to the following: In section 2 we first show the PMNS matrix and summarize the mixing and mass-difference parameters from neutrino oscillation data. With those constraints, we also show the allowed mass spectra for the three massive neutrino scheme. Our presentation is agnostic, phenomenological, and categorized according to collider signature, i.e., according to the presence of Majorana neutrinos (Type I) as in section 3, doubly charged scalars (Type II) as in section 4, new heavy charged/neutral leptons (Type III) as in section 5, and new Higgs, diquarks and leptoquarks in section 6. Particular focus is given to state-of-the-art computations, newly available Monte Carlo tools, and new collider signatures that offer expanded coverage of Seesaw parameter spaces at current and future colliders. Finally in section 7 we summarize our main results.

2. NEUTRINO MASS AND OSCILLATION PARAMETERS

In order to provide a general guidance for model construction and collider searches, we first summarize the neutrino mass and mixing parameters in light of oscillation data. Neutrino mixing can be parameterized by the PMNS matrix [1–3] as

$$U_{PMNS} = \begin{pmatrix} 1 & 0 & 0 \\ 0 & c_{23} & s_{23} \\ 0 & -s_{23} & c_{23} \end{pmatrix} \begin{pmatrix} c_{13} & 0 & e^{-i\delta} s_{13} \\ 0 & 1 & 0 \\ -e^{i\delta} s_{13} & 0 & c_{13} \end{pmatrix} \begin{pmatrix} c_{12} & s_{12} & 0 \\ -s_{12} & c_{12} & 0 \\ 0 & 0 & 1 \end{pmatrix} \text{diag}(e^{i\Phi_1/2}, 1, e^{i\Phi_2/2}) \quad (2.1)$$

$$= \begin{pmatrix} c_{12}c_{13} & c_{13}s_{12} & e^{-i\delta}s_{13} \\ -c_{12}s_{13}s_{23}e^{i\delta} - c_{23}s_{12} & c_{12}c_{23} - e^{i\delta}s_{12}s_{13}s_{23} & c_{13}s_{23} \\ s_{12}s_{23} - e^{i\delta}c_{12}c_{23}s_{13} & -c_{23}s_{12}s_{13}e^{i\delta} - c_{12}s_{23} & c_{13}c_{23} \end{pmatrix} \times \text{diag}(e^{i\Phi_1/2}, 1, e^{i\Phi_2/2}), \quad (2.2)$$

where $s_{ij} \equiv \sin\theta_{ij}$, $c_{ij} \equiv \cos\theta_{ij}$, $0 \leq \theta_{ij} \leq \pi/2$, and $0 \leq \delta, \Phi_i \leq 2\pi$, with δ being the Dirac CP phase and Φ_i the Majorana phases. While the PMNS is a well-defined 3×3 unitary matrix, throughout this review, we use the term generically to describe the 3×3 active-light mixing that may not, in general, be unitary.

The neutrino mixing matrix is very different from the quark-sector Cabbibo-Kobayashi-Maskawa (CKM) matrix, in that most of the PMNS mixing angles are large whereas CKM angles are small-to-negligible. In recent years, several reactor experiments, such as Daya Bay [68], Double Chooz [69], and RENO [70] have reported non-zero measurements of θ_{13} by searching for the disappearance of anti-electron neutrinos. Among these reactor experiments, Daya Bay gives the most conclusive result with $\sin^2 2\theta_{13} \approx 0.084$ or $\theta_{13} \approx 8.4^\circ$ [71, 72], the smallest entry of the PMNS matrix. More recently, there have been reports on indications of a non-zero Dirac CP phase, with $\delta \approx 3\pi/2$ [73–75]. However, it cannot presently be excluded that evidence for such a large Dirac phase may instead be evidence for sterile neutrinos or new neutral currents [76–79].

Neutrino oscillation experiments can help to extract the size of the mass-squared splitting between three neutrino mass eigenstates. The sign of $\Delta m^2_{31} = m^2_3 - m^2_1$, however, still remains unknown at this time. It can be either positive, commonly referred as the Normal Hierarchy (NH), or negative and referred to as the Inverted Hierarchy (IH). The terms Normal Ordering (NO) and Inverted Ordering (IO) are also often used in the literature in lieu of NH and IH, respectively. Taking into account the reactor data from the antineutrino disappearance experiments mentioned above together with other disappearance and appearance measurement, the latest global fit of the neutrino masses and mixing parameters from the NuFit collaboration [72], are listed in **Table 1** for NH (left) and IH (center). The tightest constraint on the sum of neutrino masses comes from cosmological data. Combining Planck+WMAP+highL+BAO data, this yields at 95% confidence level (CL) [80]

$$\sum_{i=1}^{3} m_i < 0.230 \text{ eV}. \quad (2.3)$$

Given this and the measured neutrino mass splittings, we show in **Figure 1** the three active neutrino mass spectra as a function of the lowest neutrino mass in (a) NH and (b) IH. With the potential sensitivity of the sum of neutrino masses being close to 0.1 eV in the near future (5–7 years) [81], upcoming cosmological probes will not be able to settle the issue of the neutrino mass hierarchy. However, the improved measurement $\sim$ 0.01 eV over a longer term (7 − 15 years) [81, 82] would be sensitive to determine the absolute mass scale of a heavier neutrino spectrum. In addition, there are multiple proposed experiments aiming to determine the neutrino mass hierarchy. The Deep Underground Neutrino Experiment (DUNE) will detect neutrino beams from the Long Baseline Neutrino Facility (LBNF), and probes the CP-phase and the mass hierarchy. With a baseline of 1,300 km, DUNE is able to determine the mass hierarchy with at least 5σ significance [83]. The Jiangmen Underground Neutrino Observatory (JUNO) plans to precisely measure the reactor electron antineutrinos and improve the accuracy of Δm^2_{21}, Δm^2_{32} and $\sin^2\theta_{12}$ to 1% level [84]. The

TABLE 1 | Three-neutrino oscillation fit based as obtained by the NuFit collaboration, taken from Esteban et al. [72], where $\Delta m^2_{3\ell} = \Delta m^2_{31} > 0$ for NO (or NH) and $\Delta m^2_{3\ell} = \Delta m^2_{32} < 0$ for IO (or IH).

	Normal Ordering (best fit)		Inverted Ordering ($\Delta\chi^2 = 0.83$)		Any Ordering
	bfp $\pm 1\sigma$	3σ range	bfp $\pm 1\sigma$	3σ range	3σ range
$\sin^2\theta_{12}$	$0.306^{+0.012}_{-0.012}$	$0.271 \to 0.345$	$0.306^{+0.012}_{-0.012}$	$0.271 \to 0.345$	$0.271 \to 0.345$
$\theta_{12}/^\circ$	$33.56^{+0.77}_{-0.75}$	$31.38 \to 35.99$	$33.56^{+0.77}_{-0.75}$	$31.38 \to 35.99$	$31.38 \to 35.99$
$\sin^2\theta_{23}$	$0.441^{+0.027}_{-0.021}$	$0.385 \to 0.635$	$0.587^{+0.020}_{-0.024}$	$0.393 \to 0.640$	$0.385 \to 0.638$
$\theta_{23}/^\circ$	$41.6^{+1.5}_{-1.2}$	$38.4 \to 52.8$	$50.0^{+1.1}_{-1.4}$	$38.8 \to 53.1$	$38.4 \to 53.0$
$\sin^2\theta_{13}$	$0.02166^{+0.00075}_{-0.00075}$	$0.01934 \to 0.02392$	$0.02179^{+0.00076}_{-0.00076}$	$0.01953 \to 0.02408$	$0.01934 \to 0.02397$
$\theta_{13}/^\circ$	$8.46^{+0.15}_{-0.15}$	$7.99 \to 8.90$	$8.49^{+0.15}_{-0.15}$	$8.03 \to 8.93$	$7.99 \to 8.91$
$\delta_{CP}/^\circ$	261^{+51}_{-59}	$0 \to 360$	277^{+40}_{-46}	$145 \to 391$	$0 \to 360$
$\frac{\Delta m^2_{21}}{10^{-5}\ \text{eV}^2}$	$7.50^{+0.19}_{-0.17}$	$7.03 \to 8.09$	$7.50^{+0.19}_{-0.17}$	$7.03 \to 8.09$	$7.03 \to 8.09$
$\frac{\Delta m^2_{3\ell}}{10^{-3}\ \text{eV}^2}$	$+2.524^{+0.039}_{-0.040}$	$+2.407 \to +2.643$	$-2.514^{+0.038}_{-0.041}$	$-2.635 \to -2.399$	$\begin{bmatrix} +2.407 \to +2.643 \\ -2.629 \to -2.405 \end{bmatrix}$

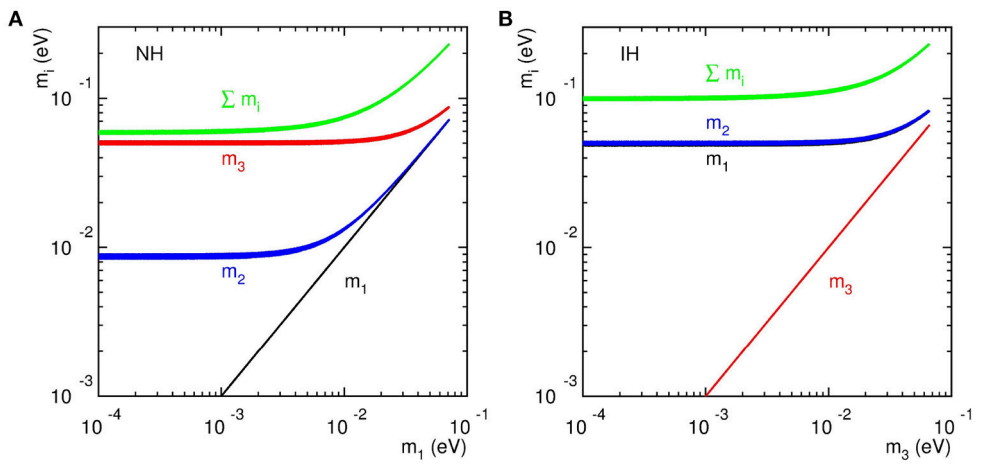

FIGURE 1 | The three active neutrino mass spectra vs. the lowest neutrino mass for **(A)** NH and **(B)** IH.

Hyper-Kamiokande (Hyper-K) experiment as an update of T2K can measure the precision of δ to be $7^\circ - 21^\circ$ and reach 3 (5)σ significance of mass hierarchy determination for 5 (10) years exposure [85]. Finally, the Karlsruhe Tritium Neutrino experiment (KATRIN) as a tritium β decay experiment aims to measure the effective electron-neutrino mass with the sensitivity of sub-eV [86].

3. THE TYPE I SEESAW AND LEPTON NUMBER VIOLATION AT COLLIDERS

We begin our presentation of collider searches for lepton number violation in the context of Type I Seesaw models. After describing the canonical Type I mechanism [8–12] and its phenomenological decoupling at collider scales in section 3.1.1, we discuss various representative, low-scale models that incorporate the Type I mechanism and its extensions. We then present collider searches for lepton number violation mediated by Majorana neutrinos (N), which is the characteristic feature of Type I-based scenarios, in section 3.2. This is further categorized according to associated phenomena of increasing complexity: N production via massive Abelian gauge bosons is reviewed in section 3.2.4, via massive non-Abelian gauge bosons in section 3.2.5, and via dimension-six operators in section 3.2.6.

3.1. Type I Seesaw Models

3.1.1. The Canonical Type I Seesaw Mechanism

In the canonical Type I Seesaw mechanism one hypothesizes a single RH neutral leptonic state, $N_R \sim (1,1,0)$, in addition to the SM matter content. However, reproducing neutrino oscillation data requires more degrees of freedom. Therefore, for our purposes, we assume $i = 1,\ldots,3$ LH states and $j = 1,\ldots,n$ RH states. Following the notation of Atre et al. [66] and Han et al. [87], the full theory is

$$\mathcal{L}_{\text{Type I}} = \mathcal{L}_{\text{SM}} + \mathcal{L}_{N\text{ Kin}} + \mathcal{L}_N, \tag{3.1}$$

where $\mathcal{L}_{\text{SM}}$ is the SM Lagrangian, $\mathcal{L}_{N\text{ Kin}}$ is N_R's kinetic term, and its interactions and mass are

$$\mathcal{L}_N = -\overline{L}\, Y_\nu^D\, \tilde{H}\, N_R - \frac{1}{2}\overline{(N^c)}_L\, M_R\, N_R + \text{H.c.}. \tag{3.2}$$

L and H are the SM LH lepton and Higgs doublets, respectively, and $\tilde{H} = i\sigma_2 H^*$. Once H settles on the vev $\langle H\rangle = v_0/\sqrt{2}$, neutrinos acquire Dirac masses $m_D = Y_\nu^D\, v_0/\sqrt{2}$ and we have

$$\mathcal{L}_N \ni -\frac{1}{2}\left(\overline{\nu}_L\, m_D\, N_R + \overline{(N^c)}_L\, m_D^T\, (\nu^c)_R + \overline{(N^c)}_L\, M_R\, N_R\right) + \text{H.c.} \tag{3.3}$$

After introducing a unitary transformation into m (m') light (heavy) mass eigenstates,

$$\begin{pmatrix} \nu \\ N^c \end{pmatrix}_L = \mathbb{N}\begin{pmatrix} \nu_m \\ N^c_{m'} \end{pmatrix}_L, \quad \mathbb{N} = \begin{pmatrix} U & V \\ X & Y \end{pmatrix}, \tag{3.4}$$

one obtains the diagonalized mass matrix for neutrinos

$$\mathbb{N}^\dagger \begin{pmatrix} 0 & m_D \\ m_D^T & M \end{pmatrix} \mathbb{N}^* = \begin{pmatrix} m_\nu & 0 \\ 0 & M_N \end{pmatrix}, \tag{3.5}$$

with mass eigenvalues $m_\nu = diag(m_1, m_2, m_3)$ and $M_N = diag(M_1, \cdots, M_{m'})$. In the limit $m_D \ll M_R$, the light (m_ν) and heavy (M_N) neutrino masses are

$$m_\nu \approx -m_D M_R^{-1} m_D^T \quad \text{and} \quad M_N \approx M_R. \tag{3.6}$$

The mixing elements typically scale like

$$UU^\dagger \approx I - m_\nu M_N^{-1}, \quad VV^\dagger \approx m_\nu M_N^{-1}, \tag{3.7}$$

with the unitarity condition $UU^\dagger + VV^\dagger = I$. With another matrix U_ℓ diagonalizing the charged lepton mass matrix, we have the approximate neutrino mass mixing matrix U_{PMNS} and the matrix $V_{\ell N}$, which transits heavy neutrinos to charged leptons, and are given by

$$U_\ell^\dagger U \equiv U_{PMNS}, \quad U_\ell^\dagger V \equiv V_{\ell N}, \quad \text{and} \quad U_{PMNS}U_{PMNS}^\dagger + V_{\ell N}V_{\ell N}^\dagger = I. \tag{3.8}$$

The decomposition of active neutrino states into a general number of massive eigenstates is then given by Atre et al. [66] and Han et al. [87], $\nu_\ell = \sum_{m=1}^{3} U_{\ell m}\nu_m + \sum_{m'=1}^{n} V_{\ell m'} N^c_{m'}$. From this, the SM EW boson couplings to heavy mass eigenstates (in the mixed mass-flavor basis) are

$$\begin{aligned}\mathcal{L}_{\text{Int.}} = &-\frac{g}{\sqrt{2}} W_\mu^+ \sum_{\ell=e}^{\tau}\left(\sum_{m=1}^{3}\overline{\nu_m}\, U^*_{\ell m} + \sum_{m'=1}^{n}\overline{N^c_{m'}}\, V^*_{\ell N_{m'}}\right)\gamma^\mu P_L \ell^- \\ &-\frac{g}{2\cos\theta_W} Z_\mu \sum_{\ell=e}^{\tau}\left(\sum_{m=1}^{3}\overline{\nu_m}\, U^*_{\ell m} + \sum_{m'=1}^{n}\overline{N^c_{m'}}\, V^*_{\ell N_{m'}}\right)\gamma^\mu P_L \nu_\ell \\ &-\frac{g}{2M_W} h \sum_{\ell=e}^{\tau}\sum_{m'=1}^{n} m_{N_{m'}}\overline{N^c_{m'}}\, V^*_{\ell N_{m'}} P_L \nu_\ell + \text{H.c.}\end{aligned} \tag{3.9}$$

There is a particular utility of using this mixed mass-flavor basis in collider searches for heavy neutrinos. Empirically, $|V_{\ell N_{m'}}| \lesssim 10^{-2}$ [88–91], which means pair production of $N_{m'}$ via EW processes is suppressed by $|V_{\ell N_{m'}}|^2 \lesssim 10^{-4}$ relative to single production of $N_{m'}$. Moreover, in collider processes involving $\nu_m - N_{m'}$ vertices, one sums over ν_m either because it is an internal particle or an undetected external state. This summation effectively undoes the decomposition of one neutrino interaction state for neutral current vertices, resulting in the basis above. In phenomenological analyses, it is common practice to consider in only the lightest heavy neutrino mass eigenstate, i.e., $N_{m'=4}$, to reduce the effective number of independent model parameters. In such cases, the mass eigenstate is denoted simply as N and one reports sensitivity on the associated mixing element, labeled correspondingly as $|V_{\ell N}|$ or $|V_{\ell 4}|$, which are equivalent to $|V_{\ell N_{m'=4}}|$. Throughout this text, the $|V_{\ell N}|$ notation is adopted where possible.

From Equation (3.5), an important relation among neutrino masses can be derived. Namely, that

$$U^*_{PMNS} m_\nu U^\dagger_{PMNS} + V^*_{\ell N} M_N V^\dagger_{\ell N} = 0\,. \tag{3.10}$$

Here the masses and mixing of the light neutrinos in the first term are measurable from the oscillation experiments, and the second term contains the masses and mixing of the new heavy neutrinos. We now consider a simple case: degenerate heavy neutrinos with mass $M_N = diag(M_1, \cdots, M_{m'}) = M_N \mathbb{I}_{m'}$. Using this assumption, we obtain from Equation (3.10),

$$M_N \sum_N (V^*_{\ell N})^2 = (U^*_{PMNS} m_\nu U^\dagger_{PMNS})_{\ell\ell}\,. \tag{3.11}$$

Using the oscillation data in **Table 1** as inputs[1], we display in **Figure 2** the normalized mixing of each lepton flavor in this scenario[2]. Interestingly, one can see the characteristic features:

$$\sum_N |V_{eN}|^2 \ll \textstyle\sum_N |V_{\mu N}|^2, \sum_N |V_{\tau N}|^2 \quad \text{for NH}, \tag{3.12}$$

$$\sum_N |V_{eN}|^2 > \textstyle\sum_N |V_{\mu N}|^2, \sum_N |V_{\tau N}|^2 \quad \text{for IH}. \tag{3.13}$$

[1] This is done for simplicity since U_{PMNS} in **Table 1** is unitary whereas here it is not; for more details, see Esteban et al. [72], and Parke and Ross-Lonergan [92].

[2] $\sum_N (V^*_{\ell N})^2 = \sum_N |V_{\ell N}|^2$ only when all phases on the right-hand side of Equation (3.11) vanish [93].

As shown in **Figure 3**, a corresponding pattern also emerges in the branching fraction[3] of the degenerate neutrinos decaying into charged leptons plus a W boson,

$$\begin{aligned} \mathrm{BR}(\mu^\pm W^\mp), \mathrm{BR}(\tau^\pm W^\mp) &\sim (20-30)\% \gg \mathrm{BR}(e^\pm W^\mp) \\ &\sim (3-4)\% \qquad \text{for NH}, \qquad (3.14) \\ \mathrm{BR}(e^\pm W^\mp) &\sim 27\% > \mathrm{BR}(\mu^\pm W^\mp), \mathrm{BR}(\tau^\pm W^\mp) \\ &\sim (10-20)\% \qquad \text{for IH}, \qquad (3.15) \end{aligned}$$

with $\mathrm{BR}(\ell^\pm W^\mp) = \mathrm{BR}(N_i \to \ell^+ W^- + \ell^- W^+)$. These patterns show a rather general feature that ratios of Seesaw partner observables, e.g., cross sections and branching fractions, encode information on light neutrinos, such as their mass hierarchy [93, 94]. Hence, one can distinguish between competing light neutrino mass and mixing patterns with high energy observables.

More generally, the $V_{\ell N}$ in Equation (3.10) can be formally solved in terms of an arbitrary orthogonal complex matrix Ω, known as the Casas-Ibarra parametrization [95], using the ansatz

$$V_{\ell N} = U_{PMNS}\, m_\nu^{1/2} \Omega M_N^{-1/2}, \qquad (3.16)$$

with the orthogonality condition $\Omega\Omega^T = I$. For the simplest incarnation with a unity matrix $\Omega = I$, $|V_{\ell N_{m'}}|^2$ are proportional to one and only one light neutrino mass, and thus the branching ratio of $N_{m'} \to \ell^\pm W^\mp$ for each lepton flavor is independent of neutrino mass and universal for both NH and IH [93]. Nevertheless, one can still differentiate between the three heavy neutrinos according to the decay rates to their leading decay channels. As shown in **Figure 4** for $\Omega = I$, one sees

$$\begin{aligned} \mathrm{BR}(e^\pm W^\mp) &\sim 40\% > \mathrm{BR}(\mu^\pm W^\mp), \mathrm{BR}(\tau^\pm W^\mp) \\ &\sim (4-15)\% \text{ for } N_1, \qquad (3.17) \\ \mathrm{BR}(e^\pm W^\mp) &\sim 20\% \approx \mathrm{BR}(\mu^\pm W^\mp) \approx \mathrm{BR}(\tau^\pm W^\mp) \\ &\sim (10-30)\% \text{ for } N_2, \qquad (3.18) \\ \mathrm{BR}(\mu^\pm W^\mp), \mathrm{BR}(\tau^\pm W^\mp) &\sim (15-40)\% \gg \mathrm{BR}(e^\pm W^\mp) \\ &\sim 1\% \text{ for } N_3. \qquad (3.19) \end{aligned}$$

A realistic Dirac mass matrix can be quite arbitrary with three complex angles parameterizing the orthogonal matrix Ω. However, this arbitrariness of the Dirac mass matrix is not a universal feature of Seesaw models; the neutrino Yukawa matrix in the Type II Seesaw, for example, is much more constrained.

Beyond this, **Figure 2** also shows another general feature of minimal, high-scale Seesaw constructions, namely that the active-sterile mixing $|V_{\ell N}|$ is vanishingly small. For a heavy neutrino mass of $M_N \sim 100$ GeV, Equation (3.11) implies $|V_{\ell N}|^2 \sim 10^{-14} - 10^{-12}$. This leads to the well-known decoupling of observable lepton number violation in the minimal, high-scale Type I Seesaw scenario at colliders experiments [27, 96, 97]. For low-scale Type I Seesaws, such decoupling of observable lepton number violation also occurs: Due to the allowed arbitrariness of the matrix Ω in Equation (3.16), it is possible to construct Ω and M_N with particular entry patterns or symmetry structures, also known as textures in the literature, such that $V_{\ell N}$ is nonzero but m_ν vanishes. Light neutrino masses can then be generated as perturbations from these textures. In Moffat et al. [27] it was proved that such delicate (and potentially fine-tuned [98–100]) constructions result in small neutrino masses being proportional to small L-violating parameters, instead of being inversely proportional as in the high-scale case. Subsequently, in low-scale Seesaw scenarios that assume only fermionic gauge singlets, tiny neutrino masses is equivalent to an approximate conservation of lepton number, and leads to the suppression of observable L violation in high energy processes. Hence, any observation of lepton number violation (and Seesaw partners in general) at collider experiments implies a much richer neutrino mass-generation scheme than just the canonical, high-scale Type I Seesaw.

[3]Where $\mathrm{BR}(A \to X) \equiv \Gamma(A \to X)/\sum_Y \Gamma(A \to Y)$ for partial width $\Gamma(A \to Y)$.

3.1.2. Type I+II Hybrid Seesaw Mechanism

While the discovery of lepton number violation in, say, $0\nu\beta\beta$ or hadron collisions would imply the Majorana nature of neutrinos [33–35], it would be less clear which mechanism or mechanisms are driving light neutrino masses to their sub-eV values. This is because in the most general case neutrinos possess both LH and RH Majorana masses in addition to Dirac masses. In such hybrid Seesaw models, two or more "canonical" tree- and loop-level mechanisms are combined and, so to speak, may give rise to phenomenology that is greater than the sum of its parts.

A well-studied hybrid model is the Type I+II Seesaw mechanism, wherein the light neutrino mass matrix M_ν, when $M_D M_R^{-1} \ll 1$, is given by Chen et al. [101], Akhmedov and Frigerio [102], Akhmedov et al. [103], Chao et al. [104, 105], Gu et al. [106], and Chao et al. [107]

$$M_\nu^{light} = M_L - M_D M_R^{-1} M_D^T. \qquad (3.20)$$

Here, the Dirac and Majorana mass terms, M_D, M_R, have their respective origins according to the Type I model, whereas M_L originates from the Type II mechanism; see section 4 for details. In this scenario, sub-eV neutrino masses can arise not only from parametrically small Type I and II masses but additionally from an incomplete cancellation of the two terms [102–104]. While a significant or even moderate cancellation requires a high-degree of fine tuning and is radiatively instable [107], this situation cannot theoretically be ruled out *a priori*. For a one-generation mechanism, the relative minus sign in Equation (3.20) is paramount for such a cancellation; however, in a multi-generation scheme, it is not as crucial as M_D is, in general, complex and can even absorb the sign through a phase rotation. Moreover, this fine-tuning scenario is a caveat of the aforementioned decoupling of L-violation in a minimal Type I Seesaw from LHC phenomenology [27, 96, 97]. As we will discuss shortly, regardless of its providence, if such a situation were to be realized in nature, then vibrant and rich collider signatures emerges.

3.1.3. Type I Seesaw in U(1)$_X$ Gauge Extensions of the Standard Model

Another manner in which the decoupling of heavy Majorana neutrinos N from collider experiments can be avoided is

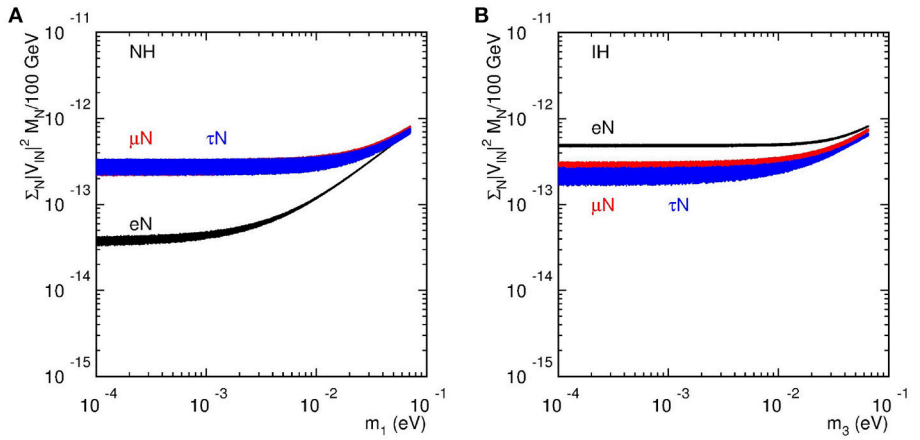

FIGURE 2 | $\Sigma_N |V_{\ell N}|^2 M_N/100$ GeV vs. the lightest neutrino mass for **(A)** NH and **(B)** IH in the case of degenerate heavy neutrinos, assuming vanishing phases.

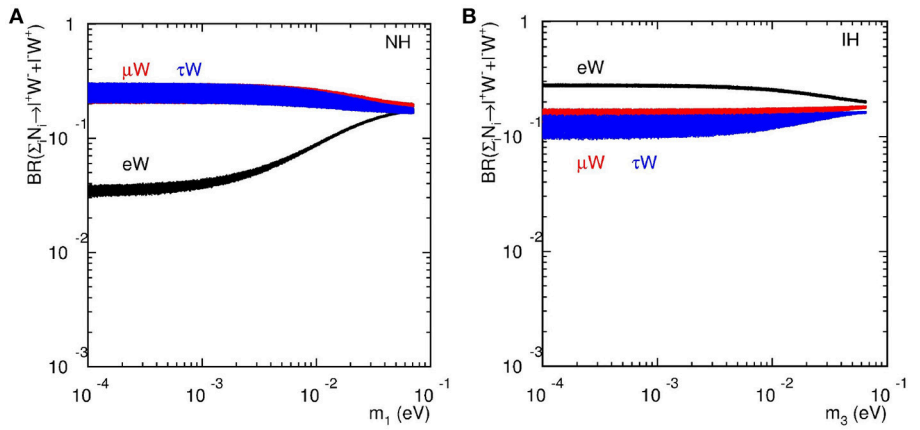

FIGURE 3 | Branching fractions of process $\sum_i N_i \to \ell^+ W^- + \ell^- W^+$ vs. the lightest neutrino mass for **(A)** NH and **(B)** IH in the degenerate case with $M_N = 300$ GeV and $m_h = 125$ GeV, assuming vanishing phases.

through the introduction of new gauge symmetries, under which N is charged. One such example is the well-studied $U(1)_X$ Abelian gauge extension of the SM [108–112], where $U(1)_X$ is a linear combination of $U(1)_Y$ and $U(1)_{B-L}$ after the spontaneous breaking of electroweak symmetry and $B - L$ (baryon minus lepton number) symmetries. In this class of models, RH neutrinos are introduced to cancel gauge anomalies and realize a Type I Seesaw mechanism.

Generally, such a theory can be described by modifying the SM covariant derivatives by Salvioni et al. [113]

$$D_\mu \ni i g_1 Y B_\mu \quad \to \quad D_\mu \ni i g_1 Y B_\mu + i(\tilde{g} Y + g_1' Y_{BL}) B_\mu', \quad (3.21)$$

where $B_\mu(Y)$ and $B'_\mu(Y_{BL})$ are the gauge fields (quantum numbers) of $U(1)_Y$ and $U(1)_{B-L}$, respectively. The most economical extension with vanishing mixing between $U(1)_Y$ and $U(1)_{B-L}$, i.e., , $U(1)_X = U(1)_{B-L}$ and $\tilde{g} = 0$ in Equation (3.21), introduces three RH neutrinos and a new complex scalar S that are all charged under the new gauge group but remain singlets under the SM symmetries [114–116]. In this extension one can then construct the neutrino Yukawa interactions

$$\mathcal{L}_I^Y = -\bar{L}_L Y_\nu^D \tilde{H} N_R - \frac{1}{2} Y_\nu^M \overline{(N^c)_L} N_R S + \text{H.c.} \quad (3.22)$$

Once the Higgs S acquires the vacuum expectation value $\langle S \rangle = v_S/\sqrt{2}$, $B - L$ is broken, spontaneously generating the RH Majorana mass matrix $M_N = Y_\nu^M v_S/\sqrt{2}$ from Equation (3.22).

It is interesting to note that the scalar vev provides a dynamical mechanism for the heavy, RH Majorana mass generation, i.e., a Type I Seesaw via a Type II mechanism; see section 4 for more details. The Seesaw formula and the mixing between the SM charged leptons and heavy neutrinos here are exactly the same as those in the canonical Type I Seesaw. The mass of neutral gauge field B'_μ, $M_{Z'} = M_{Z_{B-L}} = 2 g_{BL} v_S$, is generated from S' kinetic term, $\left(D_\mu S\right)^\dagger (D^\mu S)$ with $D_\mu S = \partial_\mu S + i 2 g_{BL} B'_\mu S$. Note that in the minimal model, $g_{BL} = g_1'$. As in other extended scalar scenarios, the quadratic term $H^\dagger H S^\dagger S$ in the scalar potential

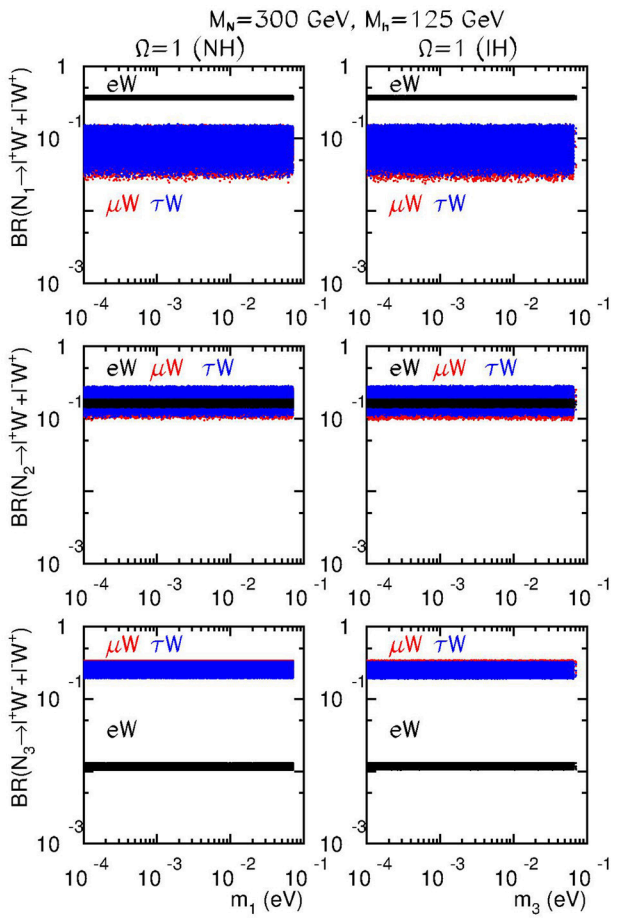

FIGURE 4 | Branching fractions of process $N_i \to \ell^+W^- + \ell^-W^+$ vs. the lightest neutrino mass for NH and IH in the case $\Omega = I$ with $M_i = 300$ GeV and $m_h = 125$ GeV, assuming vanishing Majorana phases.

results in the SM Higgs H and S interaction states mixing into two CP-even mass eigenstates, H_1 and H_2.

3.1.4. Type I+II Hybrid Seesaw in Left-Right Symmetric Model

As discussed in section 3.1.2, it may be the case the light neutrino masses result from the interplay of multiple Seesaw mechanisms. For example: the Type I+II hybrid mechanism with light neutrino masses given by Equation (3.20). It is also worth observing two facts: First, in the absence of Majorana masses, the minimum fermionic field content for a Type I+II Seesaw automatically obeys an accidental global $U(1)_{B-L}$ symmetry. Second, with three RH neutrinos, all fermions can be sorted into either $SU(2)_L$ doublets (as in the SM) or $SU(2)_R$ doublets, its RH analog. As the hallmark of the Type II model (see section 4) is the spontaneous generation of LH Majorana masses from a scalar $SU(2)_L$ triplet Δ_L, it is conceivable that RH neutrino Majorana masses could also be generated spontaneously, but from a scalar $SU(2)_R$ triplet Δ_R. (This is similar to the spontaneous breaking of $U(1)_{B-L}$ in section 3.1.3.) This realization of the Type I+II Seesaw is known as the Left-Right Symmetric Model (LRSM) [117–121], and remains one of the best-motivated and well-studied extensions of the SM. For recent, dedicated reviews, see Mohapatra and Smirnov [63], Duka et al. [122], and Senjanović [123].

The high energy symmetries of the LRSM is based on the extended gauge group

$$\mathcal{G}_{\rm LRSM} = {\rm SU}(3)_c \otimes {\rm SU}(2)_L \otimes {\rm SU}(2)_R \otimes {\rm U}(1)_{B-L}, \qquad (3.23)$$

or its embeddings, and conjectures that elementary states, in the UV limit, participate in LH and RH chiral currents with equal strength. While the original formulation of model supposes a generalized parity $\mathcal{P}_X = \mathcal{P}$ that enforces an exchange symmetry between fields charged under $SU(2)_L$ and $SU(2)_R$, it is also possible to achieve this symmetry via a generalized charge conjugation $\mathcal{P}_X = \mathcal{C}$ [124]. For fermionic and scalar multiplets $Q_{L,R}$ and Φ, the exchange relationships are [124],

$$\mathcal{P}: \begin{cases} Q_L \leftrightarrow Q_R \\ \Phi \leftrightarrow \Phi^\dagger \end{cases}, \quad \text{and} \quad \mathcal{C}: \begin{cases} Q_L \leftrightarrow (Q_R)^c \\ \Phi \leftrightarrow \Phi^T \end{cases},$$
$$\text{where} \quad (Q_R)^c = C\gamma^0 Q_R^*. \qquad (3.24)$$

A non-trivial, low-energy consequence of these complementary formulations of the LRSM is the relationship between the LH CKM matrix in the SM, $V_{ij}^{\rm L}$, and its RH analog, $V_{ij}^{\rm R}$. For generalized conjugation, one has $|V_{ij}^{\rm R}| = |V_{ij}^{\rm L}|$, whereas $|V_{ij}^{\rm R}| \approx |V_{ij}^{\rm L}| + \mathcal{O}(m_b/m_t)$ for generalized parity [124–128]. Moreover, LR parity also establishes a connection between the Dirac and Majorana masses in the leptonic sector [129, 130]. Under generalized parity, for example, the Dirac ($Y_{1,2}^D$) and Majorana ($Y_{L,R}$) Yukawa matrices must satisfy [130],

$$Y_{1,2}^D = Y_{1,2}^{D\dagger} \quad \text{and} \quad Y_L = Y_R. \qquad (3.25)$$

Such relationships in the LRSM remove the arbitrariness of neutrino Dirac mass matrices, as discussed in section 3.1.1, and permits one to calculate Ω, even for nonzero Δ_L vev [129, 131]. However, the potential cancellation between Type I and II Seesaw masses in Equation 3.20 still remains.

In addition to the canonical formulation of the LRSM are several alternatives. For example: It is possible to instead generate LH and RH Majorana neutrino masses radiatively in the absence of triplet scalars [132, 133]. One can gauge baryon number and lepton number independently, which, for an anomaly-free theory, gives rise to vector-like leptons and a Type III Seesaw mechanism [134, 135] (see section 5), as well as embed the model into an R-parity-violating Supersymmetric framework [136, 137].

Despite the large scalar sector of the LRSM (two complex triplets and one complex bidoublet), and hence a litany of neutral and charged Higgses, the symmetry structure in Equation (3.23) confines the number in independent degrees of freedom to 18 [122, 138]. These consist of three mass scales $\mu_{1,\ldots,3}$, 14 dimensionless couplings $\lambda_{1,\ldots,4}$, $\rho_{1,\ldots,4}$, $\alpha_{1,\ldots,3}$, $\beta_{1,\ldots,3}$, and one CP-violating phase, δ_2. For further discussions on the spontaneous breakdown of CP in LR scenarios, see also Senjanović [121], Basecq et al. [139], and Kiers et al. [140]. With explicit CP

conservation, the minimization conditions on the scalar potential give rise to the so-called LRSM vev Seesaw relationship [138],

$$v_L = \frac{\beta_2 k_1^2 + \beta_1 k_1 k_2 + \beta_3 k_2^2}{(2\rho_1 - \rho_3) v_R}, \tag{3.26}$$

where, $v_{L,R}$ and $k_{1,2}$ are the vevs of $\Delta_{L,R}$ and the Higgs bidoublet Φ, respectively, with $v_L^2 \ll k_1^2 + k_2^2 \approx (246\,\text{GeV})^2 \ll v_R$.

In the LRSM, the bidoublet Φ fulfills the role of the SM Higgs to generate the known Dirac masses of elementary fermions and permits a neutral scalar h_i with mass $m_{h_i} \approx 125$ GeV and SM-like couplings. In the absence of egregious fine-tuning, i.e., $\rho_3 \not\approx 2\rho_1$, Equation (3.26) suggests that v_L in the LRSM is inherently small because, in addition to $k_1, k_2 \ll v_R$, custodial symmetry is respected (up to hypercharge corrections) when all β_i are identically zero [141]. Consistent application of such naturalness arguments reveals a lower bound on the scalar potential parameters [141],

$$\begin{aligned} \rho_{1,2,4} &> \frac{g_R^2}{4}\left(\frac{m_{\text{FCNH}}}{M_{W_R}}\right)^2, \\ \rho_3 &> g_R^2\left(\frac{m_{\text{FCNH}}}{M_{W_R}}\right)^2 + 2\rho_1 \sim 6\rho_1, \\ \alpha_{1,\ldots,3} &> g_R^2\left(\frac{m_{\text{FCNH}}}{M_{W_R}}\right)^2, \end{aligned} \tag{3.27}$$

$$\mu_{1,2}^2 > (m_{\text{FCNH}})^2, \quad \mu_3^2 > \frac{1}{2}(m_{\text{FCNH}})^2, \tag{3.28}$$

where M_{W_R} and g_R are the mass and coupling of the $W_R^\pm$ gauge boson associated with $\text{SU}(2)_R$, and m_{FCNH} is the mass scale of the LRSM scalar sector participating in flavor-changing neutral transitions. Present searches for neutron EDMs [125, 126, 142, 143] and FCNCs [143–147] require $m_{\text{FCNH}} > 10 - 20$ TeV at 90% CL. Subsequently, in the absence of FCNC-suppressing mechanisms, $\rho_i > 1$ for LHC-scale W_R. Thus, discovering LRSM at the LHC may suggest a strongly coupled scalar sector. Conversely, for $\rho_i < 1$ and $m_{\text{FCNH}} \sim 15\,(20)$ TeV, one finds $M_{W_R} \gtrsim 10\,(12)$ TeV, scales that are within the reach of future hadron colliders [141, 148, 149]. For more detailed discussions on the perturbativity and stability of the LRSM scalar section, see Mitra et al. [141], Maiezza et al. [146], Bertolini et al. [150–152], Mohapatra and Zhang [153], and Maiezza and Senjanović [154] and references therein.

After Δ_R acquires a vev and LR symmetry is broken spontaneously, the neutral component of $\text{SU}(2)_R$, i.e., W_R^3, and the $\text{U}(1)_{B-L}$ boson, i.e., X_{B-L}, mix into the massive eigenstate Z'_{LRSM} (sometimes labeled Z_R) and the orthogonal, massless vector boson B. B is recognized as the gauge field associated with weak hypercharge in the SM, the generators of which are built from the remnants of $\text{SU}(2)_R$ and $\text{U}(1)_{B-L}$. The relation between electric charge Q, weak left/right isospin $T^3_{L/R}$, baryon minus lepton number B-L, and weak hypercharge Y is given by

$$Q = T_L^3 + T_R^3 + \frac{(B-L)}{2} \equiv T_L^3 + \frac{Y}{2}, \quad \text{with} \quad Y = 2T_R^3 + (B-L). \tag{3.29}$$

This in turn implies that the remaining components of $\text{SU}(2)_R$, W_R^1 and W_R^2, combine into the state $W_R^\pm$ with electric charge $Q^{W_R} = \pm 1$ and mass $M_{W_R} = g_R v_R/\sqrt{2}$. After EWSB, it is possible for the massive W_R and W_L gauge fields to mix, with the mixing angle ξ_{LR} given by $\tan 2\xi_{\text{LR}} = 2k_1k_2/(v_R^2 - v_L^2) \lesssim 2v_{\text{SM}}^2/v_R^2$. Neutral meson mass splittings [124, 147, 155–158] coupled with improved lattice calculations, e.g., [159, 160], Weak CPV [124, 158, 161], EDMs [124–126, 158], and CP violation in the electron EDM [129], are particularly sensitive to this mixing, implying the competitive bound of $M_{W_R} \gtrsim 3$ TeV at 95% CL [147]. This forces $W_L - W_R$ mixing to be, $\tan 2\xi_{\text{LR}}/2 \approx \xi_{\text{LR}} \lesssim M_W^2/M_{W_R}^2 < 7 - 7.5 \times 10^{-4}$. A similar conclusion can be reached on $Z - Z'_{LRSM}$ mixing. Subsequently, the light and heavy mass eigenstates of LRSM gauge bosons, $W_1^\pm$, $W_2^\pm$, Z_1, Z_2, where $M_{V_1} < M_{V_2}$, are closely aligned with their gauge states. In other words, to a very good approximation, $W_1 \approx W_{\text{SM}}$, $Z_1 \approx Z_{\text{SM}}$, $W_2 \approx W_R$ and $Z' \approx Z'_{LRSM}$ (or sometimes $Z' \approx Z_R$). The mass relation between the LR gauge bosons is $M_{Z_R} = \sqrt{2\cos^2\theta_W/\cos 2\theta_W} M_{W_R} \approx (1.7) \times M_{W_R}$, and implies that bounds on one mass results in indirect bounds on the second mass; see, for example, Lindner et al. [162].

3.1.5. Heavy Neutrino Effective Field Theory

It is possible that the coupling of TeV-scale Majorana neutrinos to the SM sector is dominated by new states with masses that are hierarchically larger than the heavy neutrino mass or the reach of present-day collider experiments. For example: Scalar $\text{SU}(2)_R$ triplets in the Left-Right Symmetric Model may acquire vevs $\mathcal{O}(10)$ TeV, resulting in new gauge bosons that are kinematically accessible at the LHC but, due to $\mathcal{O}(10^{-3} - 10^{-2})$ triplet Yukawa couplings, give rise to EW-scale RH Majorana neutrino masses. In such a pathological but realistic scenario, the LHC phenomenology appears as a canonical Type I Seesaw mechanism despite originating from a different Seesaw mechanism [163]. While it is generally accepted that such mimicry can occur among Seesaws, few explicit examples exist in the literature and further investigation is encouraged.

For such situations, it is possible to parameterize the effects of super-heavy degrees of freedom using the Heavy Neutrino Effective Field Theory (NEFT) framework [164]. NEFT is an extension of the usual SM Effective Field Theory (SMEFT) [165–168], whereby instead of augmenting the SM Lagrangian with higher dimension operators one starts from the Type I Seesaw Lagrangian in Equation (3.1) and builds operators using that field content. Including all $\text{SU}(3) \otimes \text{SU}(2)_L \otimes \text{U}(1)_Y$-invariant, operators of mass dimension $d > 4$, the NEFT Lagrangian before EWSB is given by

$$\mathcal{L}_{\text{NEFT}} = \mathcal{L}_{\text{Type I}} + \sum_{d=5}\sum_i \frac{\alpha_i^{(d)}}{\Lambda^{(d-4)}}\mathcal{O}_i^{(d)}. \tag{3.30}$$

Here, $\mathcal{O}_i^{(d)}$ are dimension d, Lorentz and gauge invariant permutations of Type I fields, and $\alpha_i^{(d)} \ll 4\pi$ are the corresponding Wilson coefficients. The list of $\mathcal{O}_i^{(d)}$ are known explicitly for $d = 5$ [169, 170], 6 [164, 170], and 7 [170–172], and can be built for larger d following [173–175].

After EWSB, fermions should then be decomposed into their mass eigenstates via quark and lepton mixing. For example: among the $d = 6$, four-fermion contact operations $\mathcal{O}_i^{(6)}$ that contribute to heavy N production in hadron colliders (see Equation 3.33) in the interaction/gauge basis are [164]

$$\begin{aligned}\mathcal{O}_V^{(6)} &= \left(\overline{d}\gamma^\mu P_R u\right)\left(\overline{e}\gamma_\mu P_R N_R\right) \quad \text{and} \\ \mathcal{O}_{S3}^{(6)} &= \left(\overline{Q}\gamma^\mu P_R N_R\right)\varepsilon\left(\overline{L}\gamma_\mu P_R d\right). \end{aligned} \tag{3.31}$$

In terms of light (ν_m) and heavy ($N_{m'}$) mass eigenstates and using Equation (3.4), one can generically [66, 87] decompose the heavy neutrino interaction state N_ℓ as $N_\ell = \sum_{m=1}^{3} X_{\ell m}\nu_m^c + \sum_{m'=1}^{n} Y_{\ell N_{m'}} N_{m'}$, with $|Y_{\ell N_{m'}}|$ of order the elements of U_{PMNS}. Inserting this into the preceding operators gives quantities in terms of leptonic mass eigenstates:

$$\begin{aligned}\mathcal{O}_V^{(6)} &= \sum_{m=1}^{3}\left(\overline{d}\gamma^\mu P_R u\right)\left(\overline{\ell}\gamma_\mu P_R\, X_{\ell m}\, \nu_m^c\right) \\ &\quad + \sum_{m'=1}\left(\overline{d}\gamma^\mu P_R u\right)\left(\overline{\ell}\gamma_\mu P_R\, Y_{\ell N_{m'}}\, N_{m'}\right), \quad \text{and} \\ \mathcal{O}_{S3}^{(6)} &= \sum_{m=1}^{3}\left(\overline{Q}\gamma^\mu P_R\, X_{\ell m}\nu_m^c\right)\left(\overline{\ell}\gamma_\mu P_R d\right) \\ &\quad + \sum_{m'=1}\left(\overline{Q}\gamma^\mu P_R\, Y_{\ell N_{m'}} N_{m'}\right)\left(\overline{\ell}\gamma_\mu P_R d\right). \end{aligned} \tag{3.32}$$

After EWSB, a similar decomposition for quarks gauge states in terms of CKM matrix elements and mass eigenstates should be applied. For more information on such decompositions, see, e.g., Ruiz [163] and references therein. It should be noted that after integrating out the heavy N field, the marginal operators at $d > 5$ generated from the Type I Lagrangian are not the same operators generated by integrating the analogous Seesaw partner in the Type II and III scenarios [176, 177].

3.2. Heavy Neutrinos at Colliders

The connection between low-scale Seesaw models and colliders is made no clearer than in searches for heavy neutrinos, both Majorana and (pseudo-)Dirac, in the context of Type I-based scenarios. While extensive, the topic's body of literature is still progressing in several directions. This is particularly true for the development of collider signatures, Monte Carlo tools, and high-order perturbative corrections. Together, these advancements greatly improve sensitivity to neutrinos and their mixing structures at collider experiments.

We now review the various searches for L-violating collider processes facilitated by Majorana neutrinos N. We start with low-mass (section 3.2.1) and high-mass (sections 3.2.2 and 3.2.3) neutrinos in the context of Type I-based hybrid scenarios, before moving onto Abelian (section 3.2.4) and non-Abelian (section 3.2.5) gauge extensions, and finally the semi-model independent NEFT framework (section 3.2.6). Lepton number violating collider processes involving pseudo-Dirac neutrinos are, by construction, suppressed [178–181]. Thus, a discussion of their phenomenology is outside the scope of this review and we refer readers to thorough reviews such as Ibarra et al. [94], Weiland [182], and Antusch et al. [183].

3.2.1. Low-Mass Heavy Neutrinos at *pp* and *ee* Colliders

For Majorana neutrinos below the M_W mass scale, lepton number violating processes may manifest in numerous way, including rare decays of mesons, baryons, μ and τ leptons, and even SM electroweak bosons. Specifically, one may discover L violation in three-body meson decays to lighter mesons $M_1^\pm \to M_2^\mp \ell_1^\pm \ell_2^\pm$ [66, 184–199], such as that shown in **Figure 5A**; four-body meson decays to lighter mesons $M_1^\pm \to M_2^\mp M_3^0 \ell_1^\pm \ell_2^\pm$ [195, 196, 200–202]; four-body meson decays to leptons $M^\pm \to \ell_1^\pm \ell_1^\pm \ell_2^\mp \nu$ [192, 193, 202–204]; five-body meson decays [202]; four-body baryon decays to mesons, $B \to M\ell_1^\pm \ell_2^\pm$ [205]; three-body τ decay to mesons, $\tau^\pm \to \ell^\mp M_1^\pm M_2^\pm$ [195, 206, 207]; four-body τ decays to mesons, $\tau^\pm \to \ell_1^\pm \ell_1^\pm M^\mp \nu$ [195, 206, 208–210]; four-body W boson decays, $W^\pm \to \ell_1^\pm \ell_1^\pm \ell_2^\mp \nu$ [211–215]; Higgs boson decays, $h \to NN \to \ell_1^\pm \ell_2^\pm + X$ [216–219]. and even top quark decays, $t \to bW^{+*} \to b\ell_1^+ N \to b\ell_1^+ \ell_2^\pm q\overline{q'}$ [7, 211, 220, 221]. The W boson case is notable as azimuthal and polar distributions [87] or exploiting endpoint kinematics [214] can differentiate between L conservation and non-conservation. Of the various collider searches for GeV-scale N, great complementarity is afforded by B-factories. As shown in **Figure 5B**, an analysis of Belle I [45] and LHCb Run I [46, 47] searches for L-violating final states from meson decays excluded [222] $|V_{\mu N}|^2 \gtrsim 3 \times 10^{-5}$ for $M_N = 1 - 5$ GeV. Along these same lines, the observability of displaced decays of heavy neutrinos [217, 223–227] and so-called "neutrino-antineutrino oscillations" [228–231] (in analogy to $\mathcal{B}-\overline{\mathcal{B}}$ oscillations) and have also been discussed.

Indirectly, the presence of heavy Majorana neutrinos can appear in precision EW measurements as deviations from lepton flavor unitarity and universality, and is ideally suited for e^+e^- colliders [88–91, 183, 232, 233], such as the International Linear Collider (ILC) [234, 235], Circular e^-e^+ Collider (CepC) [236], and Future Circular Collider-*ee* (FCC-ee) [232]. An especially famous example of this is the number of active, light neutrino flavors N_ν, which can be inferred from the Z boson's invisible width Γ_{Inv}^Z. At lepton colliders, Γ_{Inv}^Z can be determined in two different ways: The first is from line-shape measurements of the Z resonance as a function of $\sqrt{s}$, and is measured to be $N_\nu^{\text{Line}} = 2.9840 \pm 0.0082$ [237]. The second is from searches for invisible Z decays, i.e., , $e^+e^- \to Z\gamma$, and is found to be $N_\nu^{\text{Inv}} = 2.92 \pm 0.05$ [238]. Provocatively, both measurements deviate from the SM prediction of $N_\nu^{\text{SM}} = 3$ at the 2σ level. It is unclear if deviations from N_ν^{SM} are the result of experimental uncertainty or indicate the presence of, for example, RH neutrinos [224, 239]. Nonetheless, a future Z-pole machine can potentially clarify this discrepancy [224]. For investigations into EW constraints on heavy neutrinos, see del Águila et al. [88], Antusch and Fischer [89], de Gouvêa and Kobach [90], and Fernandez-Martinez et al. [91].

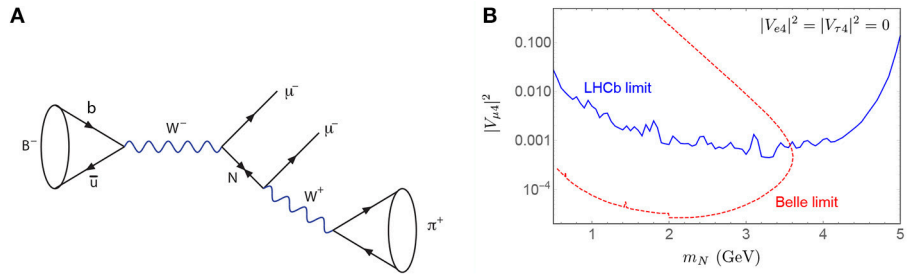

FIGURE 5 | (A) B^- meson decay to L-violating final state via heavy Majorana N [47]. **(B)** LHCb and Belle I limits on $|V_{\mu N}|^2$ (labeled $|V_{\mu 4}|^2$ in the figure) as a function of N mass after $\mathcal{L} = 3$ fb^{-1} at 7-8 TeV LHC [222].

3.2.2. High-Mass Heavy Neutrinos at *pp* Colliders

Collider searches for heavy Majorana neutrinos with masses above M_W have long been of interest to the community [240–243], with exceptionally notable works appearing in the early 1990s [96, 244–247] and late-2000s [66, 97, 248–253]. In the past decade, among the biggest advancements in Seesaw phenomenology is the treatment of collider signatures for such hefty N in Type I-based models. While coupled to concurrent developments in Monte Carlo simulation packages, the progression has been driven by attempts to reconcile conflicting reports of heavy neutrino production cross sections for the LHC. This was at last resolved in Alva et al. [254] and Degrande et al. [255], wherein new, infrared- and collinear- (IRC-)safe definitions for inclusive and semi-inclusive[4] production channels were introduced. The significance of such collider signatures is that they are well-defined at all orders in α_s, and hence correspond to physical observables. We now summarize this extensive body of literature, emphasizing recent results.

For Majorana neutrinos with $M_N > M_W$, the most extensively studied [66, 105, 183, 230, 240, 241, 246, 248–253, 256] collider production mechanism is the L-violating, charged current (CC) Drell-Yan (DY) process [240], shown in **Figure 6A**, and given by

$$q_1\,\overline{q}_2 \to W^{\pm *} \to N\,\ell_1^{\pm}, \quad \text{with} \quad N \to \ell_2^{\pm} W^{\mp} \to \ell_2^{\pm} q_1'\,\overline{q}'_2. \tag{3.33}$$

A comparison of **Figure 6A** to the meson decay diagram of **Figure 5A** immediately reveals that Equation (3.33) is the former's high momentum transfer completion. Subsequently, much of the aforementioned kinematical properties related to L-violating meson decays also hold for the CC DY channel [87, 257]. Among the earliest studies are those likewise focusing on neutral current (NC) DY production [241, 242, 245–247], again shown in **Figure 6A**, and given by

$$q\,\overline{q} \to Z^* \to N\,\overset{(-)}{\nu}_{\ell}, \tag{3.34}$$

as well as the gluon fusion mechanism [242, 245], shown in **Figure 6B**, and given by

$$g\,g \to Z^*/h^* \to N\,\overset{(-)}{\nu}_{\ell}. \tag{3.35}$$

Interestingly, despite gluon fusion being formally an $\mathcal{O}(\alpha_s^2)$ correction to Equation (3.34), it is non-interfering, separately gauge invariant, and the subject of renewed interest [255, 258, 259]. Moreover, in accordance to the Goldstone Equivalence Theorem [260, 261], the ggZ^* contribution has been shown [258, 259] to be as large as the ggh^* contribution, and therefore should not be neglected. Pair production of N via s-channel scattering [242, 246], e.g., $gg \to NN$, or weak boson scattering [244, 247, 248], e.g., $W^{\pm}W^{\mp} \to NN$, have also been discussed, but are relatively suppressed compared to single production by an additional mixing factor of $|V_{\ell N_{m'}}|^2 \lesssim 10^{-4}$.

A recent, noteworthy development is the interest in semi-inclusive and exclusive production of heavy neutrinos at hadron colliders, i.e., , N production in association with jets. In particular, several studies have investigated the semi-inclusive, photon-initiated vector boson fusion (VBF) process [247, 254, 255, 262], shown in **Figure 6C**, and given by

$$q\,\gamma \to N\,\ell^{\pm}\,q', \tag{3.36}$$

and its deeply inelastic, $\mathcal{O}(\alpha)$ radiative correction [247, 254, 255, 262–266],

$$q_1\,q_2 \xrightarrow{W\gamma + WZ \to N\ell^{\pm}} N\,\ell^{\pm}\,q_1'\,q_2'. \tag{3.37}$$

At $\mathcal{O}(\alpha^4)$ (here we do not distinguish between α and α_W), the full, gauge invariant set of diagrams, which includes the sub-leading $W^{\pm}Z \to N\ell^{\pm}$ scattering, is given in **Figure 7**.

Treatment of the VBF channel is somewhat subtle in that it receives contributions from collinear QED radiation off the proton [262], collinear QED radiation off initial-states quarks [254], and QED radiation in the deeply inelastic/high momentum transfer limit [247]. For example: In the top line

[4] A note on terminology: High-p_T hadron collider observables, e.g., fiducial distributions, are inherently inclusive with respect to jets with arbitrarily low p_T. In this sense, we refer to hadronic-level processes with a fixed multiplicity of jets satisfying kinematical requirements (and with an arbitrary number of additional jets that do not) as *exclusive*, e.g., $pp \to W^{\pm} + 3j + X$; those with a minimum multiplicity meeting these requirements are labeled *semi-inclusive*, e.g., $pp \to W^{\pm} + \geq 3j + X$; and those with an arbitrary number of jets are labeled *inclusive*, e.g., $pp \to W^{\pm} + X$. Due to DGLAP-evolution, exclusive, partonic amplitudes convolved with PDFs are semi-inclusive at the hadronic level.

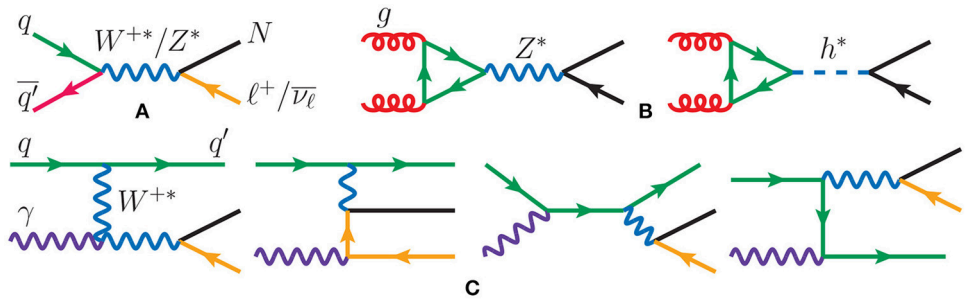

FIGURE 6 | Born diagrams for heavy neutrino (*N*) production via **(A)** Drell-Yan, **(B)** gluon fusion, and **(C)** electroweak vector boson fusion; from Ruiz et al. [259] and drawn using `JaxoDraw` [267].

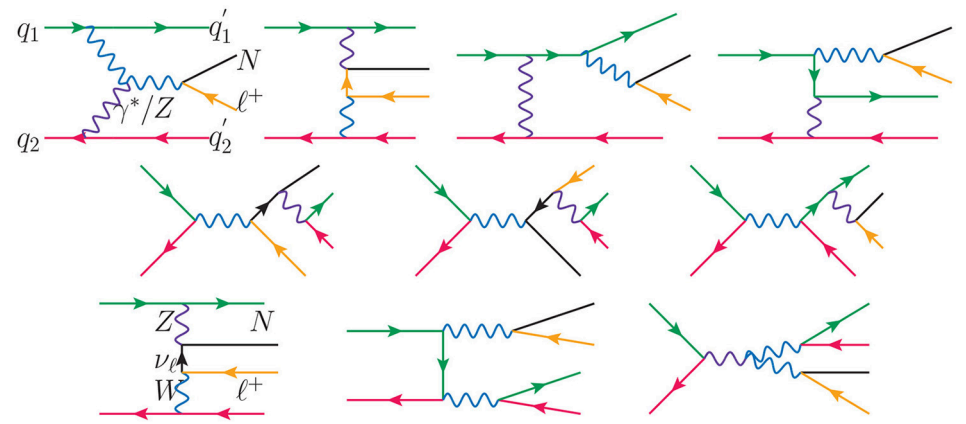

FIGURE 7 | Born diagrams for the $\mathcal{O}(\alpha^4)$ heavy neutrino (*N*) production process $q_1 q_2 \to N\ell^\pm q_1' q_2'$ [254].

of diagrams in **Figure 7**, one sees that in the collinear limit of the $q_2 \to \gamma^* q_2'$ splitting, the virtual γ^* goes on-shell and the splitting factorizes into a photon parton distribution function (PDF), recovering the process in Equation (3.36) [254, 255]. As these sub-channels are different kinematic limits of the same process, care is needed when combining channels so as to not double count regions of phase space. While ingredients to the VBF channel have been known for some time, consistent schemes to combine/match the processes are more recent [254, 255]. Moreover, for inclusive studies, Degrande et al. [255] showed that the use of Equation (3.36) in conjunction with a γ-PDF containing both elastic and inelastic contributions [268] can reproduce the fully matched calculation of Ref. [254] within the $\mathcal{O}(20\%)$ uncertainty resulting from missing NLO in QED terms. Neglecting the collinear $q_2 \to \gamma^* q_2'$ splitting accounts for the unphysical cross sections reported in Deppisch et al. [67] and Dev et al. [262] . Presently, recommended PDF sets containing such γ-PDFs include: MMHT QED (no available `lhaid`) [268, 269], NNPDF 3.1+LUXqed (`lhaid=324900`) [270], LUXqed17+PDF4LHC15 (`lhaid=82200`) [271, 272], and CT14 QED Inclusive (`lhaid = 13300`) [273]. Qualitatively, the MMHT [268] and LUXqed [271, 272] treatments of photon PDFs are the most rigorous. In analogy to the gluon fusion and NC DY, Equation (3.36) (and hence Equation 3.37) is a non-interfering, $\mathcal{O}(\alpha)$ correction to the CC DY process. Thus, the CC DY and VBF channels can be summed coherently.

In addition to these channels, the semi-inclusive, associated *n*-jet production mode,

$$p\,p \to W^* + \geq nj + X \quad \to \quad N\,\ell^\pm + \geq nj + X, \quad \text{for} \quad n \in \mathbb{N}, \tag{3.38}$$

has also appeared in the recent literature [255, 262, 274]. As with VBF, much care is needed to correctly model Equation (3.38). As reported in Degrande et al. [255] and Ruiz [275], the production of heavy leptons in association with QCD jets is nuanced due to the presence of additional *t*-channel propagators that can lead to artificially large cross sections if matrix element poles are not sufficiently regulated. (It is not enough to simply remove the divergences with phase space cuts). After phase space integration, these propagators give rise to logarithmic dependence on the various process scales. Generically Ruiz [275] and Collins et al. [276], the cross section for heavy lepton and jets in Equation (3.38) scales as:

$$\sigma(pp \to N\ell^\pm + nj + X) \sim \sum_{k=1}^{n} \alpha_s^k(Q^2) \log^{(2k-1)}\left(\frac{Q^2}{q_T^2}\right), \tag{3.39}$$

Here, $Q \sim M_N$ is the scale of the hard scattering process, $q_T = \sqrt{|\vec{q}_T|^2}$, and $\vec{q}_T \equiv \sum_k^n \vec{p}_{T,k}^{\,j}$, is the $(N\ell)$-system's transverse momentum, which recoils against the vector sum of all jet $\vec{p}_T$. It is clear for a fixed M_N that too low jet p_T cuts can lead to too small q_T and cause numerically large (collinear) logarithms such that $\log(M_N^2/q_T^2) \gg 1/\alpha_s(Q)$, spoiling the perturbative convergence of Equation (3.39). Similarly, for a fixed q_T, arbitrarily large M_N can again spoil perturbative convergence. As noted in Alva et al. [254] and Degrande et al. [255], neglecting this fact has led to conflicting predictions in several studies on heavy neutrino production in pp collisions.

It is possible [255], however, to tune p_T cuts on jets with varying M_N to enforce the validity of Equation (3.39). Within the Collins-Soper-Sterman (CSS) resummation formalism [276], Equation (3.39) is only trustworthy when $\alpha_s(Q^2)$ is perturbative and $q_T \sim Q$, i.e.,

$$\log(Q/\Lambda_{\rm QCD}) \gg 1 \quad \text{and} \quad \alpha_s(Q)\log^2(Q^2/q_T^2) \lesssim 1. \tag{3.40}$$

Noting that at 1-loop $\alpha_s(Q)$ can be expressed by $1/\alpha_s(Q) \approx (\beta_0/2\pi)\log(Q/\Lambda_{\rm QCD})$, and setting $Q = M_N$, one can invert the second CSS condition and obtain a consistency relationship [255]:

$$q_T = |\vec{q}_T| = \left|\sum_{k=1}^{n} \vec{p}_{T,k}^{\,j}\right| \gtrsim M_N \times e^{-(1/2)\sqrt{(\beta_0/2\pi)\log(M_N/\Lambda_{\rm QCD})}}. \tag{3.41}$$

This stipulate a minimum q_T needed for semi-inclusive processes like Equation (3.39) to be valid in perturbation theory. When q_T of the $(N\ell)$-system is dominated by a single, hard radiation, Equation (3.41) is consequential: In this approximation, $q_T \approx |\vec{p}_{T,1}^{\,j}|$ and Equation (3.41) suggests a *scale-dependent*, minimum jet p_T cut to ensure that specifically the semi-inclusive $pp \to N\ell + \geq 1j + X$ cross section is well-defined in perturbation theory. Numerically, this is sizable: for $M_N = 30$ (300) [3000] GeV, one requires that $|\vec{p}_{T,1}^{\,j}| \gtrsim 9$ (65) [540] GeV, or alternatively $|\vec{p}_{T,1}^{\,j}| \gtrsim 0.3$ (0.22) [0.18] $\times M_N$, and indicates that naïve application of fiducial p_T^j cuts for the LHC do not readily apply for $\sqrt{s} = 27$-100 TeV scenarios, where one can probe much larger M_N. The perturbative stability of this approach is demonstrated by the (roughly) flat K-factor of $K^{\rm NLO} \approx 1.2$ for the semi-inclusive $pp \to N\ell^\pm + 1j$ process, shown in the lower panel of **Figure 8A**. Hence, the artificially large N production cross sections reported in Deppisch et al. [67], Dev et al. [262], and Das et al. [274] can be attributed to a loss of perturbative control over their calculation, not the presence of an enhancement mechanism. Upon the appropriate replacement of M_N, Equation (3.41) holds for other color-singlet processes [255], including mono-jet searches, and is consistent with explicit p_T resummations of high-mass lepton [275] and slepton [277, 278] production.

A characteristic of heavy neutrino production cross sections is that the active-sterile mixing, $|V_{\ell N}|$, factorizes out of the partonic and hadronic scattering expressions. Exploiting this one can define [248] a "bare" cross section σ_0, given by

$$\sigma_0(pp \to N + X) \equiv \sigma(pp \to N + X)/|V_{\ell N}|^2. \tag{3.42}$$

Assuming resonant production of N, a similar expression can be extracted at the N decay level,

$$\sigma_0(pp \to \ell_1^\pm \ell_2^\pm + X) \equiv \sigma(pp \to \ell_1^\pm \ell_2^\pm + X)/S_{\ell_1\ell_2},$$
$$S_{\ell_1\ell_2} = \frac{|V_{\ell_1 N}|^2 |V_{\ell_2 N}|^2}{\sum_{\ell=e}^{\tau} |V_{\ell N}|^2}. \tag{3.43}$$

These definitions, which hold at all orders in α_s [255, 275], allow one to make cross section predictions and comparisons independent of a particular flavor model, including those that largely conserve lepton number, such as the inverse and linear Seesaws. It also allows for a straightforward reinterpretation of limits on collider cross sections as limits on $S_{\ell_1\ell_2}$, or $|V_{\ell N}|$ with additional but generic assumptions. An exception to this factorizablity is the case of nearly degenerate neutrinos with total widths that are comparable to their mass splitting [228, 249, 279, 280].

Figure 8 shows a comparison of the leading, single N hadronic production cross sections, divided by active-heavy mixing $|V_{\ell N}|^2$, as a function of (a) heavy neutrino mass M_N at $\sqrt{s} = 14$ [255] and (b) collider energy $\sqrt{s}$ up to 100 TeV for $M_N = 500$, 1000 GeV [259]. The various accuracies reported reflect the maturity of modern Seesaw calculations. Presently, state-of-the-art predictions for single N production modes are automated up to NLO+PS in QCD for the Drell-Yan and VBF channels [255, 281], amongst others, and known up to N^{3}LL(threshold) for the gluon fusion channel [259]. With Monte Carlo packages, predictions are available at LO with multi-leg merging (MLM) [251, 255, 282, 283] as well as up to NLO with parton shower matching and merging [255, 283]. The NLO accurate [284], `HeavyNnlo` universal FeynRules object (UFO) [285] model file is available from Degrande et al. [255, 283]. Model files built using `FeynRules` [285–287] construct and evaluate L-violating currents following the Feynman rules convention of Denner et al. [288]. A brief comment is needed regarding choosing MLM+PS or NLO+PS computations: To produce MLM Monte Carlo samples, one must sum semi-inclusive channels with successively higher leg multiplicities in accordance with Equations (3.39)–(3.41) and correct for phase space double-counting. However, such MLM samples are formally LO in $\mathcal{O}(\alpha_s)$ because of missing virtual corrections. NLO+PS is formally more accurate, under better perturbative control, and thus is recommended for modeling heavy N at colliders. Such computations are possible with modern, general-purpose event generators, such as Herwig [289], MadGraph5_aMC@NLO [290], and Sherpa [291].

At the 13 and 14 TeV LHC, heavy N production is dominated by charged-current mechanisms for phenomenologically relevant mass scales, i.e., $M_N \lesssim 700$ GeV [254]. At more energetic colliders, however, the growth in the gluon-gluon luminosity increases the $gg \to N\nu$ cross section faster than the CC DY channel. In particular, at $\sqrt{s} = 20 - 30$ TeV, neutral-current mechanisms surpass charged-current modes for heavy

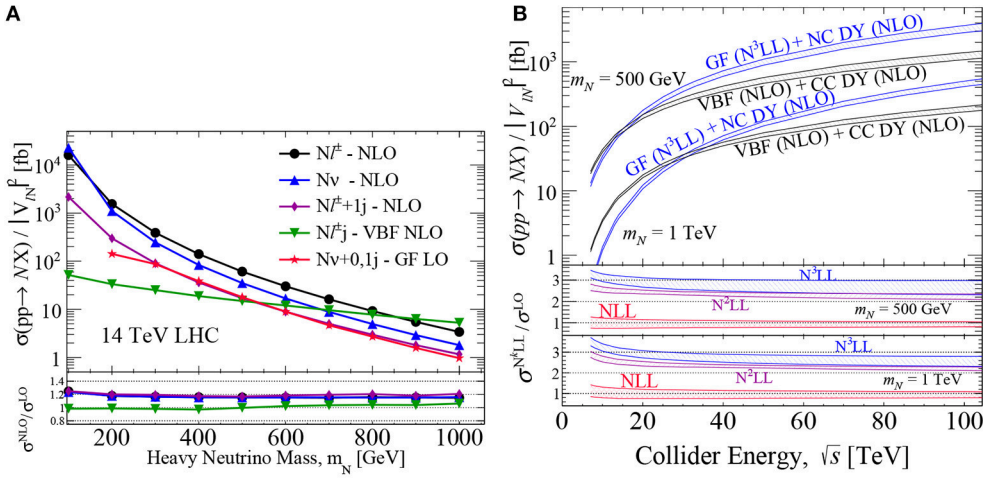

FIGURE 8 | Heavy neutrino (N) hadron collider production cross sections, divided by active-heavy mixing $|V_{\ell N}|^2$, for various production modes as a function of **(A)** N mass at $\sqrt{s} = 14$ [255] and **(B)** collider energy for representative M_N (band thickness corresponds to residual scale uncertainty) [259].

N production with $M_N = 500 - 1000$ GeV [259]. As seen in the sub-panel of **Figure 8A**, NLO in QCD contributions only modify inclusive, DY-type cross section normalizations by +20 to +30% and VBF negligibly, indicating that the prescriptions of Degrande et al. [255] are sufficient to ensure perturbative control over a wide-range of scales. One should emphasize that while VBF normalizations do not appreciably change under QCD corrections [292], VBF kinematics do change considerably [255, 293–295]. The numerical impact, however, is observable-dependent and can be large if new kinematic channels are opened at higher orders of α_s. In comparison to this, the sub-panel of **Figure 8B** shows that QCD corrections to gluon fusion are huge (+150 to +200%), but convergent and consistent with SM Higgs, heavy Higgs, and heavy pseudoscalar production [296–298]; for additional details, see Ruiz et al. [259].

With these computational advancements, considerable collider sensitivity to L-violating processes in the Type I Seesaw has been reached. In **Figure 9** is the expected sensitivity to active-sterile neutrino mixing via the combined CC DY+VBF channels and in same-sign $\mu^\pm\mu^\pm + X$ final-state. With $\mathcal{L} = 1$ ab^{-1} of data for $M_N > M_W$ at $\sqrt{s} = 14$ (100) TeV, one can exclude at 2σ $S_{\mu\mu} \approx |V_{\mu N}|^2 \gtrsim 10^{-4}$ (10^{-5}) [254]. This is assuming the 2013 Snowmass benchmark detector configuration for $\sqrt{s} = 100$ TeV [299]. Sensitivity to the $e^\pm e^\pm$ and $e^\pm\mu^\pm$ channels is comparable, up to detector (in)efficiencies for electrons and muons. As shown in **Figure 10**, with $\mathcal{L} \approx 20$ fb^{-1} at 8 TeV, the ATLAS and CMS experiments have excluded at 95% CLs $|V_{\ell N}|^2 \gtrsim 10^{-3} - 10^{-1}$ for $M_N = 100 - 450$ GeV [48–52]. For heavier M_N, quarks from the on-shell W boson decay can form a single jet instead of the usual two-jet configuration. In such cases, well-known "fat jet" techniques can be used [300, 301]. Upon discovery of L-violating processes involving heavy neutrinos, among the most pressing quantities to measure are N's chiral couplings to other fields [87, 257], its flavor structure [129, 228, 230, 256], and a potential determination if the signal is actually made of multiple, nearly degenerate N [105, 229].

3.2.3. High-Mass Heavy Neutrinos at *ep* Colliders

Complementary to searches for L violation in pp collisions are the prospects for heavy N production at ep deeply inelastic scattering (DIS) colliders [183, 302–309], such as proposed Large Hadron-electron Collider (LHeC) [310], or a μp analog [304]. As shown in **Figure 10**, DIS production of Majorana neutrinos can occur in multiple ways, including (a) W exchange and (b) $W\gamma$ fusion. For treatment of initial-state photons from electron beams, see Frixione et al. [311]. Search strategies for Majorana neutrinos at DIS experiments typically rely on production via the former since $e\gamma \to NW$ associated production can suffer from large phase space suppression, especially at lower beam energies. On the other hand, at higher beam energies, the latter process can provide additional polarization information on N and its decays [183].

At DIS facilities, one usually searches for L violation by requiring that N decays to a charged lepton of opposite sign from the original beam configuration, i.e.,

$$\ell_1^\pm\, q_i \to N\, q_f, \quad \text{with} \quad N \to \ell_2^\mp W^\pm \to \ell_2^\mp\, q\, \overline{q'}, \qquad (3.44)$$

which is only possible of N is Majorana and is relatively free of SM backgrounds: As in the pp case, the existence of a high-p_T charged lepton without accompanying MET (at the partonic level) greatly reduces SM backgrounds. At the hadronic level, this translates to requiring one charged lepton and three high-p_T jets: two that arise from the decay of N, which scale as $p_T^j \sim M_N/4$, and the third from the W exchange, which scales as $p_T^j \sim M_W/2$. However, it was recently noted [312] that tagging this third jet is not necessary to reconstruct and identify the heavy neutrino, and that a more inclusive search may prove more sensitive. Although Equation (3.44) represents the so-called "golden channel," searches for $N \to Z/h + \nu$ decays, but

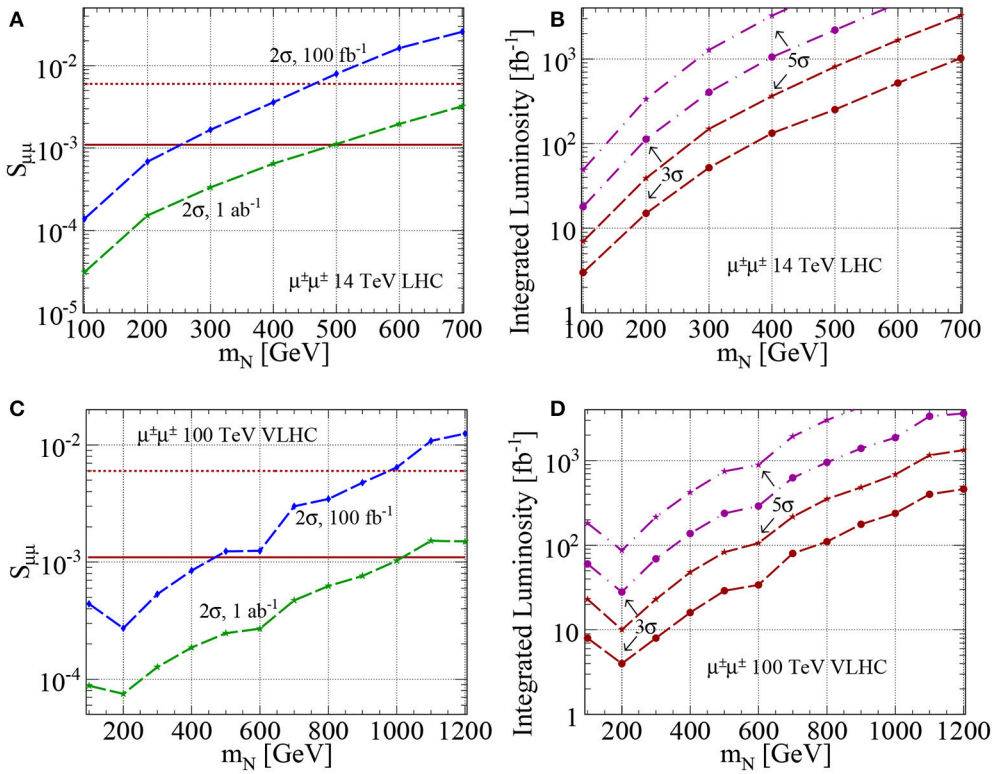

FIGURE 9 | At 14 TeV and as a function of M_N, **(A)** the 2σ sensitivity to $S_{\ell\ell'}$ for the $pp \to \mu^{\pm}\mu^{\pm} + X$ process. **(B)** The required luminosity for a 3 (dash-circle) and 5σ (dash-star) discovery in the same channel **(C,D)** Same as **(A,B)** but for 100 TeV [254].

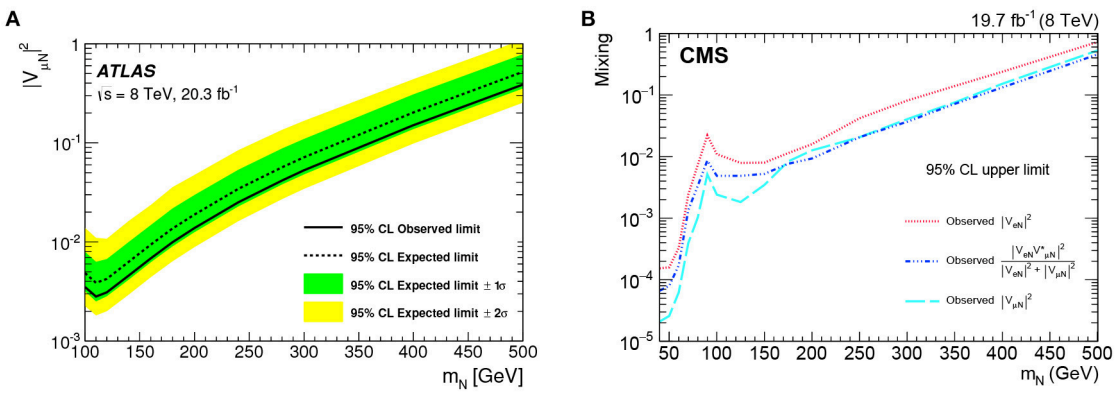

FIGURE 10 | 8 TeV LHC limits on neutrino mixing $|V_{\ell N}|^2$ from searches for $pp \to \ell_1^{\pm}\ell_2^{\pm} + nj$ at **(A)** ATLAS [52] and **(B)** CMS [50] with $\mathcal{L} \approx 20$ fb^{-1} of data.

which do not manifestly violate lepton number, have also been proposed [308].

While the lower beam energies translate to a lower mass reach for M_N, large luminosity targets and relative cleaner hadronic environment result in a better sensitivity than the LHC to smaller active-sterile mixing for smaller neutrino Majorana masses. In **Figure 11**, one sees the expected 90% CL active-sterile mixing $|\theta|^2$ (or $|V_{\ell N}|^2$) sensitivity assuming (c) ep configuration with $E_e = 150$ GeV and (d) μp configuration with $E_\mu = 2$ TeV. For $\mathcal{L} \sim \mathcal{O}(100)$ fb^{-1}, one can probe $|V_{\ell N}|^2 \sim 10^{-5} - 10^{-3}$ for $M_N = 250 - 750$ GeV [304].

3.2.4. Heavy Neutrinos and U(1)$_X$ Gauge Extensions at Colliders

Due to the small mixing between the heavy neutrinos and the SM leptons in minimal Type I Seesaw scenarios, typically of the order $|V_{\ell N}|^2 \sim \mathcal{O}(m_\nu/M_N)$, the predicted rates for collider-scale lepton number violation is prohibitively small. With a new gauge

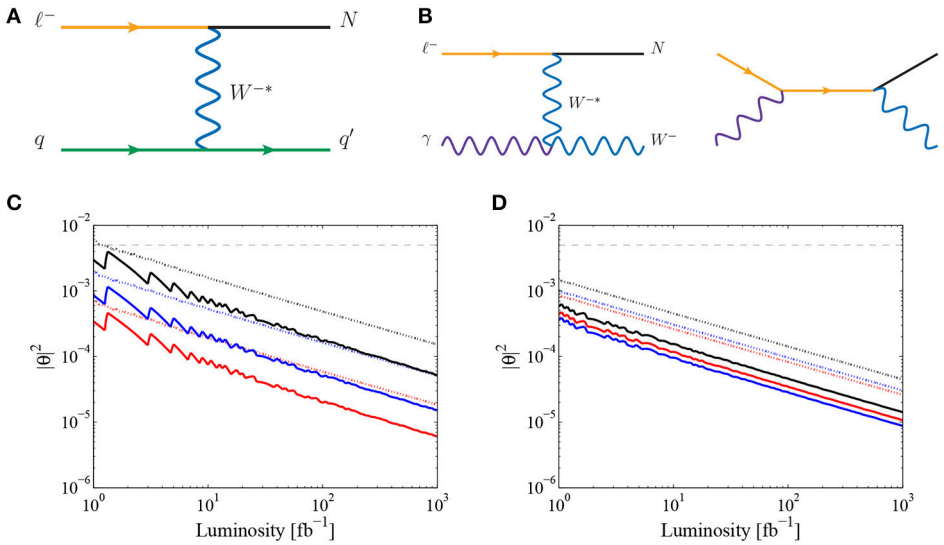

FIGURE 11 | Born diagrams for DIS heavy neutrino (N) production via **(A)** W-exchange and **(B)** $W\gamma$ fusion. 90% CL active-sterile mixing $|\theta|^2$ (or $|V_{\ell N}|^2$) sensitivity vs. integrated luminosity at DIS experiment assuming **(C)** ep configuration with $E_e = 150$ GeV and **(D)** μp configuration with $E_\mu = 2$ TeV; red (blue) [black] line in **(C,D)** correspond to $M_N = 250$ (500) [750] GeV, whereas the solid/dotted lines are the sensitivities with/without cuts [304].

interaction, say, from U(1)$_{B-L}$, the gauge boson $Z' = Z_{BL}$ can be produced copiously in pp and $p\bar{p}$ collisions via gauge interactions in quark annihilation [113, 313–319] and at Linear Colliders in e^+e^- annihilation [317, 320–322],

$$q\bar{q} \to Z' \to NN \quad \text{and} \quad e^+e^- \to Z' \to NN. \tag{3.45}$$

Z_{BL}'s subsequent decay to a pair of heavy Majorana neutrinos may lead to a large sample of events without involving the suppression from a small active-sterile mixing angles [93, 323–330]. As a function of $M_{Z_{BL}}$, **Figure 12A** shows the NLO+NLL(Thresh.) $pp \to Z_{BL} \to \ell^+\ell^-$ production and decay rate for $\sqrt{s} = 13$ TeV and representative values of coupling g_{BL}. As a function of Majorana neutrino mass M_{N_1}, **Figure 12B** shows the LO $pp \to Z_{BL} \to NN$ production and decay rate for $\sqrt{s} = 14$ TeV and 100 TeV and representative $M_{Z_{BL}}$. As N is Majorana, the mixing-induced decays modes $N \to \ell^\pm W^\mp, \nu Z, \nu h$ open for $M_{N_1} > M_W, M_Z, M_h$, respectively. Taking these into account, followed by the leptonic and/or hadronic decays of W, Z and h, the detectable signatures include the lepton number violating, same-sign dileptons, $NN \to \ell^\pm\ell^\pm W^\mp W^\mp \to \ell^\pm\ell^\pm + nj$ [93, 301]; final states with three charged leptons, $\ell^\pm\ell^\pm\ell^\mp + nj$+MET [325, 330, 331]; and four-charged lepton, $\ell^\pm\ell^\pm\ell^\mp\ell^\mp$+MET [324, 332]. Assuming only third generation fermions charged under $B - L$ symmetry, HL-LHC can probe Z' mass up to 2.2 TeV and heavy neutrino mass in the range of $0.2 - 1.1$ TeV as shown in **Figure 13** [301].

For super-heavy Z_{BL}, *e.g.*, $M_{Z_{BL}} \gtrsim 5$ TeV $\gg M_N$, one should note that at the 13 TeV LHC, a nontrivial contribution of the total $pp \to Z_{BL} \to NN$ cross section comes from the kinematical threshold region, where the (NN) system's invariant mass is near $m_{NN} \sim 2M_N$ and Z^*_{BL} is far off-shell. This implies that the L-violating process $pp \to NN \to \ell^\pm\ell^\pm + nj$ can still proceed despite Z_{BL} being kinematically inaccessible [163]. For more details, see section 3.2.6. Additionally, for such heavy Z_{BL} that are resonantly produced, the emergent N are highly boosted with Lorentz factors of $\gamma \sim M_{Z_{BL}}/2M_N$. For $M_N \ll M_{Z_{BL}}$, this leads to highly collimated decay products, with separations scaling as $\Delta R \sim 2/\gamma \sim 4M_N/M_{Z_{BL}}$, and eventually the formation of lepton jets [225, 333], i.e., collimated clusters of light, charged leptons and electromagnetic radiation, and neutrino jets [141, 301, 312, 334], i.e., collimated clusters of electromagnetic and hadronic activity from decays of high-p_T heavy neutrinos.

Leading Order-accurate Monte Carlo simulations for tree-level processes involving Z' bosons and heavy neutrinos in $U(1)_X$ theories are possible using the `SM+B-L` FeynRules UFO model [325, 335, 336]. At NLO+PS accuracy, Monte Carlo simulations can be performed using the `Effective LRSM at NLO in QCD` UFO model [312, 337], and, for light, long-lived neutrinos and arbitrary Z' boson couplings, the `SM + W' and Z' at NLO in QCD` UFO model [338, 339].

In $B - L$ models, heavy neutrino pairs can also be produced through the gluon fusion process mediated by the two H_1 and H_2 [330, 340–342], and given by

$$gg \to H_1, H_2 \to NN. \tag{3.46}$$

For long-lived heavy neutrinos with $M_N \lesssim 200$ GeV, this process becomes important compared to the channel mediated by Z'. **Figure 14A** shows that for $M_{H_2} < 500$ GeV, $M_N < 200$ GeV, and $M_{Z'} = 5$ TeV, the cross section $\sigma(pp \to H_2 \to NN)$ can be above 1 fb at the $\sqrt{s} = 13$ TeV LHC. For $M_N < 60$ GeV, decays of the SM-like Higgs H_1 also contributes to neutrino pair

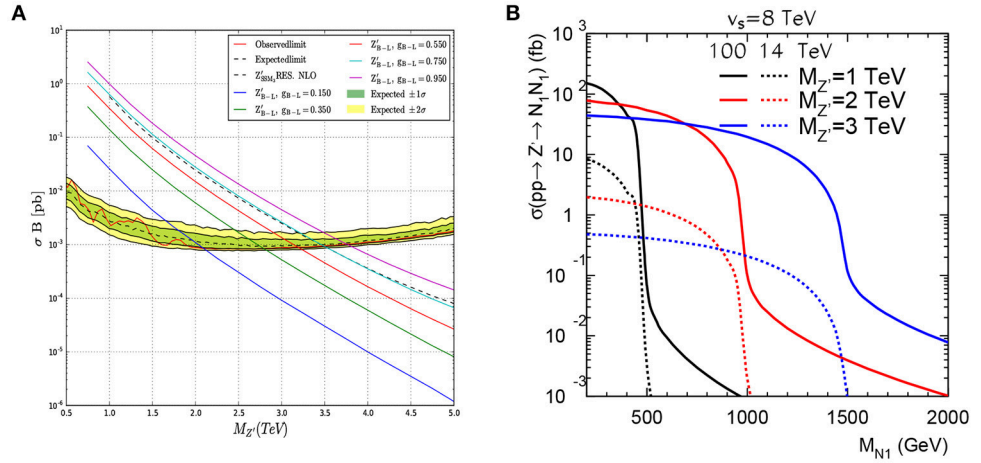

FIGURE 12 | (A) The total cross section of $pp \to Z_{BL} \to \ell^+\ell^-$ as a function of for various representative values of g_{BL} at NLO+NLL(thresh.) for $\sqrt{s} = 13$ TeV [343]. **(B)** The total cross section of $pp \to Z' \to NN$ as a function of M_N for $M_{Z'} = 1, 2, 3$ TeV, $v_S = 8$ TeV, with $\sqrt{s} = 14$ TeV and 100 TeV.

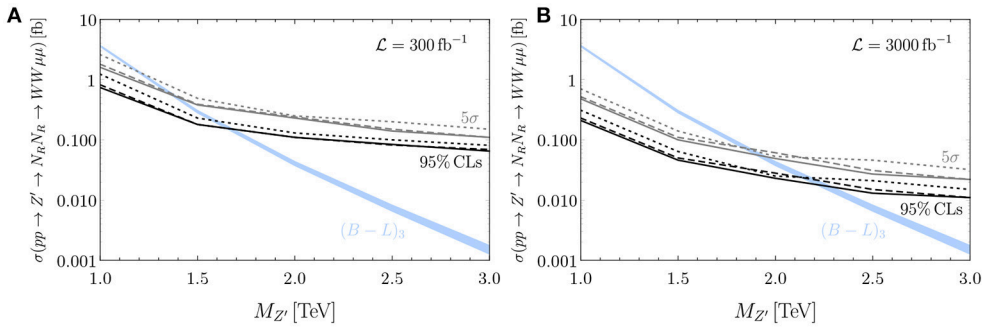

FIGURE 13 | HL-LHC sensitivity for $pp \to Z' \to NN$ with $\sqrt{s} = 14$ TeV for **(A)** $\mathcal{L} = 300$ fb^{-1} and for **(B)** $\mathcal{L} = 3,000$ fb^{-1}, assuming $M_N = M_{Z'}/4$ and $g'_1 = 0.6$ [301].

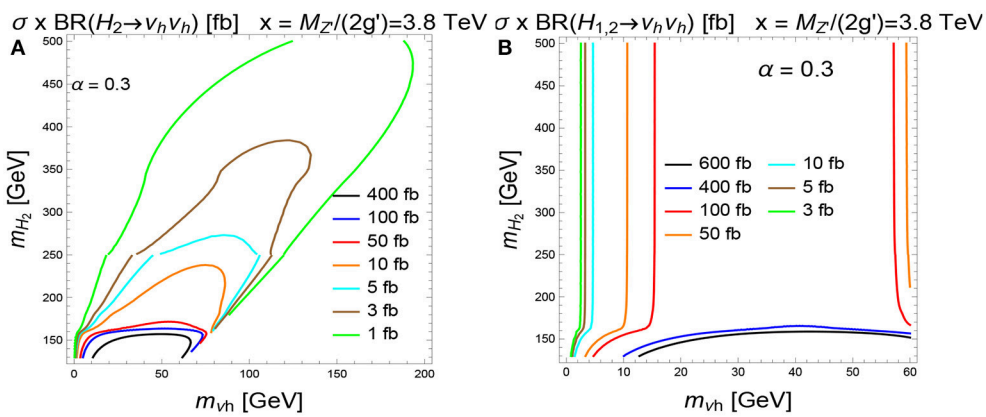

FIGURE 14 | (A) Contour of the cross section for $pp \to H_2 \to NN$ with $\sqrt{s} = 13$ TeV in the plane of M_{H_2} vs. M_N for $M_{Z'} = 5$ TeV and $g'_1 = 0.65$; **(B)** the same but for $pp \to H_1, H_2 \to NN$ with $\sqrt{s} = 13$ TeV and $M_N < M_W$ [330].

production. Summing over the contributions via H_1 and H_2 the total cross section can reach about 700 fb for $M_{H_2} < 150$ GeV as shown in **Figure 14B**.

Owing to this extensive phenomenology, collider experiments are broadly sensitive to Z' bosons from U(1)$_{BL}$ gauge theories. For example: Searches at LEP-II have set the lower bound

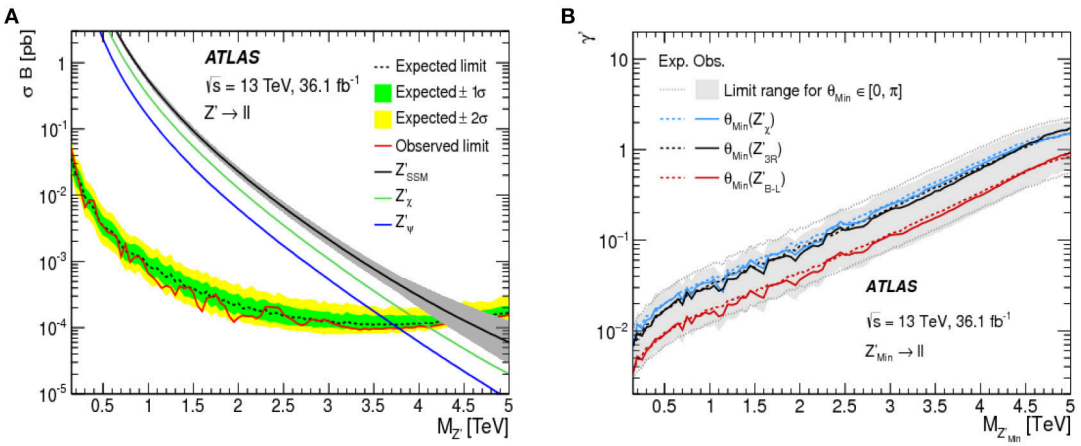

FIGURE 15 | (A) Exclusion limit on $pp \to Z' \to \ell^+\ell^-$ by ATLAS at $\sqrt{s} = 13$ TeV with 36.1 fb^{-1}; **(B)** 13 TeV upper limit at 95% CL on the coupling strength $\gamma' = g_{BL}/g_Z$ as a function of $M_{Z'}$ [344].

$M_{Z'}/g_{BL} \gtrsim 6$ TeV [314]. For more generic Z' (including Z_R in LRSM models), comparable limits from combined LEP+EW precision data have been derived in del Águila et al. [345, 346]. Direct searches for a Z' with SM-like couplings to fermions exclude $M_{Z'} < 2.9$ TeV at 95% CLs by ATLAS [347] and CMS [348] at $\sqrt{s} = 8$ TeV. Z_{BL} gauge bosons with the benchmark coupling $g_1{}' = g_{BL}$ are stringently constrained by searches for dilepton resonances at the LHC, with $M_{Z'} \lesssim 2.1 - 3.75$ TeV excluded at 95% CLs for $g_{BL} = 0.15 - 0.95$, as seen in **Figure 12A** [343]. Searches for Z' decays to dijets at the LHC have exclude $M_{Z'} < 1.5 - 3.5$ TeV for $g_{BL} = 0.07 - 0.27$ [349, 350]. **Figure 15A** shows that ATLAS excludes $M_{Z'} < 4.5$ TeV at $\sqrt{s} = 13$ TeV. Further constraints are given in the plane of coupling strength $\gamma' = g_{BL}/g_Z$ vs. $M_{Z'}$ by ATLAS at $\sqrt{s} = 13$ TeV with 36.1 fb^{-1} [344] as shown in the lower curve of **Figure 15B**. For $\sqrt{s} = 27$ TeV, early projections show that with $\mathcal{L} = 1$ (3) ab^{-1}, $M_{Z'} \lesssim 19$ (20) TeV can be probed in the dijet channel [351].

3.2.5. Heavy Neutrinos and the Left-Right Symmetric Model at Colliders

In addition to the broad triplet scalar phenomenology discussed later in section 4.2, the LRSM predicts at low scales massive $W_R^\pm$ and Z_R gauge bosons that couple appreciably to SM fields as well as to heavy Majorana neutrinos N. The existence of these exotic states leads to a rich collider phenomenology that we now address, focusing, of course, on lepton number violating final states. The collider phenomenology for Z_R searches is very comparable to that for Z' gauge bosons in U(1)$_X$ theories [93, 323–330], and thus we refer readers to section 3.2.4 for more generic collider phenomenology.

In the LRSM, for $M_N < M_{W_R}$ or $M_N < M_{Z_R}/2$, the most remarkable collider processes are the single and pair production of heavy Majorana neutrinos N through resonant charged and neutral SU(2)$_R$ currents,

$$q\overline{q'} \to W_R^\pm \to N_i\,\ell^\pm \quad \text{and} \quad q\overline{q'} \to Z_R \to N_i\,N_j. \tag{3.47}$$

As first observed in Keung and Senjanović [240], N_i can decay into L-violating final-states, giving rise to the collider signatures,

$$\begin{aligned} pp \to W_R^\pm \to N_i\,\ell^\pm \to \ell_1^\pm\,\ell_2^\pm + nj \quad \text{and} \\ pp \to Z_R \to N_i\,N_j \to \ell_1^\pm\,\ell_2^\pm + nj. \end{aligned} \tag{3.48}$$

In the minimal/manifest LRSM, the decay of N_i proceeds primarily via off-shell three-body right-handed currents, as shown in **Figure 16A**, due to mixing suppression to left-handed currents. In a generic LRSM scenario, the naïve mixing suppression of $|V_{\ell N}|^2 \sim \mathcal{O}(m_\nu/M_N)$ is not guaranteed due to the interplay between the Types I and II Seesaws, e.g., as in Anamiati et al. [228] and Das et al. [230]. (However, heavy-light neutrino mixing in the LRSM is much less free than in pure Type I scenarios due to constraints on Dirac and RH masses from LR parity; see section 3.1.4 for more details). Subsequently, if $|V_{\ell N}|$ is not too far from present bounds (see e.g., [91]), then decays of N_i to on-shell EW bosons, as shown in **Figure 16B**, can occur with rates comparable to decays via off-shell W_R^* [87]. The inverse process [352], i.e., N_i production via off-shell EW currents and decay via off-shell RH currents as well as vector boson scattering involving t-channel W_R and Z_R bosons [353] are in theory also possible but insatiably phase space-suppressed. For $M_N > M_{W_R}, M_{Z_R}$, resonant N production via off-shell SU(2)$_R$ currents is also possible, and is analogous to the production through off-shell, SU(2)$_L$ currents in Equations (3.33)–(3.34). As M_{W_R}, M_{Z_R} are bound to be above a few-to-several TeV, the relevant collider phenomenology is largely the same as when $M_N < M_{W_R}, M_{Z_R}$ [144], and hence will not be individually discussed.

Aside from the mere possibility of L violation, what makes these channels so exceptional, if they exist, are their production rates. Up to symmetry-breaking corrections, the RH gauge coupling is $g_R \approx g_L \approx 0.65$, which is not a small number. In **Figure 17**, we show for $\sqrt{s} = 13$ and 100 TeV the production rate for resonant W_R at various accuracies as a function of mass [141]; rates for Z_R are marginally smaller due to slight coupling

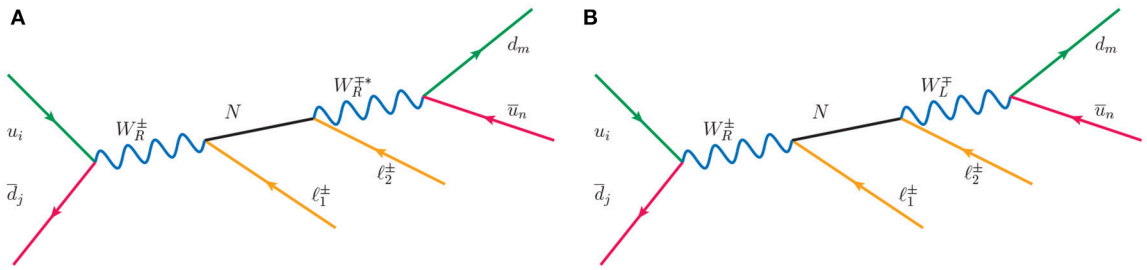

FIGURE 16 | Born-level diagrams depicting resonant W_R, N production and decay to same-sign leptons in LRSM via **(A)** successive right-handed currents and **(B)** mixed right- and left-handed currents.

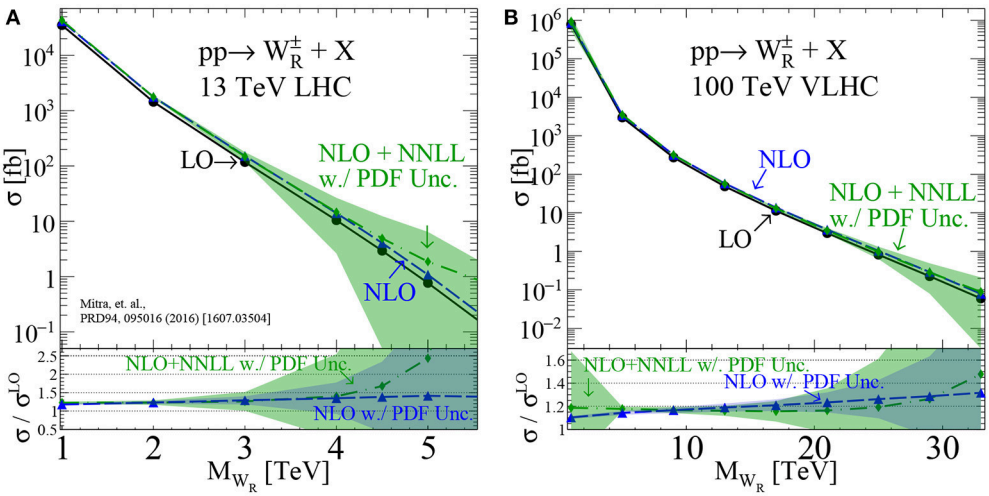

FIGURE 17 | Upper panel: As a function of M_{W_R}, $pp \to W_R$ production cross section for $\sqrt{s}$ = **(A)** 13 and **(B)** 100 TeV, at LO (solid), NLO (dash), and NLO+NNLL (dash-dot) with 1σ PDF uncertainty (shaded); Lower: NLO (dash) and NLO+NNLL (dash-dot) K-factors and PDF uncertainties [141].

suppression. As in other Seesaw scenarios, much recent progress has gone into advancing the precision of integrated and differential predictions for the LRSM: The inclusive production of W_R and Z_R are now known up to NLO+NNLL(Thresh) [141], automated at NLO+NLL(Thresh+k_T) [354, 355], automated at NNLO [356, 357], and differentially has been automated at NLO with parton shower matching for Monte Carlo simulations [312]. For $\sqrt{\tau_0} = M_{W_R/Z_R}/\sqrt{s} \gtrsim 0.3$, threshold corrections become as large as (N)NLO corrections, which span roughly +20% to +30%, and have an important impact cross section normalizations [141, 358]. For example: The inclusive W_R cross section at LO (NLO+NNLL) for $M_{W_R} = 5$ TeV is $\sigma \sim 0.7$ (1.7) fb. After $\mathcal{L} = 1\,\text{ab}^{-1}$ and assuming a combined branching-detection efficiency-selection acceptance of BR$\times\varepsilon\times\mathcal{A} = 2\%$, the number of observed events is $N \sim 14$ (34). For simple Gaussian statistics with a zero background hypothesis, this is the difference between a 6σ "discovery" and 4σ "evidence". Clearly, the HL-LHC program is much more sensitive to ultra-high-mass resonances than previously argued.

For the collider processes in Equation (3.48), such estimations of branching, acceptance/selection, and background rates resemble actual rates: see, e.g., [87, 141, 240, 352, 353, 359–361]. For $M_{W_R}, M_{Z_R} \gg M_N$, one finds generically that BR($W_R \to \ell^{\pm} N_i$) $\sim 1/(1+3N_c) \sim \mathcal{O}(10\%)$, BR($Z_R \to N_i N_j$) $\sim \mathcal{O}(10\%)$, and, for the lightest heavy N_i in this limit, BR($N_1 \to \ell^{\pm} X$) $\sim \mathcal{O}(100\%)$. Trigger rates for multi-TeV, stable charged leptons (e, μ) at ATLAS and CMS exceed 80–95%, but conversely, the momentum resolution for such energetic muons begins to degrade severely; for additional information, see Aad et al. [52], Collaboration [362], Khachatryan [363, 364] and references therein. As in searches for Majorana neutrinos in the previous Type I-based scenarios, the final-states in Equation (3.48) possess same-sign, high-p_T charged leptons without accompanying MET at the partonic level [240, 248, 359]. For the LRSM, this is particularly distinct since the kinematics of the signal process scale with the TeV-scale W_R and Z_R masses. Accordingly, top quark and EW background processes that can mimic the fiducial collider definition correspondingly must carry *multi*-TeV system invariant masses, and are inherently more phase space suppressed than the signal processes at the LHC [359]. Consequently, so long as $M_N \lesssim M_{W_R}, M_{Z_R} \ll \sqrt{s}$, s-channel production of W_R and Z_R remains the most promising

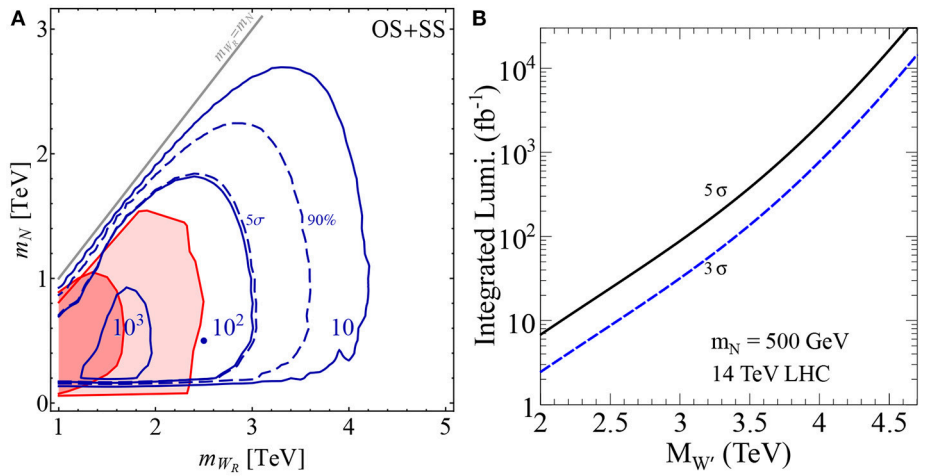

FIGURE 18 | Discovery potential at 14 TeV LHC of W_R and N in **(A)** the minimal LRSM as in **Figure 16A** after $\mathcal{L} = 30$ fb^{-1} [360] and **(B)** the agnostic mixing scenario as in **Figure 16B** [87].

mechanism for discovering L violation in the LRSM at hadron colliders. In **Figure 18** we show the discovery potential at 14 TeV LHC of W_R and N in (a) the minimal LRSM as in **Figure 16A** after $\mathcal{L} = 30$ fb^{-1} [360] and (b) the agnostic mixing scenario as in **Figure 16B** [87]. Final-states involving τ leptons are also possible, but inherently suffer from the difficult signal event reconstruction and larger backgrounds due to partonic-level MET induced by τ decays [365].

Unfortunately, direct searches at the $\sqrt{s} = 7/8$ TeV LHC via the DY channels have yielded no evidence for lepton number violating processes mediated by W_R and Z_R gauge bosons from the LRSM [52, 300, 363, 366]. As shown in **Figure 19**, searches for W_R/Z_R in the $e^\pm e^\pm + nj$ and $\mu^\pm\mu^\pm + nj$ final state have excluded, approximately, $M_{W_R/Z_R} \lesssim 1.5 - 2.5$ TeV and $M_N \lesssim 2$ TeV. However, sensitivity to the $e^\pm e^\pm + nj$ greatly diminishes for $M_N \ll M_{W_R/Z_R}$.

Interestingly, for $M_N \ll M_{W_R}, M_{Z_R}$, decays of N become highly boosted and its decay products, i.e., $\ell_2^\pm q\overline{q'}$, become highly collimated. In such cases, the isolation criterion for electrons (and some muons) in detector experiments fail, particularly when $\sqrt{r} = M_N/M_{W_R} < 0.1$ [52, 87, 141, 359]. Instead of requiring the identification of two well-isolated charged leptons for the processes given in Equation (3.48), one can instead consider the N-decay system as a single, high-p_T *neutrino jet* [141, 312]. The hadronic-level collider signature is then

$$pp \to W_R \to \ell^\pm N \to \ell^\pm j_N, \tag{3.49}$$

where the neutrino jet j_N is comprised of three "partons", $(\ell_2, q, \overline{q'})$, with an invariant mass of $m_j \sim M_N$. (Neutrino jets are distinct from so-called "lepton jets" [225], which are built from collimated charged leptons and largely absent of hadrons). This alternative topology for $M_N \ll M_{W_R}$ recovers the lost sensitivity of the same-sign dilepton final state, as seen in **Figure 20**. Inevitably, for N masses below the EW scale, rare L-violating decay modes also of SM particles open. In particular, for M_N below the top quark mass m_t, one has the rare decay mode, $t \to bW_R^{+*} \to b\ell_1^+ N \to b\ell_1^+\ell_2^\pm q\overline{q'}$ [220]. Such processes, however, can be especially difficult to distinguish from rare SM processes, e.g., $t \to Wb\ell^+\ell^-$ [367], particularly due to the large jet combinatorics.

For too small M_N/M_{W_R} ratio, the lifetime for N, which scales as $\tau_N \sim M_{W_R}^4/M_N^5$, can become quite long. In such instances, the decays of N are no longer prompt and searches for $pp \to W_R \to N\ell$ map onto searches for Sequential Standard Model W' bosons [338, 368]. Likewise, searches for L-violating top quark decays become searches for RH currents in $t \to b\ell p_T$ decays. For intermediate lifetimes, displaced vertex searches become relevant [223, 228, 230, 334, 369].

Another recent avenue of exploration is the reassessment for resonant production of W_R and Z_R in Equation (3.48). In the limit where $M_{W_R} \gtrsim \sqrt{s}$ but $M_N \ll \sqrt{s}$, resonant production of N, and hence a lepton number violating final state, is still possible despite W_R being kinematically inaccessible [163]. In such cases, N is produced near mass threshold with $p_T^N \sim M_N$ instead of the usual $p_T^N \sim M_{W_R}/2$. The same-sign leptons discovery channel is then kinematically and topologically identical to Type I Seesaw searches, and hence is actively searched for at the LHC, despite this kinematic regime not being well-studied in the literature. Reinterpretation of observed and expected sensitivities at the 14 and 100 TeV LHC are shown in **Figure 21**. One sees that with the anticipated cache of LHC data, $M_{W_R} \lesssim 9$ TeV can be excluded for $M_N \lesssim 1$ TeV.

In addition to the aforementioned DY and VBF channels, there has been recent attention [312, 353, 370, 371] given to the production of LRSM scalar and vector bosons in association with heavy flavor quarks, e.g.,

$$g\,\overset{(-)}{b} \to \overset{(-)}{t}\,W_R^\pm \text{ or } \overset{(-)}{t}\,H_R^\pm \quad \text{and} \quad gg \to t\bar{t}Z_R \text{ or } t\bar{t}H_R^0. \tag{3.50}$$

As in the SM, such processes are critical in measuring the couplings of gauge bosons to quarks as well as determining

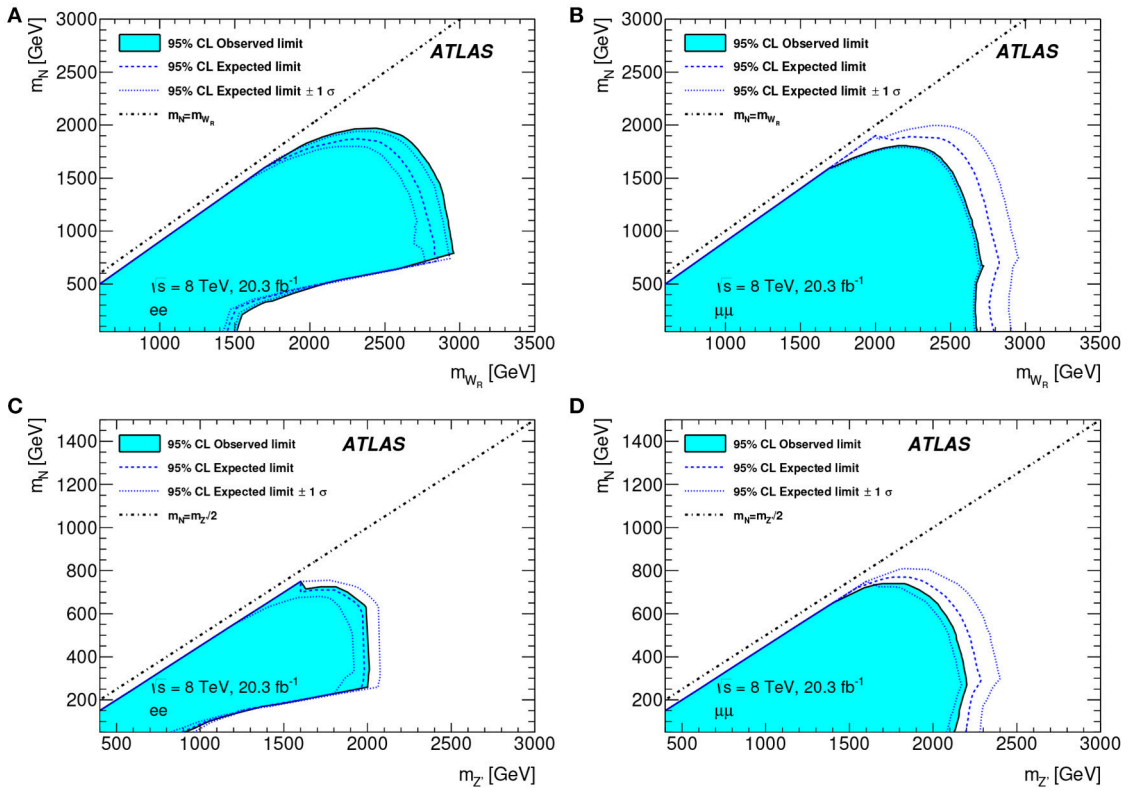

FIGURE 19 | 95% CL exclusion of the (M_V, M_N) parameter space by the ATLAS experiment at $\sqrt{s} = 8$ for $V = W_R$ **(Top)** and $V = Z_R$ **(Bottom)** production in the (L) $e^{\pm}e^{\pm} + nj$ and (R) $\mu^{\pm}\mu^{\pm} + nj$ final state [52].

heavy flavor PDFs. However, also as in the SM, care is needed in calculating the rates of these processes when $M_R \gg m_b,\ m_t$. Here, M_R is generically the mass of the RH scalar or vector boson. As discussed just after Equation (3.38), it has been noted recently in Mattelaer et al. [312] that such associated processes possess logarithmic dependence on the outgoing top quarks' kinematics, i.e., that the inclusive cross section scales as $\sigma \sim \alpha_s^k \log^{2k-1}\left(M_R^2/(m_t^2 + p_T^{t\,2})\right)$. Subsequently, for $M_R \gtrsim 1 - 2$ TeV, these logarithms grow numerically large since $\log^2(M_R^2/m_t^2) \gtrsim 1/\alpha_s$ and can spoil the perturbativity convergence of fixed order predictions. For example, the (N)NLO K-factor of $K^{(\mathrm{N})\mathrm{NLO}} \gtrsim 1.6 - 2.0$ claimed in Dev et al. [353] indicate a loss of perturbative control, not an enhancement, and leads to a significant overestimation of their cross sections. As in the case of EW boson production in association with heavy flavors [372, 373], the correct treatment requires either a matching/subtraction scheme with top quark PDFs to remove double counting of phase space configurations [374, 375] or kinematic requirements on the associated top quarks/heavy quark jets, e.g., Equation (3.41) [255].

In all of these various estimates for discovery potential, it is important to also keep in mind what can be learned from observing L violation and LR symmetry at the LHC or a future collider, including ep machines [312, 376–382]. Primary goals post-discovery include: determination of W_R and Z_R chiral coupling to fermions [87, 129, 383], which can be quantified for quarks and leptons independently [87], determination of the leptonic and quark mixing [129, 130, 228, 230, 384–387], as well as potential CP violation [228, 230, 386–388]. We emphasize that the discovery of TeV-scale LRSM could have profound implications on high-scale baryo- and leptogenesis [10, 389–392] as well as searches for $0\nu\beta\beta$ [129, 162, 385, 393, 394]. The latter instance is particularly noteworthy as the relationship between m_ν^{ee} and m_{ν_1} in the LRSM is different because of the new mediating fields [385].

We finish this section by noting our many omissions, in particular: supersymmetric extensions of the LRSM, e.g., Frank and Saif [395], and Demir et al. [396]; embeddings into larger internal symmetry structures, e.g., Goh and Krenke [361] and Appelquist and Shrock [397]; as well as generic extensions with additional vector-like or mirror quarks, e.g., Goh and Krenke [361], and de Almeida et al. [398]. While each of these extensions have their phenomenological uniquenesses, their collider signatures are broadly indistinguishable from the minimal LRSM scenario. With regard to Type I-based Seesaws in extra dimensional frameworks, it is worthwhile to note that it has recently [399–401] been observed that in warped five-dimensional models, a more careful organization of Kaluza-Klein states and basis decomposition results in an inverse Seesaw mechanism as opposed to a canonical Type I-like Seesaw

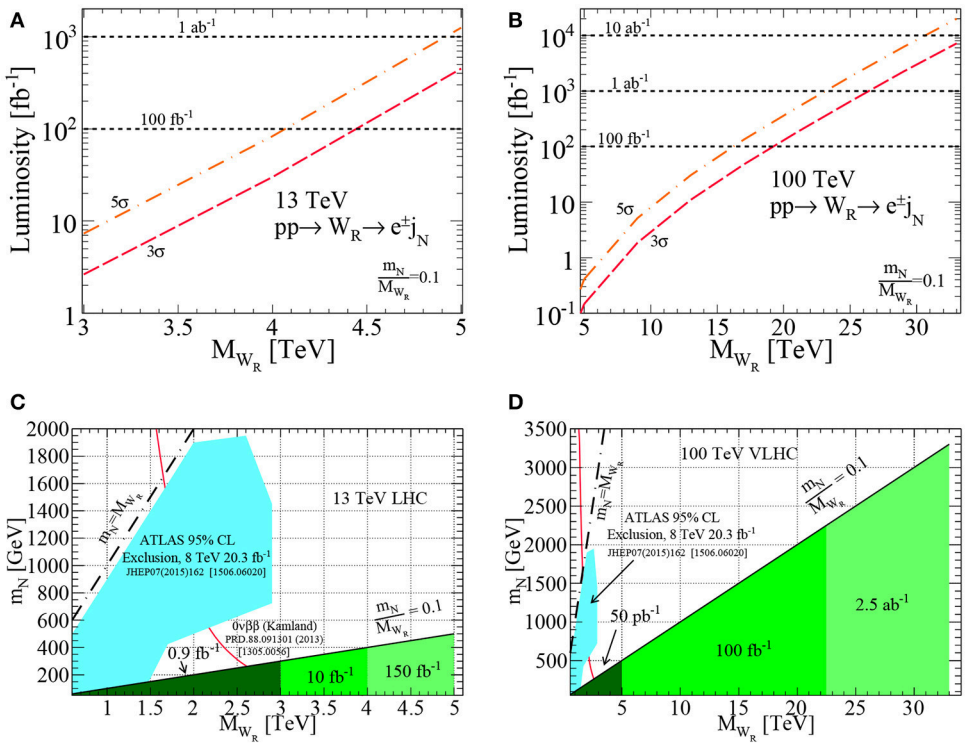

FIGURE 20 | Discovery **(A,B)** and 95% CL exclusion **(C,D)** potential of neutrino jet searches, i.e., $pp \to W_R \to e^{\pm} j_N$, at **(A,C)** $\sqrt{s} = 13$ and **(B,D)** 100 TeV. Also shown in **(C,D)**, ATLAS experiment's 8 TeV 95% CL [52] and KamLAND-Zen 90% CL [36, 402] exclusion limits. Figure from Mitra et al. [141].

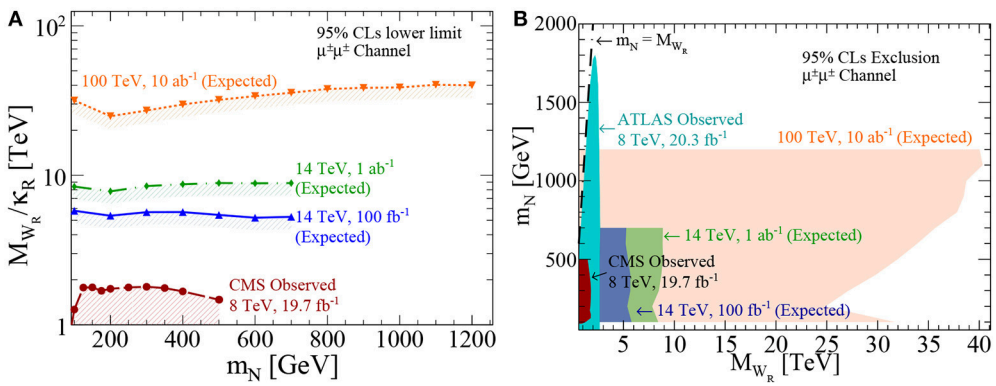

FIGURE 21 | (A) As a function of M_N and for right-left coupling ratio $\kappa_R = g_R/g_L$, the observed 8 TeV LHC 95% CLs lower limit on (M_{W_R}/κ_R) (dash-dot), expected 14 TeV sensitivity with $\mathcal{L} = 100$ fb^{-1} (solid-triangle) and 1 ab^{-1} (dash-dot-diamond), and expected 100 TeV VLHC sensitivity with 10 ab^{-1} (dot-star). **(B)** Observed and expected 95% CL$_s$ sensitivities to the (M_{W_R}, M_N) parameter space for various collider configurations via direct and indirect searches in the $\mu^{\pm}\mu^{\pm}$ final state [163].

mechanism, as conventionally believed. Again, this leads to greatly suppressed L violation at collider experiments.

3.2.6. Heavy Neutrino Effective Field Theory at Colliders

As discussed in section 3.1.5, the production and decay of Majorana neutrinos in colliders may occur through contact interactions if mediating degrees of freedom are much heavier than the hard scattering process scale. Such scenarios have recently become a popular topic [163, 171, 172, 218, 305, 403–406], in part because of the considerable sensitivity afforded by collider experiments. This is particularly true for L-violating final-states in pp collisions, which naturally have small experimental backgrounds. As shown in **Figure 22**, for various operators, searches for L-violating process $pp \to N\ell_1^{\pm} \to \ell_1^{\pm}\ell_2^{\pm} + X$ by the ATLAS and CMS experiments have set wide

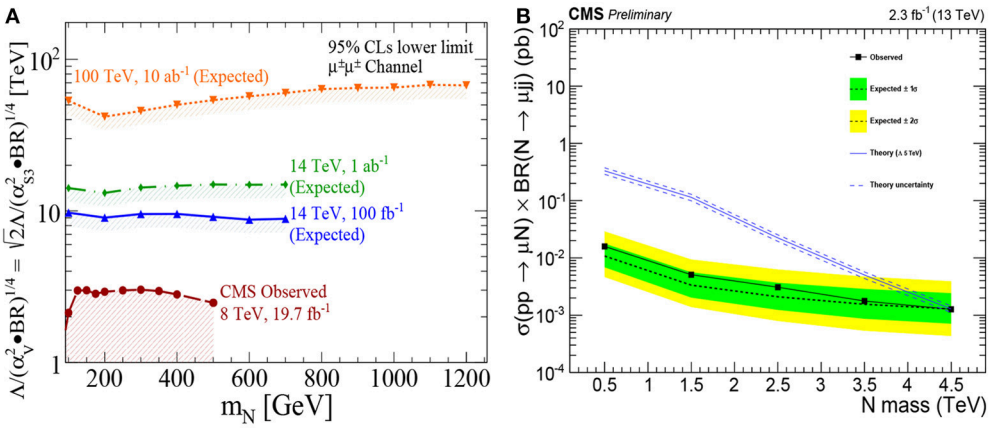

FIGURE 22 | Observed limits and expected sensitivities at current and future hadron collider experiments on NEFT mass scale Λ for **(A)** low-mass [163] and **(B)** high-mass [59] Majorana neutrinos N via the L-violating $pp \to \ell_1^\pm \ell_2^\pm + X$.

limits on the effective mass scale of $\Lambda > 1-5$ TeV for $M_N = 100$ GeV$-$4.5 TeV [59, 163, 403]. Projections for $\sqrt{s} = 14$ (100) TeV after $\mathcal{L} = 1$ (10) ab^{-1} show that $\Lambda \lesssim 9$ (40) TeV can be achieved [163]. These search strategies are also applicable for the more general situation where L violation is mediated entirely via SMEFT operators [176, 177] as introduced in section 3.1.5.

4. THE TYPE II SEESAW AND LEPTON NUMBER VIOLATION AT COLLIDERS

In this section we review lepton number violating collider signatures associated with the Type II Seesaw mechanism [14–18, 407] and its extensions. The Type II model is unique among the original tree-level realizations of the Weinberg operator in that lepton number is spontaneously broken; in the original formulations of the Type I and III Seesaws, lepton number violation is explicit by means of a Majorana mass allowed by gauge invariance. In section 4.1, we summarize the main highlights of the canonical Type II Seesaw and other Type II-based scenarios. We then review in section 4.2 collider searches for lepton number violation mediated by exotically charged scalars ($H^\pm, H^{\pm\pm}$), which is the characteristic feature of Type II-based scenarios.

4.1. Type II Seesaw Models

In the Type II mechanism [14–18, 407], tiny neutrino masses arise through the Yukawa interaction,

$$\Delta\mathcal{L}_{II}^m = -\overline{L^c}\, Y_\nu\, i\sigma_2\, \Delta_L\, L + \text{ H.c.}, \tag{4.1}$$

between the SM LH lepton doublet L, its charge conjugate, and an SU(2)$_L$ scalar triplet (adjoint representation) Δ_L with mass M_Δ and Yukawa coupling Y_ν. More precisely, the new scalar transforms as $(1, 3, 1)$ under the full SM gauge symmetry and possesses lepton number $L = -2$, thereby ensuring that Equation (4.1) conserves lepton number before EWSB. Due to its hypercharge and L assignments, Δ_L does not couple to quarks at tree-level. It does, however, couple to the SM Higgs doublet, particularly through the doublet-triplet mixing operator

$$\Delta\mathcal{L}_{H\Delta_L} \ni \mu H^T\, i\sigma_2\, \Delta_L^\dagger H + \text{ H.c.} \tag{4.2}$$

The importance of this term is that after minimizing the full Type II scalar potential $V_{\text{Type II}}$, Δ_L acquires a small vev v_Δ that in turn induces a LH Majorana mass for SM neutrinos, given by

$$M_\nu = \sqrt{2} Y_\nu v_\Delta \quad \text{with} \quad v_\Delta = \langle \Delta_L \rangle = \frac{\mu v_0^2}{\sqrt{2} M_\Delta^2}. \tag{4.3}$$

In the above, $v_0 = \sqrt{2}\langle H \rangle$ is the vev of the SM Higgs and $v_0^2 + v_\Delta^2 = (\sqrt{2} G_F)^{-1} \approx (246 \text{ GeV})^2$. As a result of $B-L$ being spontaneously broken by Δ_L, tiny 0.1 eV neutrino masses follow from the combination of three scales: μ, v_0, and M_Δ. In addition, after EWSB, there are seven physical Higgses, including the singly and doubly electrically charged $H^\pm$ and $H^{\pm\pm}$ with masses $M_{H^\pm, H^{\pm\pm}} \sim M_\Delta$. As v_Δ contributes to EWSB at tree-level, and hence the EW ρ/T-parameter, v_Δ is constrained by precision EW observables, with present limits placing $v_\Delta \lesssim \mathcal{O}(1 \text{ GeV})$ [408–416]. The impact of triplet scalars on the naturalness of the SM-like Higgs at 125 GeV has also been studied [412, 417, 418]. The simultaneous sensitivity of M_ν to collider, neutrino mass measurement, and neutrino oscillation experiments is one of the clearest examples of their complementarity and necessity to understanding neutrinos physics.

For SM-like Yukawas $Y_\nu \sim 10^{-6} - 1$, one finds that $v_\Delta \sim 0.1\,\text{eV} - 100\,\text{keV}$ are needed in order to reproduce 0.1 eV neutrino masses. Subsequently, for $\mu \sim M_\Delta$, then $M_\Delta \sim \mu \sim 10^8 - 10^{14}$ GeV, and for $\mu \sim v_0$, then $M_\Delta \sim 10^5 - 10^8$ GeV. In either case, these scales are too high for present-day experiments. However, as nonzero μ is associated with both lepton number and custodial symmetry non-conservation, one may expect it to be small [121] and natural, in the t'Hooft sense [419]. Imposing technical naturalness can have dramatic impact on LHC phenomenology: for example, if $\mu \sim 1$ MeV (keV), then

$M_\Delta \sim 10^2 - 10^5$ $(10^1 - 10^4)$ GeV, scales well within the LHC's energy budget. Moreover, this also indicates that proposed future hadron collider experiments [148, 149] will be sensitive to MeV-to-GeV values of the scalar-doublet mixing parameter μ, independent of precision Higgs coupling measurements, which are presently at the 10% level [420]. Assuming Higgs coupling deviations of $\mathcal{O}(\mu/M_h)$, this implies the weak 7/8 TeV LHC limit of $\mu \lesssim \mathcal{O}(10\text{ GeV})$. While not yet competitive with constraints from EW precision data, improvements on Higgs coupling measurements will be greatly improved over the LHC's lifetime.

After decomposition of leptons into their mass eigenstates, the Yukawa interactions of the singly and doubly charged Higgses are

$$\nu_L^T\, C\, \Gamma_+\, H^+\, \ell_L, \quad : \quad \Gamma_+ = \cos\theta_+\, \frac{m_\nu^{diag}}{v_\Delta}\, U^\dagger_{PMNS},\ \theta_+ \approx \frac{\sqrt{2}v_\Delta}{v_0}, \tag{4.4}$$

$$\ell_L^T\, C\, \Gamma_{++}\, H^{++}\, \ell_L \quad : \quad \Gamma_{++} = \frac{M_\nu}{\sqrt{2}v_\Delta} = U^*_{PMNS}\, \frac{m_\nu^{diag}}{\sqrt{2}\, v_\Delta}\, U^\dagger_{PMNS}. \tag{4.5}$$

The constrained neutrino mass matrix $M_\nu = \sqrt{2}v_\Delta \Gamma_{++}$ and squared Yukawa coupling $Y_+^i \equiv \sum_j |\Gamma_+^{ji}|^2 v_\Delta^2$ with vanishing Majorana phases are shown in **Figures 23**, **24** respectively. The results reveal the following mass and Yukawa patterns:

$$M_\nu^{22}, M_\nu^{33} \gg M_\nu^{11}; \quad Y_+^2, Y_+^3 \gg Y_+^1 \qquad \text{for NH;} \tag{4.6}$$

$$M_\nu^{11} \gg M_\nu^{22}, M_\nu^{33}; \quad Y_+^1 \gg Y_+^2, Y_+^3 \qquad \text{for IH.} \tag{4.7}$$

Below $v_\Delta \approx 10^{-4}$ GeV, the doubly charged Higgs $H^{\pm\pm}$ decays dominantly to same-sign lepton pairs. For vanishing Majorana phases $\Phi_1 = \Phi_2 = 0$, we show in **Figures 25**, **26** the branching fraction of the decays into same-flavor and different-flavor leptonic final states, respectively. Relations among the branching fractions of the lepton number violating Higgs decays of both the singly- and doubly-charged Higgs in the NH and IH, with vanishing Majorana phases, are summarized in **Table 2**.

The impact of Majorana phases can be substantial in doubly charged Higgs decays [421, 422]. In the case of the IH, a large cancellation among the relevant channels occurs due to the phase at $\Phi_1 = \pi$. As a result, in this scenario, the dominant channels swap from $H^{++} \to e^+e^+,\ \mu^+\tau^+$ when $\Phi_1 \approx 0$ to $H^{++} \to e^+\mu^+,\ e^+\tau^+$ when $\Phi_1 \approx \pi$, as shown in **Figure 27**. Therefore this qualitative change can be made use of to extract the value of the Majorana phase Φ_1. In the NH case, however, the dependence of the decay branching fractions on the phase is rather weak because of the lack of a subtle cancellation [408].

The Type II mechanism can be embedded in a number of extended gauge scenarios, for example the LRSM as discussed in section 3.1.4, as well as GUTs, such as (331) theories [423–426] and the extensions of minimal SU(5) [427]. For (331) models, one finds the presence of bileptons [428, 429], i.e., gauge bosons with $L = \pm 2$ charges and hence $Q = \pm 2$ electric charges. In a realistic extension of the Georgi-Glashow model, a scalar 15-dimensional representation is added [430] and the scalar triplet stays in the **15** representation together with scalar leptoquark $\Phi \sim (3, 2, 1/6)$. The SU(5) symmetry thus indicates that the couplings of the leptoquark to matter gain the same Yukawas Y_ν responsible for neutrino mass matrix [431]. Extensions with vector-like leptons in nontrivial $SU(2)_L$ representations are also possible [432]. Unsurprisingly, the phenomenology [423, 425, 433–435] and direct search constraints [433, 434] for L-violating, doubly charged vector bosons are similar to L-violating, doubly charged scalar bosons, which we now discuss.

4.2. Triplet Higgs Scalars at Colliders

4.2.1. Triplet Higgs Scalars and the Type II Seesaw at Colliders

If kinematically accessible, the canonical and well-studied [145, 408, 436, 437] triplet scalars production channels at hadron colliders are the neutral and charged current DY processes, given by

$$pp \to \gamma^*/Z^* \to H^{++}H^{--}, \quad pp \to W^{\pm *} \to H^{\pm\pm}H^{\mp}, \tag{4.8}$$

and shown in **Figure 28A**. Unlike Type I models, scalars in the Type II Seesaw couple to EW bosons directly via gauge couplings. Subsequently, their production rates are sizable and can be predicted as a function of mass without additional input. In **Figure 29** we show the LO pair production cross section of triplet scalars via the (a) neutral and (b) charged current DY process at $\sqrt{s} = 14$ and 100 TeV. NLO in QCD corrections to these processes are well-known [438] and span $K^{\rm NLO} = \sigma^{\rm NLO}/\sigma^{\rm LO} = 1.1 - 1.3$ away from boundaries of collider phase space; moreover, due to the color-structure of DY-like processes, inclusive kinematics of very heavy scalar triplets are Born-like and thus naïve normalization of kinematics by $K^{\rm NLO}$ gives reliable estimates of both NLO- and NLO+PS-accurate results [275, 338]. For $M_{H^{\pm\pm}} = 1$ TeV, one finds that the LO pair production rates can reach $\sigma \sim 0.1$ (10) fb at $\sqrt{s} = 14$ (100) TeV, indicating $\mathcal{O}(10^2)$ ($\mathcal{O}(10^4)$) of events with the ab^{-1}-scale data sets expected at the respective collider program.

In addition to the DY channels are: single production of charged Higgses via weak boson scatter, as shown in **Figure 28B** and investigated in Han et al. [410], and Chen et al. [439]; charged Higgs pair production via $\gamma\gamma$ scattering, as shown in **Figure 28C**, studied in Dutta et al. [409], Han et al. [440], Drees et al. [441], Bambhaniya et al. [442], and Babu and Jana [443], and computed at $\sqrt{s} = 14$ TeV [440] in **Figure 29C**; as well as pair production through weak boson scattering, as studied in Dutta et al. [409] and Bambhaniya et al. [442] and computed for the 14 TeV LHC [409] in **Figure 29D**. As in the case of $W\gamma$ scattering in heavy N production in section 3, there is renewed interest [442] in the $\gamma\gamma$-mechanisms due to the new availability of photon PDFs that include both elastic and (deeply) inelastic contributions, e.g., NNPDF 2.3 and 3.0 QED PDF sets [444, 445]. However, care should be taken in drawing conclusions based on these specific PDF sets due to the (presently) large γ-PDF uncertainty, particularly at large Bjorken-x where this can reach greater than 100% [444]. For example: As shown in **Figure 29C**, $\gamma\gamma$ production is unambiguously sub-leading to the DY mechanism and only contributes about 10% despite recent claims to the contrary [443, 446]. The collinear behavior and the

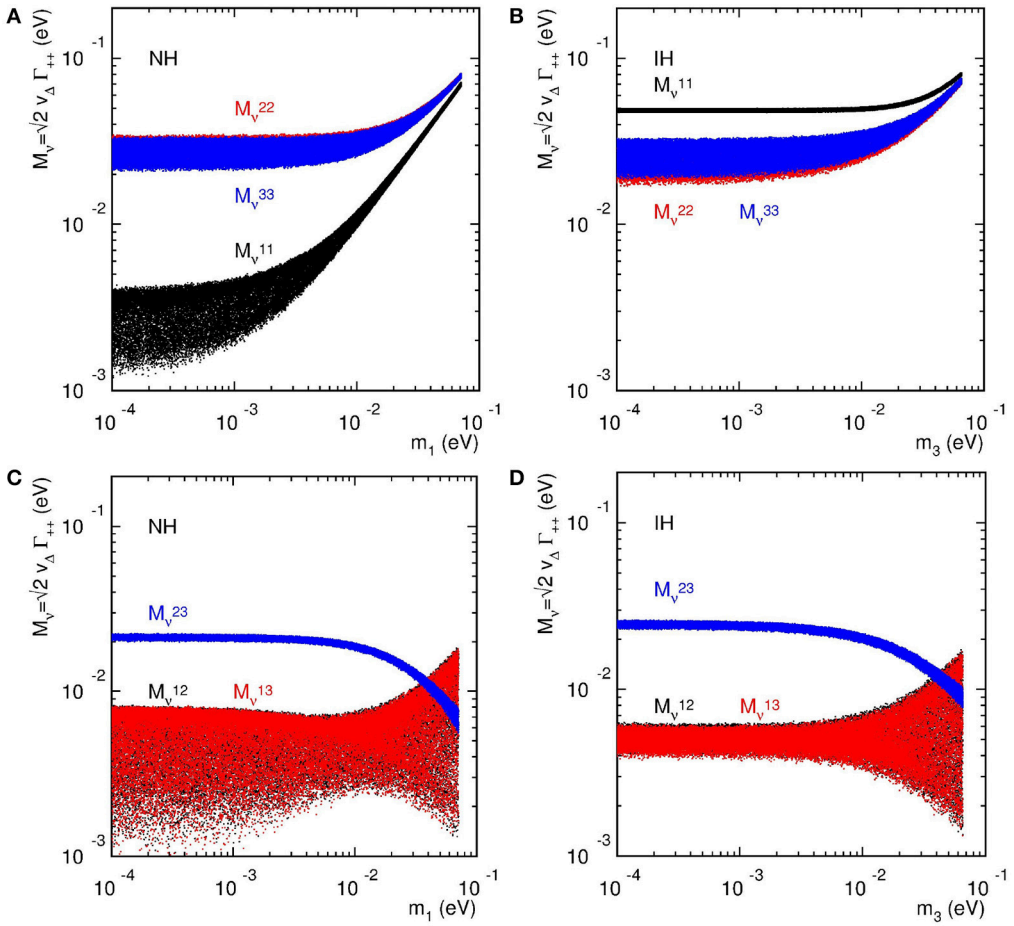

FIGURE 23 | Constraints on the diagonal **(A,B)** and off-diagonal **(C,D)** elements of the neutrino mass matrix $M_\nu \equiv \sqrt{2}v_\Delta \Gamma_{++}$ vs. the lowest neutrino mass for NH **(A,C)** and IH **(B,D)** when $\Phi_1 = 0$ and $\Phi_2 = 0$.

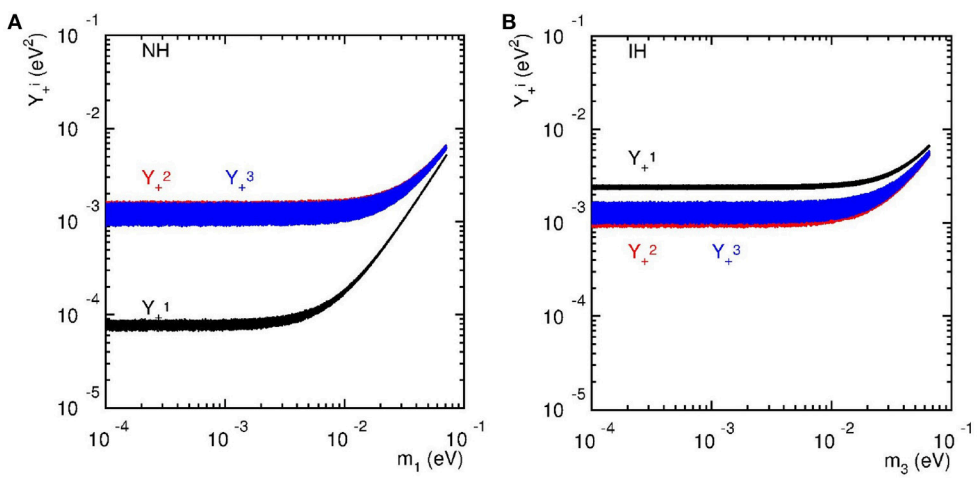

FIGURE 24 | Constraints on the squared coupling $Y_+^i \equiv \sum_j |\Gamma_+^{ji}|^2 v_\Delta^2$, vs. the lowest neutrino mass for NH **(A)** and IH **(B)**.

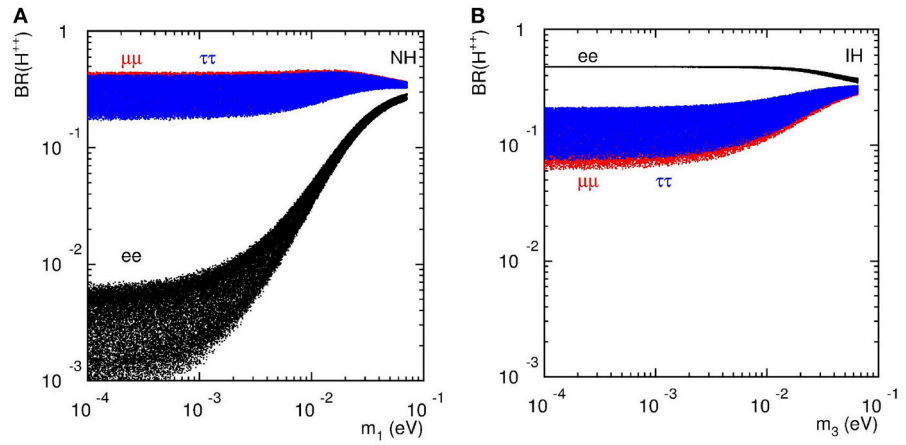

FIGURE 25 | Scatter plots for the H^{++} decay branching fractions to the flavor-diagonal like-sign dileptons vs. the lowest neutrino mass for NH **(A)** and IH **(B)** with $\Phi_1 = \Phi_2 = 0$.

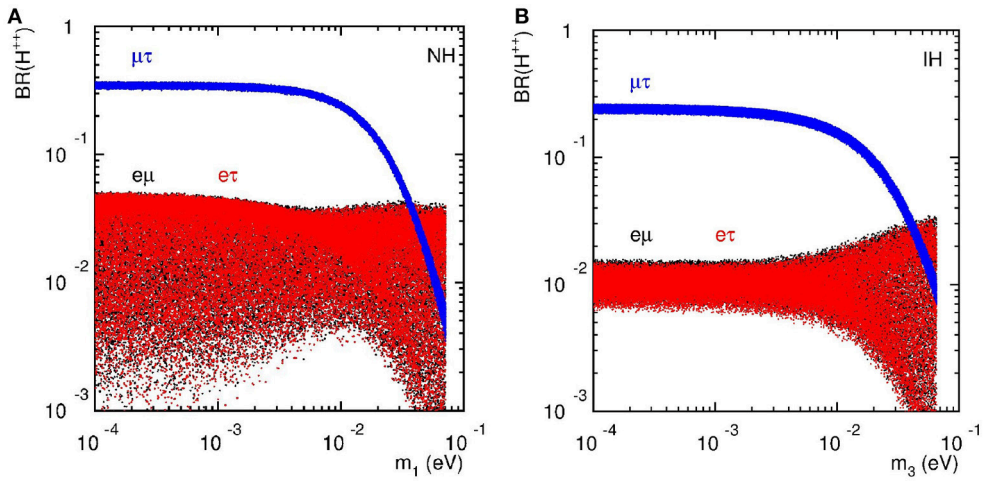

FIGURE 26 | H^{++} decay to the flavor-off-diagonal like-sign dileptons vs. the lowest neutrino mass for NH **(A)** and IH **(B)** with $\Phi_1 = \Phi_2 = 0$.

TABLE 2 | Relations among the branching fractions of the lepton number violating Higgs decays for the neutrino mass patterns of NH and IH, with vanishing Majorana phases.

	Relations
NH	$\text{BR}(H^{++} \to \tau^+\tau^+/\mu^+\mu^+) \sim (20-40)\% \gg \text{BR}(H^{++} \to e^+e^+) \sim (0.1-0.6)\%$ $\text{BR}(H^{++} \to \mu^+\tau^+) \sim (30-40)\% \gg \text{BR}(H^{++} \to e^+\mu^+/e^+\tau^+) \lesssim 5\%$ $\text{BR}(H^{+} \to \tau^+\bar{\nu}/\mu^+\bar{\nu}) \sim (30-60)\% \gg \text{BR}(H^{+} \to e^+\bar{\nu}) \sim (2.5-3)\%$
IH	$\text{BR}(H^{++} \to e^+e^+) \sim 50\% > \text{BR}(H^{++} \to \mu^+\mu^+/\tau^+\tau^+) \sim (6-20)\%$ $\text{BR}(H^{++} \to \mu^+\tau^+) \sim (20-30)\% \gg \text{BR}(H^{++} \to e^+\mu^+/e^+\tau^+) \sim (0.1-4)\%$ $\text{BR}(H^{+} \to e^+\bar{\nu}) \sim 50\% > \text{BR}(H^{+} \to \mu^+\bar{\nu}/\bar{\nu}) \sim (20-30)\%$

factorization scale dependence of the incoming photons must be treated with great care. As more data is collected and γ-PDF methodology further matures, one anticipates these uncertainties to greatly shrink; for further discussions of γ-PDFs, see Alva et al. [254], Degrande et al. [255], Martin and Ryskin [268], Harland-Lang et al. [269], Manohar et al. [271, 272]. For a list of recommended γ-PDFs, see the discussion just above Equation (3.38).

Similar to the $\gamma\gamma$ channel, production of triplet scalars from gluon fusion is sub-leading with respect to DY due to multiple vanishing contributions [258, 447] and despite an expectedly large QCD correction of $K^{\text{N}^3\text{LL}} = \sigma^{\text{N}^3\text{LL}}/\sigma^{\text{LO}} \sim 2.5-3$ [259]. If triplet scalar couplings to the SM-like Higgs are not too small and if sufficiently light, then such scalars may appear in pairs as rare decays of the 125 GeV scalar boson [448]. Likewise, if neutral triplet scalars mix appreciably with the SM-like Higgs, then single production via gluon fusion is also possible [448]; one should note that in such cases, the QCD K-factors calculated in Ruiz et al. [259] are applicable.

A noteworthy direction of progress in searches for triplet scalars at colliders are the implementation of exotically charged

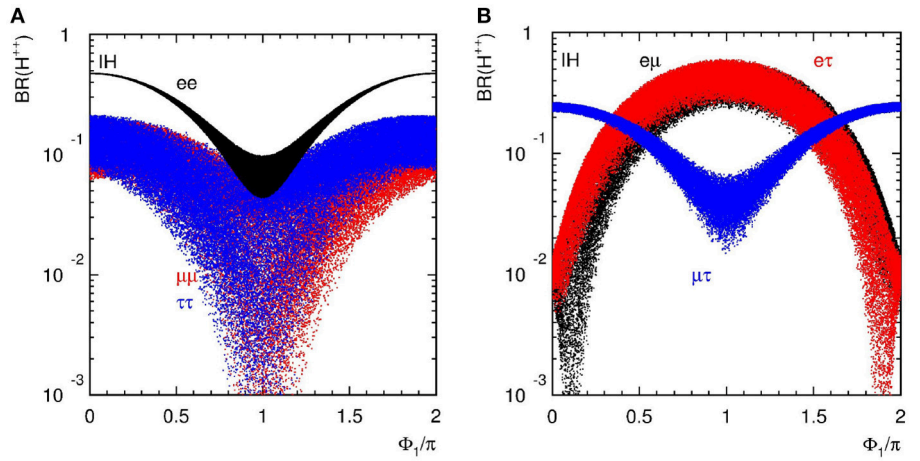

FIGURE 27 | Scatter plots of the same **(A)** and different **(B)** flavor leptonic branching fractions for the H^{++} decay vs. the Majorana phase Φ_1 for the IH with $m_3 = 0$ and $\Phi_2 \in (0, 2\pi)$.

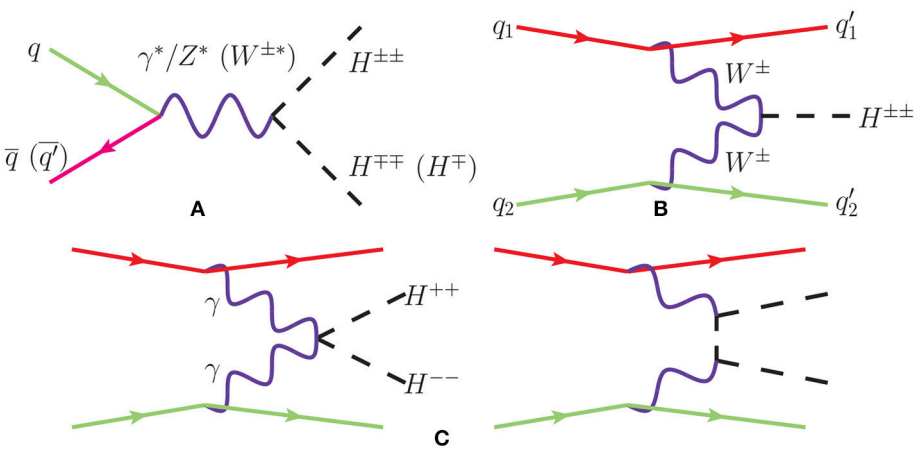

FIGURE 28 | Born-level diagrams depicting Type II triplet scalar production in *pp* collisions via **(A)** the DY mechanism, **(B)** same-sign $W^{\pm}W^{\pm}$ scattering, and **(C)** $\gamma\gamma$ fusion.

scalars into FeynRules model files. In particular, lepton number violating scalars are available in the `LNV-Scalars` [449, 450] model file as well as in a full implementation of LRSM at LO accuracy [451, 452]; the Georgi-Machacek model [453] is also available at NLO in QCD accuracy [293, 454]. These permit simulation of triplet scalar production in inclusive $\ell\ell/\ell p/pp$ collisions using modern, general-purpose event generators, such as Herwig [289], MadGraph5_aMC@NLO [290], and Sherpa [291].

Due to the unknown Yukawa structure in Equation (4.1), the decays of the triplet scalars to SM states are much more ambiguous than their production. Subsequently, branching rates of $H^{\pm} \to \ell^{\pm}\nu$ and $H^{\pm\pm} \to \ell_1^{\pm}\ell_2^{\pm}$ are often taken as phenomenological parameters in analyses and experimental searches. When taking such a model-agnostic approach, it may be necessary to also consider the lifetimes of scalar triplets: In a pure Type II scenario, for $M_{H^{\pm\pm}} < 270$ GeV and sub-MeV values of the triplet vev v_L, the proper decay length of $H^{\pm\pm}$ can exceed 10 μm [410]. As a result, exotically charged triplet scalars may manifest at collider experiments in searches for long-lived, multi-charged particles such as Aad et al. [455, 456], Collaboration [457], and Barrie et al. [458].

For prompt decays of triplet scalars, the discovery potential at hadron colliders is quantified in **Figure 30**. In particular, following the analysis of Fileviez Pérez et al. [408], **Figures 30A,B** show event contours in the BR($H^{++} \to \mu^+\mu^+$) vs. $M_{H^{\pm\pm}}$ plane after $\mathcal{L} = 300$ (3000) fb^{-1} of data at $\sqrt{s} = 14$ TeV and 100 TeV, respectively. At the 2σ level, one finds the sensitivity to doubly charged Higgs is about $M_{H^{\pm\pm}} = 0.75$ (1.1) TeV at 14 TeV and $M_{H^{\pm\pm}} = 2$ (3.5) TeV at 100 TeV. In **Figures 30C,D**, one similarly has the signal significance $\sigma = S/\sqrt{S+B}$ after $\mathcal{L} = 1$ and 3 ab^{-1} at the 14 TeV LHC for VBF production of doubly charged Higgs pairs and their decays to $e^{\pm}\mu^{\pm}$ and $\tau^{\pm}\tau^{\pm}$

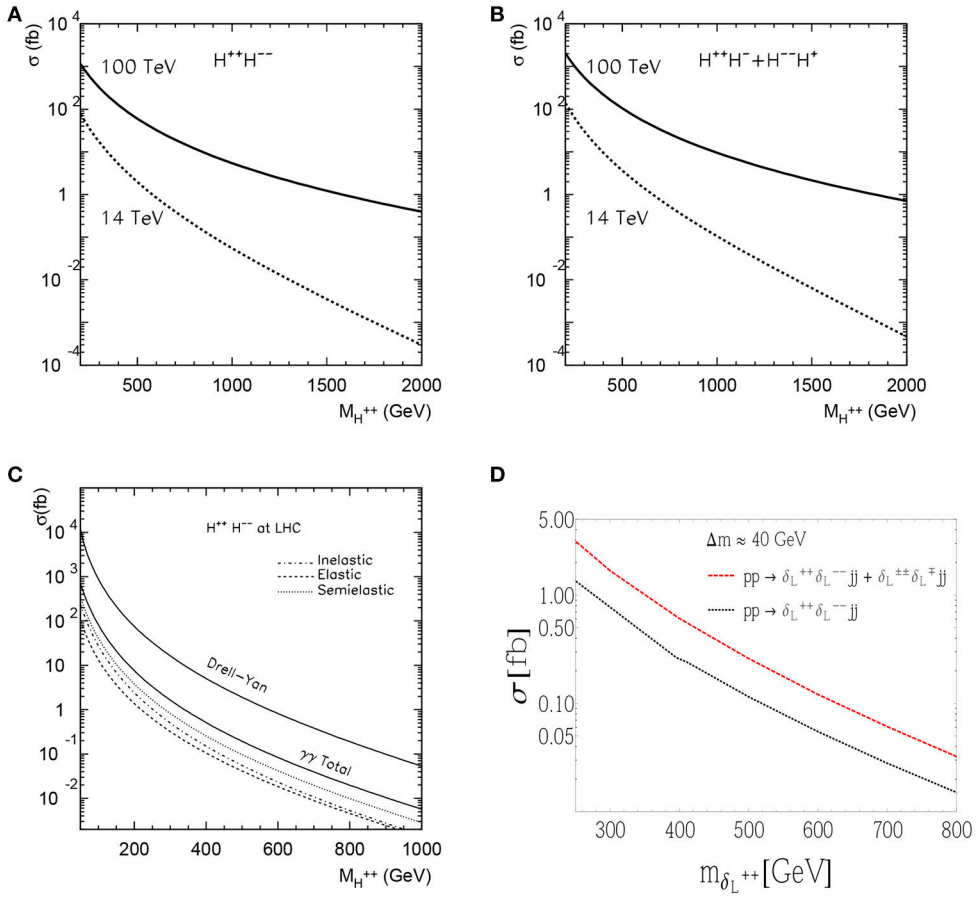

FIGURE 29 | Production cross section for **(A)** $pp \to H^{++}H^{--}$ and **(B)** $H^{\pm\pm}H^{\mp}$ at $\sqrt{s} = 14$ and 100 TeV, as well as for **(C)** $pp \to H^{++}H^{--}jj$ from $\gamma\gamma$ fusion [440] and **(D)** $pp \to H^{++}H^{--}jj + H^{\pm\pm}H^{\mp}$ from VBF at $\sqrt{s} = 14$ TeV [409].

final-states, respectively [409]. Upon the fortuitous discovery of a doubly charged scalar, however, will require also observing other charged scalars to determine its precise weak isospin and hypercharge quantum numbers [145, 449, 459].

In light of such sensitivity at hadron colliders, it is unsurprising then that null results from searches at the 7/8/13 TeV LHC [54, 55, 460, 461] have placed stringent constraints on EW-scale triplet scalar masses, assuming benchmark branching rates. As seen in **Figure 31**, results from the ATLAS experiment in searches for doubly charged Higgs pairs decaying to leptons, after collecting $\mathcal{L} = 36\,\text{fb}^{-1}$ of data at 13 TeV, have ruled out $M_{H^{\pm\pm}} > 600 - 900$ GeV at 95% CLs in both the (a) single-flavor and (b) mixed light-lepton final states [460]. Comparable limits have been reached by the CMS experiment [461].

At future e^-e^+ colliders, triplet scalars can appear in t-channel exchanges, inducing charged lepton flavor violation (cLFV) and forward-backward asymmetries [462]; in three-body decays of taus that are absent of light-neutrinos in the final state, i.e., $\tau^{\pm} \to \ell^{\mp}H^{\pm\pm *} \to \ell^{\mp}\mu^{\pm}\mu^{\pm}$ [463]; and, of course, in pairs via s-channel gauge currents [464]. In the event of such observations, the nontrivial conversion of an e^-e^+ beam into an $e^-e^-/e^-\mu^-/\mu^-\mu^-$ facility could provide complimentary information on scalar triplet Yukawa couplings by means of the "inverse" $0\nu\beta\beta$ processes, $\ell_i^-\ell_j^- \to W_{L/R}^-W_{L/R}^-$ [465–467].

4.2.2. Triplet Higgs Scalars and the Left-Right Symmetric Model at Colliders

Turning to scalars in the LRSM, as introduced in section 3.1.4, it was recently observed [368, 448] that in a certain class of neutrino mass models, decays of the SM-like Higgs boson $h(125\,\text{GeV})$ to heavy neutrino pairs, $h \to NN$, may occur much more readily than previously thought. The significance of this reaction is one's ability to confirm neutrino masses are generated, in part, through EWSB. It would also indicate sensitivity to the scalar sector responsible for generating RH Majorana masses. Interactions between SM particles and N typically proceed through heavy-light neutrino mixing, $|V_{\ell N}|$, which, is a numerically small quantity. As $h \to NN$ involves two N, the issue is compounded and usually renders the decay rate prohibitively small in a pure Type I scenario. For $H \in \{H^0, H^{\pm}, H^{\pm\pm}\}$ predicted in Type I+II Seesaws, and in particular the LRSM, the situation is more interesting: it may be that $h(125\,\text{GeV})$ and the RH neutral scalars mix sufficiently that decays to relatively light ($2M_N < 125\,\text{GeV}$) heavy neutrino pairs are possible [368]. This is allowed as H

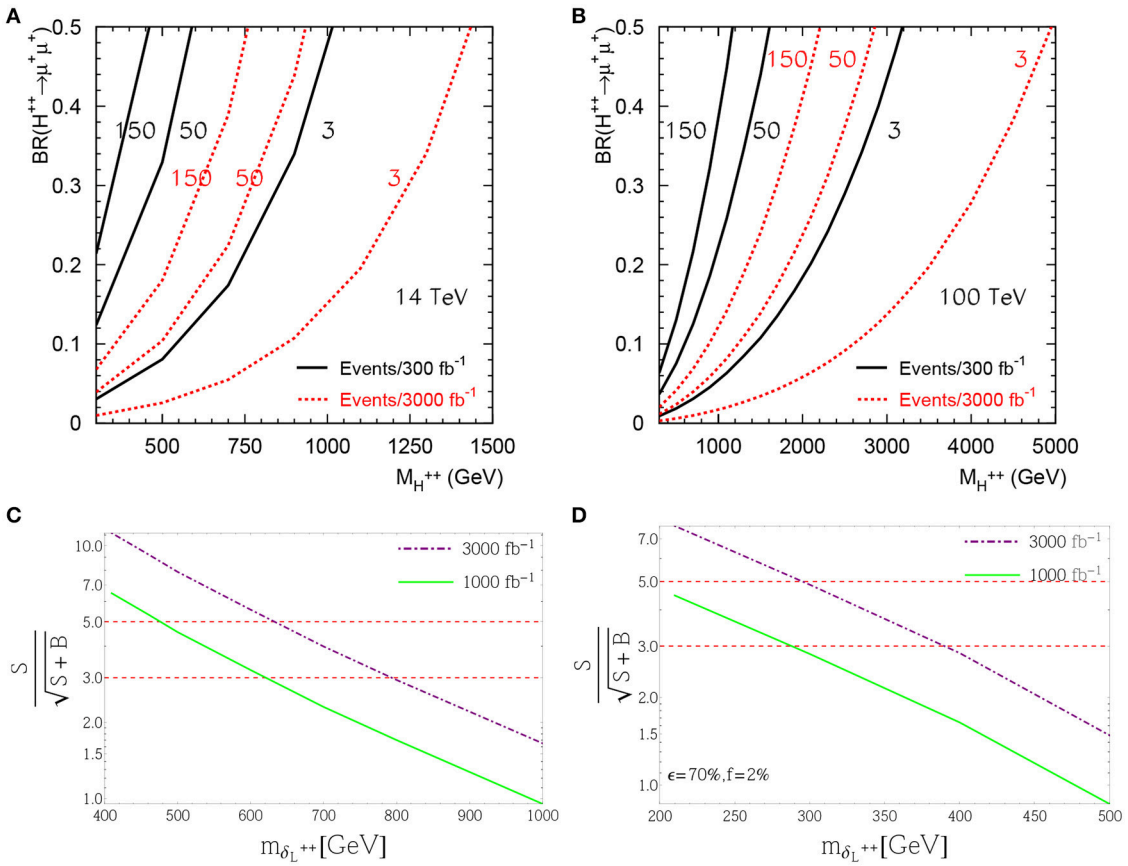

FIGURE 30 | Event contour for $H^{++}H^{--} \to \mu^+\mu^+\mu^-\mu^-$ in the BR($H^{++} \to \mu^+\mu^+$) vs. $M_{H^{++}}$ plane at **(A)** $\sqrt{s}$ =14 TeV and **(B)** 100 TeV, assuming $\mathcal{L}$ =300 fb^{-1} and 3,000 fb^{-1}, and based on the analysis of Fileviez Perez et al. [408]. Signal significance for VBF production of doubly charged Higgs pairs and their decays to **(C)** $e^{\pm}\mu^{\pm}$ and **(D)** $\tau^{\pm}\tau^{\pm}$ final-states, after $\mathcal{L}$ = 1 and 3 ab^{-1} at the 14 TeV LHC [409].

can couple appreciable to N and the mixing between H^0 and h is much less constrained. Subsequently, the naïve neutrino mixing suppression is avoided by exploiting that $h \to NN$ decays can proceed instead through $H^0 - h$ mixing. In a similar vein, it may be possible for h to decay to triplet pairs and subsequently to N or same-sign charged leptons, or for single H^0 production to proceed directly [448]. Such processes are shown diagrammatically in **Figure 32**. As a result, the L-violating Higgs decays,

$$h(125\,\text{GeV}) \to N\,N \to W_R^{\pm *} W_R^{\pm *} \ell_1^{\mp} \ell_2^{\mp} \to \ell_1^{\mp}\,\ell_2^{\mp} + nj, \quad (4.9)$$

$$h(125\,\text{GeV}) \to H^0\,H^0 \to 4N \to \ell_1^{\pm}\,\ell_2^{\mp}\,\ell_3^{\pm}\,\ell_4^{\mp} + nj, \quad (4.10)$$

$$h(125\,\text{GeV}) \to H^{++}\,H^{--} \to \ell_1^{\pm}\,\ell_2^{\pm}\,\ell_3^{\mp}\,\ell_4^{\mp}, \quad (4.11)$$

are not only possible, but also provide complementary coverage of low-mass N scenarios that are outside the reach of $0\nu\beta\beta$ experiments and direct searches for W_R at colliders. The sensitivity of such modes are summarized in **Figure 33** [368, 448]. The associated production channels,

$$pp \to H^{0,\pm\pm}\,W_R^{\mp} \quad \text{and} \quad pp \to H^0 Z_R, \quad (4.12)$$

are also possible. However, as in the SM, these channels are s-channel and phase space suppressed, which lead to prohibitively small cross sections in light of present mass limits [145].

Lastly, one should note that the search for such Higgs decays is not limited to hadron colliders. As presently designed future lepton colliders are aimed at operating as Higgs factories, searches for such L-violating Higgs decays [468–470] at such facilities represent an attractive discovery prospect. In this context, a relatively understudied topic is the possible manifestation of Seesaw in precision measurements of the known SM-like Higgs boson [216, 368, 471]. Some related studies also exist in the literature such as for generic pheno [440, 440, 449]; for little Higgs [410, 472]; and for decay ratios and mixing patterns of exotically charged Higgs [473, 474].

5. THE TYPE III SEESAW AND LEPTON NUMBER VIOLATION AT COLLIDERS

We now turn to collider searches for lepton number violation in the context of the Type III Seesaw mechanism [19] as well

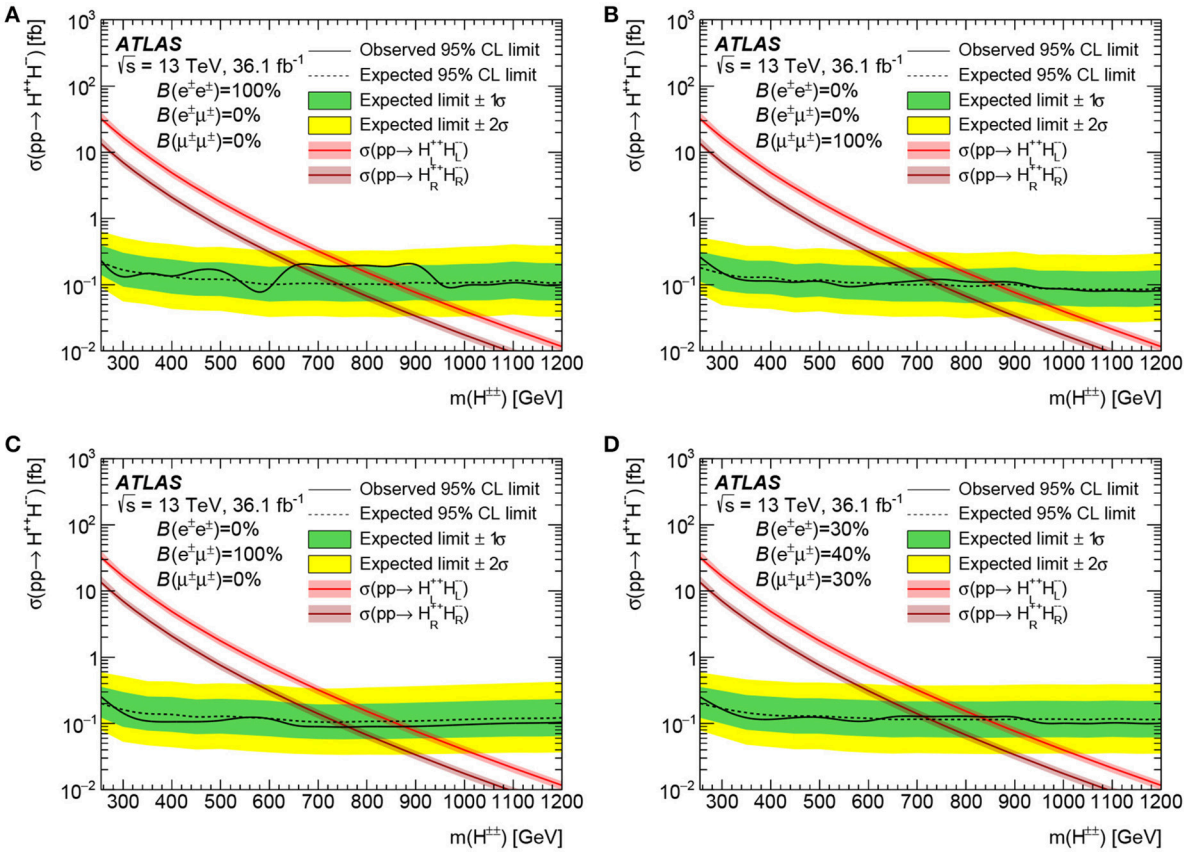

FIGURE 31 | ATLAS 95% CLs exclusion at 13 TeV after $\mathcal{L} = 36$ fb^{-1} on $\sigma(pp \to H^{++}H^{--})$ for various representative branching rates to SM charged leptons in the **(A)** pure $e^{\pm}e^{\pm}$, **(B)** pure $\mu^{\pm}\mu^{\pm}$, **(C)** pure $e^{\pm}\mu^{\pm}$, and **(D)** mixed final-states [460].

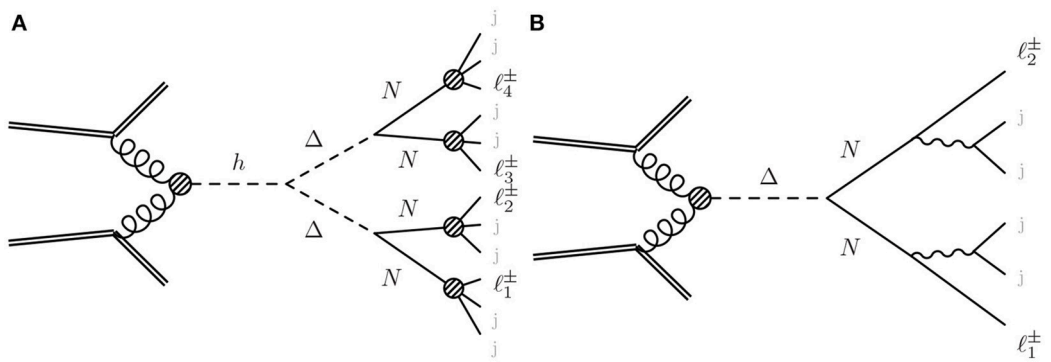

FIGURE 32 | Feynman diagrams depicting gluon fusion production of Majorana neutrinos via **(A)** SM Higgs boson (h) and **(B)** SU(2)$_R$ triplet Higgs (H) through their mixing in pp collisions [368, 448].

as its embedding in GUTs and other SM extensions. In some sense, the Type III model is the fermionic version of the Type II scenario, namely that Seesaw partner fermions couple to the SM via both weak gauge and Yukawa couplings. Subsequently, much of the Type III collider phenomenology resembles that of Type I-based models. However, quantitatively, the presence of gauge couplings lead to a very different outlook and level of sensitivity. We now summarize the main highlights of the canonical Type III Seesaw (section 5.1.1), Type III-based models (section 5.1.2), and then review their L-violating collider phenomenology (section 5.2). As with the previous Seesaw scenarios, a discussion of cLFV is outside the scope of this review. For recent summaries on cLFV in the Type III Seesaw, see Abada et al. [176, 475], Eboli

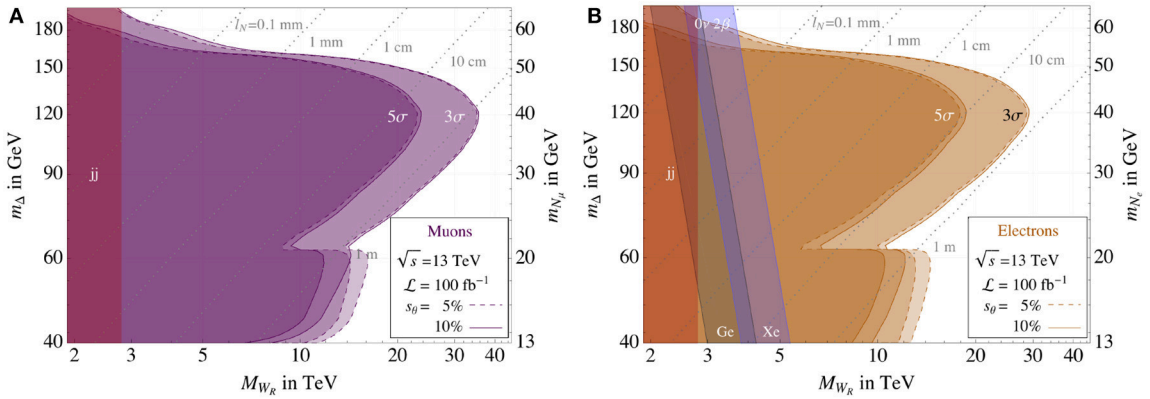

FIGURE 33 | (A,B) 13 TeV LHC sensitivity to the LRSM in the (M_N, M_{W_R}) plane to the processes shown in **Figure 32** after $\mathcal{L} = 100$ fb^{-1} [368, 448].

et al. [476], and Agostinho et al. [477] and references therein.

5.1. Type III Seesaw Models

5.1.1. The Canonical Type III Seesaw Mechanism

In addition to the SM field content, the Type III Seesaw [19] consists of SU(2)$_L$ triplet (adjoint) leptons,

$$\Sigma_L = \Sigma_L^a \sigma^a = \begin{pmatrix} \Sigma_L^0/\sqrt{2} & \Sigma_L^+ \\ \Sigma_L^- & -\Sigma_L^0/\sqrt{2} \end{pmatrix}, \quad \Sigma_L^\pm \equiv \frac{\Sigma_L^1 \mp i\Sigma_L^2}{\sqrt{2}}, \quad \Sigma_L^0 = \Sigma_L^3, \tag{5.1}$$

which transform as $(1, 3, 0)$ under the SM gauge group. Here $\Sigma_L^\pm$ have U(1)$_{\rm EM}$ charges $Q = \pm 1$, and the σ^a for $a = 1, \ldots, 3$, are the usual Pauli SU(2) matrices. The RH conjugate fields are related by

$$\Sigma_R^c = \begin{pmatrix} \Sigma_R^{0c}/\sqrt{2} & \Sigma_R^{-c} \\ \Sigma^{+c} & -\Sigma_R^{0c}/\sqrt{2} \end{pmatrix}, \quad \text{for} \quad \psi_R^c \equiv (\psi^c)_R = (\psi_L)^c. \tag{5.2}$$

The Type III Lagrangian is given by the sum of the SM Lagrangian, the triplet's kinetic and mass terms,

$$\mathcal{L}_T = \frac{1}{2}\,\mathrm{Tr}\left[\overline{\Sigma_L} i \not{D} \Sigma_L\right] - \left(\frac{M_\Sigma}{2}\overline{\Sigma_L^0}\Sigma_R^{0c} + M_\Sigma \overline{\Sigma_L^-}\Sigma_R^{+c} + \text{H.c.}\right), \tag{5.3}$$

and the triplet's Yukawa coupling to the SM LH lepton (L) and Higgs (H) doublet fields,

$$\mathcal{L}_Y = -Y_\Sigma \overline{L}\, \Sigma_R^c\, i\sigma^2 H^* + \text{H.c.} \tag{5.4}$$

From Equation (5.4), one can deduce the emergence of a Yukawa coupling between the charged SM leptons and the charged triplet leptons. This, in turn, induces a mass mixing among charged leptons that is similar to doublet-singlet and doublet-triplet neutrino mass mixing, and represents one of the more remarkable features of the Type III mechanism. The impact of EW fermion triplets on the SM Higgs, naturalness in the context of the Type III Seesaw has been discussed in Gogoladze et al. [478], He et al. [479], and Gogoladze et al. [480].

After expanding Equations (5.3)–(5.4), the relevant charged lepton and neutrino mass terms are [481]

$$\mathcal{L}_{\rm III}^m = -\left(\overline{l_R}\ \overline{\Psi_R}\right)\begin{pmatrix} m_l & 0 \\ Y_\Sigma v_0 & M_\Sigma \end{pmatrix}\begin{pmatrix} l_L \\ \Psi_L \end{pmatrix} - \left(\overline{\nu_L^c}\ \overline{\Sigma_L^{0c}}\right)\begin{pmatrix} 0 & Y_\Sigma^T v_0/2\sqrt{2} \\ Y_\Sigma v_0/2\sqrt{2} & M_\Sigma/2 \end{pmatrix}\begin{pmatrix} \nu_L \\ \Sigma_L^0 \end{pmatrix} + \text{H.c.}, \tag{5.5}$$

with $\Psi_L \equiv \Sigma_L^-$, $\Psi_R \equiv \Sigma_L^{+c}$, and $\Psi = \Psi_L + \Psi_R$. After introducing unitarity matrices to transit light doublet and heavy triplet lepton fields as below

$$\begin{pmatrix} l_{L,R} \\ \Psi_{L,R} \end{pmatrix} = U_{L,R}\begin{pmatrix} l_{mL,R} \\ \Psi_{mL,R} \end{pmatrix}, \quad \begin{pmatrix} \nu_L \\ \Sigma_L^0 \end{pmatrix} = U_0\begin{pmatrix} \nu_{mL} \\ \Sigma_{mL}^0 \end{pmatrix}, \tag{5.6}$$

$$U_L \equiv \begin{pmatrix} U_{Ll} & U_{L\Psi} \\ U_{L\Psi l} & U_{L\Psi\Psi} \end{pmatrix}, \quad U_R \equiv \begin{pmatrix} U_{Rl} & U_{R\Psi} \\ U_{R\Psi l} & U_{R\Psi\Psi} \end{pmatrix}, \quad U_0 \equiv \begin{pmatrix} U_{0\nu\nu} & U_{0\nu\Sigma} \\ U_{0\Sigma\nu} & U_{0\Sigma\Sigma} \end{pmatrix}, \tag{5.7}$$

one obtains the diagonal mass matrices and mass eigenvalues for neutrinos and charged leptons,

$$\mathrm{diag}(\mathcal{N}) = U_0^\dagger \begin{pmatrix} 0 & Y_\Sigma^\dagger v_0/\sqrt{2} \\ Y_\Sigma^* v_0/\sqrt{2} & M_\Sigma^* \end{pmatrix} U_0^* = \begin{pmatrix} m_\nu^{diag} & 0 \\ 0 & M_N^{diag} \end{pmatrix}, \tag{5.8}$$

$$\mathrm{diag}(\mathcal{E}) = U_L^\dagger \begin{pmatrix} m_l^\dagger & Y_\Sigma^\dagger v_0 \\ 0 & M_\Sigma^\dagger \end{pmatrix} U_R = \begin{pmatrix} m_l^{diag} & 0 \\ 0 & M_E^{diag} \end{pmatrix}. \tag{5.9}$$

The light neutrino mass eigenstates are denoted by ν_j for $j = 1, \ldots, 3$; whereas the heavy neutral and charged leptons are respectively given by $N_{j'}$ and $E_{k'}^\pm$. In the literature, N and $E^\pm$ are often denoted as T^0, $T^\pm$ or Σ^0, $\Sigma^\pm$. However, there is no standard convention as to what set of symbols are used to

denote gauge and mass eigenstates. Where possible, we follow the convention of Arhrib et al. [482] and generically denote triplet-doublet mixing by Y_T and ε_T. This means that in the mass basis, triplet gauge states are given by

$$\Psi^{\pm} = Y_T\, E^{\pm} + \sqrt{2}\varepsilon_T\, \ell^{\pm} \quad \text{and} \quad \Psi^0 = Y_T\, N + \varepsilon_T\, \nu_m, \\ \text{with } |Y_T| \sim \mathcal{O}(1) \quad \text{and} \quad |\varepsilon_T| \sim \frac{Y_\Sigma v_0}{\sqrt{2}M_\Sigma} \ll 1. \tag{5.10}$$

The resulting interaction Lagrangian, in the mass eigenbasis then contains [482]

$$\begin{aligned}\mathcal{L}^{\text{Mass Basis}}_{\text{Type III}} \ni & -\overline{E^-_{k'}}\left(eY_T A_\mu \gamma^\mu + g\cos\theta_W Y_T Z_\mu \gamma^\mu\right) E^-_{k'} \\ & - gY_T \overline{E^-_{k'}} W^-_\mu \gamma^\mu N_{j'} \\ & - \frac{e}{2s_w c_w} Z_\mu \left(\varepsilon_T \overline{N_{j'}} \gamma^\mu P_R \nu_j + \sqrt{2}\varepsilon_T \overline{E^-_{k'}} \gamma^\mu P_R \ell^-_k\right) \\ & - \frac{e}{s_w} W^+_\mu \left(\varepsilon_T \overline{\nu_j} \gamma^\mu P_L E^-_{k'} + \frac{1}{\sqrt{2}} \varepsilon_T \overline{N_{j'}} \gamma^\mu P_R \ell^-_k\right) + \text{H.c.}\end{aligned} \tag{5.11}$$

From this, one sees a second key feature of the Type III Seesaw, that gauge interactions between heavy lepton pairs proceeds largely through pure vector currents with axial-vector deviations (not shown) suppressed by $\mathcal{O}(\varepsilon_T^2)$ at the Lagrangian level. This follows from the triplet fermions vector-like nature. Similarly, the mixing-suppressed gauge couplings between heavy and light leptons proceeds through SM-like currents.

Explicitly, the light and heavy neutrino mass eigenvalues are

$$m_\nu \approx \frac{Y_\Sigma^2 v_0^2}{2M_\Sigma}, \quad M_N \approx M_\Sigma, \tag{5.12}$$

and for the charged leptons are

$$m_l - m_l \frac{Y_\Sigma^2 v_0^2}{2M_\Sigma^2} \approx m_l, \quad M_E \approx M_\Sigma. \tag{5.13}$$

This slight deviation in the light, charged leptons' mass eigenvalues implies a similar variation in the anticipated Higgs coupling to the same charged leptons. At tree-level, the heavy leptons N and $E^{\pm}$ are degenerate in mass, a relic of $\text{SU}(2)_L$ gauge invariance. However, after EWSB, and for $M_\Sigma \gtrsim 100$ GeV, radiative corrections split this degeneracy by Arhrib et al. [482],

$$\Delta M_T \equiv M_E - M_N = \frac{\alpha_W}{2\pi} \frac{M_W^2}{M_\Sigma} \left[f\left(\frac{M_\Sigma}{M_Z}\right) - f\left(\frac{M_\Sigma}{M_W}\right)\right] \\ \approx 160 \text{ MeV}, \tag{5.14}$$

$$\text{where} \quad f(y) = \frac{1}{4y^2} \log y^2 - \left(1 + \frac{1}{2y^2}\right) \sqrt{4y^2 - 1} \arctan \\ \sqrt{4y^2 - 1}, \tag{5.15}$$

and opens the $E^{\pm} \to N\pi^{\pm}$ decay mode. Beyond this are the heavy lepton decays to EW bosons and light leptons that proceed through doublet-triplet lepton mixing. The mixings are governed by the elements in the unitary matrices $U_{L,R}$ and U_0. Expanding $U_{L,R}$ and U_0 up to order $Y_\Sigma^2 v_0^2 M_\Sigma^{-2}$, one gets the following results [475, 483]

$$\begin{aligned} & U_{Ll} = 1 - \epsilon\,, \quad U_{L\Psi} = Y_\Sigma^\dagger M_\Sigma^{-1} v_0\,, \qquad U_{L\Psi l} = -M_\Sigma^{-1} Y_\Sigma v_0\,, \\ & \quad U_{L\Psi\Psi} = 1 - \epsilon'\,, \\ & U_{Rl} = 1\,, \quad U_{R\Psi} = m_l Y_\Sigma^\dagger M_\Sigma^{-2} v_0\,, \; U_{R\Psi l} = -M_\Sigma^{-2} Y_\Sigma m_l v_0\,, \\ & \quad U_{R\Psi\Psi} = 1\,, \\ & U_{0\nu\nu} = (1 - \epsilon/2) U_{PMNS}\,, \quad U_{0\nu\Sigma} = Y_\Sigma^\dagger M_\Sigma^{-1} v_0/\sqrt{2}\,, \quad U_{0\Sigma\nu} = \\ & \quad -M_\Sigma^{-1} Y_\Sigma U_{0\nu\nu} v_0/\sqrt{2}\,, \\ & U_{0\Sigma\Sigma} = 1 - \epsilon'/2\,, \qquad \epsilon = Y_\Sigma^\dagger M_\Sigma^{-2} Y_\Sigma v_0^2/2\,, \\ & \quad \epsilon' = M_\Sigma^{-1} Y_\Sigma Y_\Sigma^\dagger M_\Sigma^{-1} v_0^2/2\,. \end{aligned}$$

To the order of $Y_\Sigma v_0 M_\Sigma^{-1}$, the mixing between the SM charged leptons and triplet leptons, i.e., $V_{\ell N} = -Y_\Sigma^\dagger v_0 M_\Sigma^{-1}/\sqrt{2}$, follows the same relation as Equation (3.10) in the Type I Seesaw [481] and the couplings in the interactions in Equation (5.11) are all given by $V_{\ell N}$ [326, 481].

Hence, the partial widths for both the heavy charged lepton and heavy neutrino are proportional to $|V_{\ell N}|^2$. For $M_E \approx M_N \gg M_W, M_Z, M_h$, the partial widths behave like [252, 326]

$$\begin{aligned} & \frac{1}{2}\Gamma(N \to \sum_\ell \ell^+ W^- + \ell^- W^+) \approx \Gamma(N \to \sum_\nu \nu Z + \bar{\nu} Z) \\ & \quad \approx \Gamma(N \to \sum_\nu \nu h + \bar{\nu} h) \\ \approx\; & \frac{1}{2}\Gamma(E^{\pm} \to \sum_\nu \overset{(-)}{\nu} W^{\pm}) \approx \Gamma(E^{\pm} \to \sum_\ell \ell^{\pm} Z) \\ & \quad \approx \Gamma(E^{\pm} \to \sum_\ell \ell^{\pm} h) \\ \approx\; & \frac{G_F}{8\sqrt{2}\pi} \sum_\ell |V_{\ell N}|^2 M_\Sigma^3. \end{aligned} \tag{5.16}$$

Thus the heavy lepton branching ratios exhibit asymptotic behavior consistent with the Goldstone Equivalence Theorem [260, 261], and are given by the relations [252, 326, 482, 484],

$$\begin{aligned} & \frac{1}{2}\text{BR}(N \to \sum_\ell \ell^+ W^- + \ell^- W^+) \approx \text{BR}(N \to \sum_\nu \nu Z + \bar{\nu} Z) \\ & \quad \approx \text{BR}(N \to \sum_\nu \nu h + \bar{\nu} h) \\ \approx\; & \frac{1}{2}\text{BR}(E^{\pm} \to \sum_\nu \overset{(-)}{\nu} W^{\pm}) \approx \text{BR}(E^{\pm} \to \sum_\ell \ell^{\pm} Z) \\ & \quad \approx \text{BR}(E^{\pm} \to \sum_\ell \ell^{\pm} h) \approx \frac{1}{4}. \end{aligned} \tag{5.17}$$

As displayed in **Figure 34** by Franceschini et al. [484], as the triplet mass grows, this asymptotic behavior can be seen explicitly in the triplet lepton partial widths.

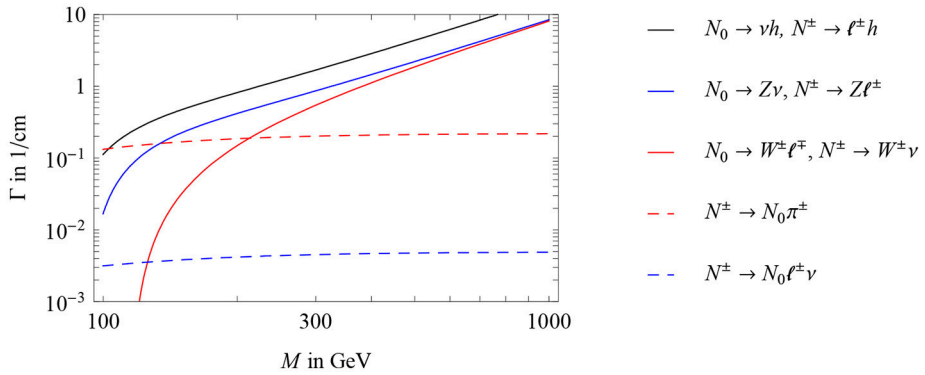

FIGURE 34 | Triplet decay widths as function of the triplet mass and assuming $M_{h_{\rm SM}} = 115$ GeV [484].

5.1.2. Type I+III Hybrid Seesaw in Grand Unified and Extended Gauge Theory

One plausible possibility to rescue the minimal grand unified theory, i.e., SU(5), is to introduce an adjoint 24_F fermion multiplet in addition to the original 10_F and $\bar{5}_F$ fermionic representations [5, 485]. As the 24_F contains both singlet and triplet fermions in this non-supersymmetric SU(5), the SM gauge couplings unify and neutrino masses can generated through a hybridization of the Types I and III Seesaw mechanisms. The Yukawa interactions and Majorana masses in this Type I+III Seesaw read [482]

$$\Delta\mathcal{L}^{Y}_{\rm I+III} = Y_S LHS + Y_T LHT - \frac{M_S}{2}SS - \frac{M_T}{2}TT + \text{H.c.}, \quad (5.18)$$

where S and $T = \left(\frac{T^- + T^+}{\sqrt{2}}, \frac{T^- - T^+}{i\sqrt{2}}, T^0\right)$ are the fermionic singlet and triplet fields, respectively, with masses M_S and M_T. In the limit that $M_S, M_T \gg Y_S v_0, Y_T v_0$, the light neutrino masses are then given by the sum of the individual Type I and III contributions

$$m_\nu = -(Y_S v_0/\sqrt{2})^2 M_S^{-1} - (Y_T v_0/\sqrt{2})^2 M_T^{-1}, \quad (5.19)$$

The most remarkable prediction of this SU(5) theory is that the unification constraint and the stability of proton require the triplet mass to be small: $M_T \lesssim 1$ TeV [485, 486]. Thus, in SU(5) scenarios, the triplet leptons of this Type I+III Seesaw are within the LHC's kinematic reach and can be tested via L-violating collider signatures [5, 487–491].

Other GUT models that can accommodate the Type III Seesaw and potentially lead to collider-scale L-violation include variations of SO(10) [492] theories. It is also possible to embed the Type III scenario into extended gauge sectors, including Left-Right Symmetric theories [134, 135, 493, 494], which also represents a Type I+II+III hybrid Seesaw hat trick. Additionally, Type III-based hybrid Seesaws can be triggered via fermions in other $SU(2)_L \times U(1)_Y$ representations [495–498], The collider phenomenology in many of these cases is very comparable to that of the Type I and II Seesaws, as discussed in sections 3 and 4, or the more traditional Type III scenario, which we now discuss.

5.2. Heavy Charged Leptons and Neutrinos at Colliders

5.2.1. Heavy Charged Leptons and Neutrinos at *pp* Colliders

Due to the presence of both gauge and Yukawa couplings to SM fields, the collider phenomenology for triplet leptons is exceedingly rich. In hadron collisions, for example, pairs of heavy triplet leptons are produced dominantly via charged and neutral Drell-Yan (DY) currents, given by

$$q\bar{q}' \to W^{*\pm} \to T^\pm T^0 \text{and} q\bar{q} \to \gamma^*/Z^* \to T^+T^-, \quad (5.20)$$

and shown in **Figure 35A**. For the DY process, the total cross section is now known up to NLO and differentially at NLO+LL in p_T resummation [275]. As function of mass, the $N\ell^\pm$ (singlet) as well as T^+T^- and $T^\pm T^0$ (triplet) DY production cross sections at $\sqrt{s} = 14$ and 100 TeV are displayed in **Figure 36A**. While the three rates are naïvely comparable, one should assign a mixing factor of $|V_{\ell N}|^2 \lesssim 10^{-2}$ to the singlet production since it proceeds through active-sterile neutrino mixing, i.e., Yukawa couplings, whereas triplet lepton pair production proceeds through gauge couplings. Heavy triplet leptons can also be produced singly in the association with light leptons and neutrinos,

$$q\bar{q}' \to W^{*\pm} \to T^\pm \nu,\ T^0 \ell^\pm \text{ and } q\bar{q} \to \gamma^*/Z^* \to T^\pm \ell^\mp. \quad (5.21)$$

As single production modes are proportional to the small [88] doublet-triplet mixing, denoted by $|V_{\ell T}|$, these processes suffer from the same small signal rates at colliders as does singlet production in Type I-based Seesaws (see section 3.1.1). However, as heavy-light lepton vertices also posses axial-vector contributions, new production channels are present, such as through the gluon fusion mechanism [242, 245, 258, 259], shown in **Figure 35B** and given by

$$gg \to Z^*/h^* \to T^\pm \ell^\mp. \quad (5.22)$$

It is noteworthy that the partonic expression for gluon fusion channels $gg \to Z^*/h^* \to T^\pm \ell^\mp$ is equal to the Type I analog $gg \to N\nu_\ell$ [258], and hence its QCD corrections [259], but that

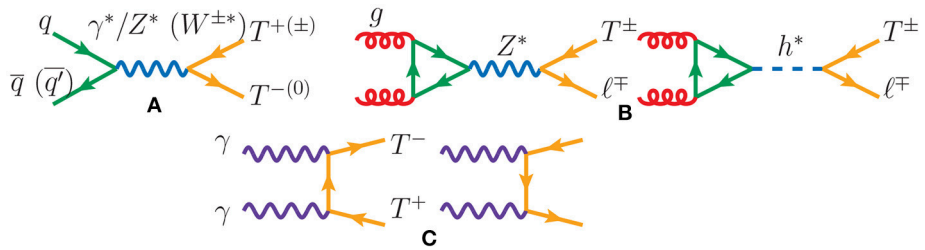

FIGURE 35 | Born level production of Type III lepton pairs via **(A)** Drell-Yan, **(B)** gluon fusion, and **(C)** photon fusion.

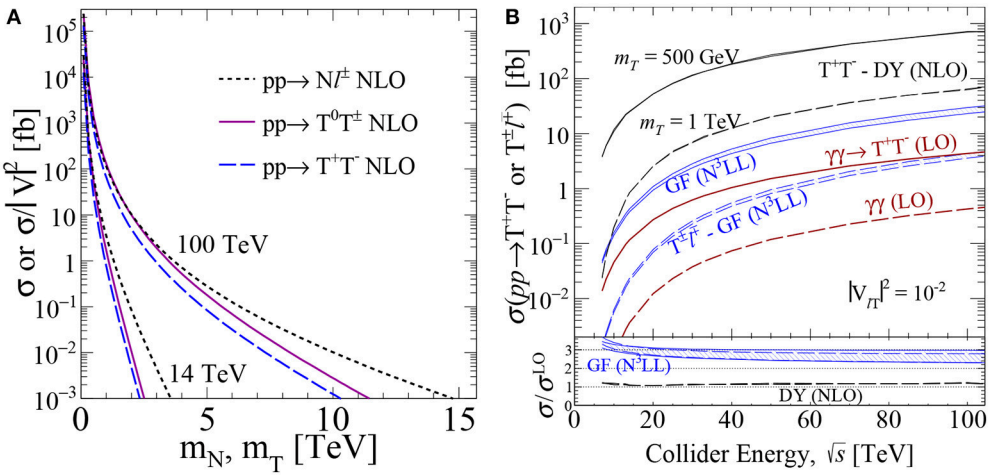

FIGURE 36 | (A) As a function of mass, the $N\ell^\pm$ (singlet) as well as T^+T^- and $T^\pm T^0$ (triplet) DY production cross sections at $\sqrt{s} = 14$ and 100 TeV. **(B)** As a function of collider energy $\sqrt{s}$, the T^+T^- and $T^\pm\ell^\mp$ (assuming benchmark $|V_{\ell T}|^2 = 10^{-2}$) production cross sections via various production mechanisms.

heavy triplet pair production through gluon fusion, i.e., $gg \to T\overline{T}$, is zero since their couplings to weak bosons are vector-like, and hence vanish according to Furry's Theorem [242, 245, 447]. For $\sqrt{s} = 7 - 100$ TeV, the N^{3}LL(Threshold) corrections to the Born rates span +160% to +260% [259]. Hence, for singly produced triplet leptons, the gluon fusion mechanism is dominant over the DY channel for $\sqrt{s} \gtrsim 20 - 25$ TeV, over a wide range of EW- and TeV-scale triplet masses [258, 259]. More exotic production channels also exist, such as the $\gamma\gamma \to T^+T^-$ VBF channel, shown in **Figure 35C**, as well as permutations involving W and Z. However, their contributions are sub-leading due to coupling and phase space suppression.

For representative heavy lepton masses of $M_T = 500$ GeV and 1 TeV as well as doublet-triplet mixing of $|V_{\ell T}|^2 = 10^{-2}$, we display in **Figure 36B** the $pp \to T^+T^-$ and $T^\pm\ell^\mp$ production cross sections via various hadronic production mechanisms as a function of collider energy $\sqrt{s}$. In the figure, the dominance of pair production over single production is unambiguous. Interestingly, considering that the triplet mass splitting is $\Delta M_T \sim \mathcal{O}(200)$ MeV as stated above, one should not expect to discover the neutral current single production mode without also observing the charged channel almost simultaneously. Hence, despite sharing much common phenomenology, experimentally differentiating a Type I scenario from a Type III (or I+III) scenario is straightforward.

Leading order-accurate Monte Carlo simulations for tree-level processes involving Type III leptons are possible with the `Type III Seesaw` FeynRules UFO model [475, 499, 500], as well as a Minimal Lepton Flavor Violation variant `MLFV Type III Seesaw` [476, 477, 501]. The models can be ported into modern, general-purpose event generators, such at Herwig [289], MadGraph5_aMC@NLO [290], and Sherpa [291].

Hadron collider tests of the Type III Seesaw can be categorized according to the final-state lepton multiplicities, which include: the L-violating, same-sign dilepton and jets final state, $\ell_1^\pm\ell_2^\pm + nj$ [252, 326, 481, 482, 484, 485, 499, 502]; the four-lepton final state, $\ell_1^\pm\ell_2^\pm\ell_3^\mp\ell_4^\mp + nj$ [252, 326, 481, 484, 499]; other charged lepton multiplicities [252, 326, 484, 499, 503]; and also displaced charged lepton vertices [484, 504]. Other "displaced" signatures, include triplet lepton decays to displaced Higgs bosons [505]. Direct searches for Type III Seesaw partners at the $\sqrt{s} = 7/8$ TeV [56, 57, 506] and $\sqrt{s} = 13$ TeV [58, 507, 508] LHC have yet to show evidence of heavy leptons. As shown in **Figure 37A**, triplet masses below $M_T \lesssim 800$ GeV have been excluded at 95% CLs [508]. **Figure 37B** displays the discovery potential of

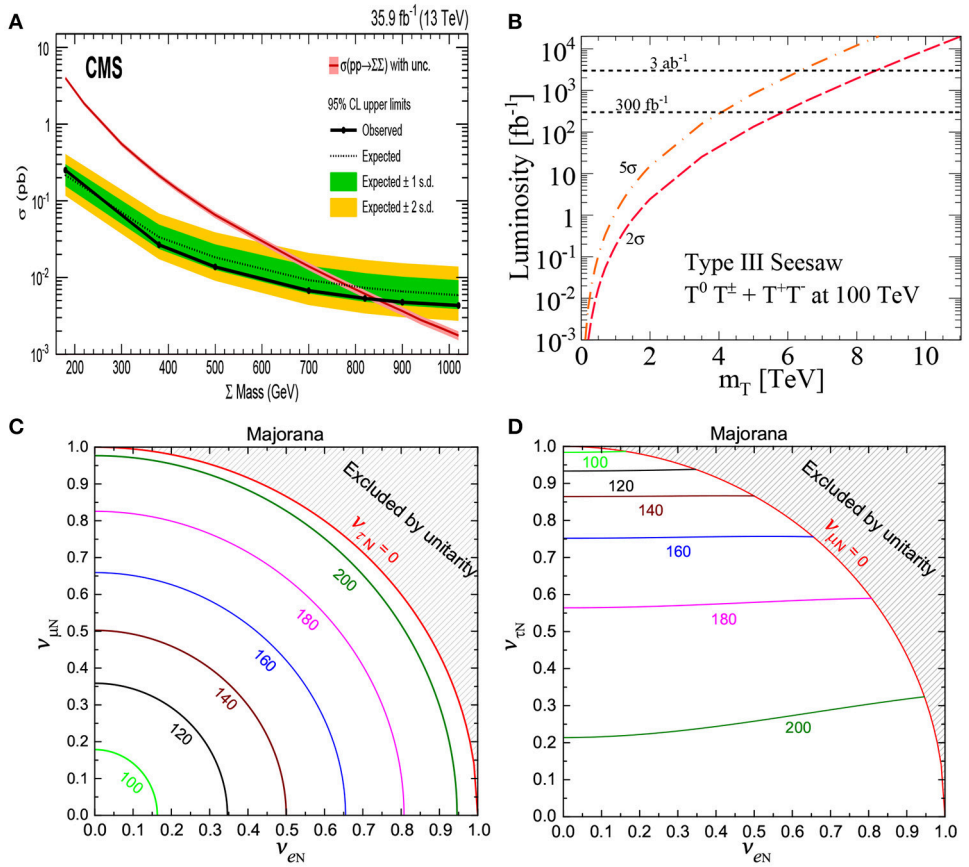

FIGURE 37 | (A) Limits on Type III leptons at $\sqrt{s} = 13$ TeV LHC [58, 508]; **(B)** required luminosity for 2 (5)σ sensitivity (discovery) with fully reconstructible final states [149, 275]. **(C,D)** Exclusion contours of doublet-triplet neutrino mixing in $|V_{\mu N}| - |V_{eN}|$ and $|V_{\tau N}| - |V_{eN}|$ spaces after $\mathcal{L} = 4.9$ fb^{-1} of data at CMS (labels denote heavy neutral lepton mass in GeV) [490].

triplet leptons at high-luminosity 100 TeV collider. One can discover triplet lepton as heavy as 4 (6.5) TeV with 300 (3000) fb^{-1} integrated luminosity. The absence of triplet leptons in multi-lepton final states can also be interpreted as a constrain on doublet-triplet neutrino mixing. In **Figures 37C,D**, one sees the exclusion contours of doublet-triplet neutrino mixing in $|V_{\mu N}| - |V_{eN}|$ and $|V_{\tau N}| - |V_{eN}|$ spaces after $\mathcal{L} = 4.9$ fb^{-1} of data at CMS (labels denote heavy neutral lepton mass in GeV) [490].

5.2.2. Heavy Charged Leptons and Neutrinos at *ee* and *ep* Colliders

The triplet leptons can also be produced at the leptonic colliders like the ILC and the Compact Linear Collider (CLIC) [482, 509], and the electron-hadron collider like LHeC [309]. Besides the similar s-channels as hadron colliders, at e^+e^- colliders, the triplet lepton single and pair productions can also happen in t-channel via the exchange of h, W, or Z boson. Triplet leptons can also lead to anomalous pair production of SM weak bosons [470]. Assuming $M_\Sigma = 500$ GeV and $V_{eN} = 0.05$, the cross sections of triplet lepton single and pair productions are shown in **Figure 38A**. For the single production at 1 TeV e^+e^- collider, the triplet lepton with mass up to about 950-980 GeV can be reached with 300 fb^{-1}. To discover the heavy charged lepton through $e^+e^- \to \Sigma^+\Sigma^-$ production at $\sqrt{s} = 2$ TeV, the luminosity as low (high) as 60 (480) fb^{-1} is needed as shown in **Figure 38B**.

6. RADIATIVE NEUTRINO MASS MODELS AND LEPTON NUMBER VIOLATION AT COLLIDERS

A common feature of the Seesaw mechanisms discussed in the previous sessions is that they are all tree-level, UV completion of the dimension-5 Weinberg operator in of Equation (1.1). Though economical and elegant, these models often imply subtle balancing between a Seesaw mass scale at TeV or below and small Yukawa couplings, in the hope for them to be observable in the current and near future experiments. In an altogether different paradigm, it may be the case that small neutrino masses are instead generated radiatively. In *radiative neutrino mass models*, loop and (heavy) mass factors can contribute to the suppression of light neutrino masses and partly explain their smallness. A key feature of radiative neutrino mass models is that the Weinberg

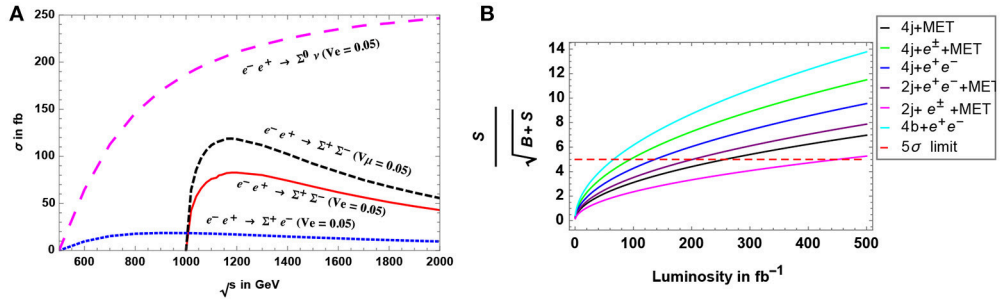

FIGURE 38 | (A) Production cross section of $e^+e^- \to \Sigma^0\nu, \Sigma^\pm e^\mp, \Sigma^+\Sigma^-$ as a function of the center of mass energy for e^+e^- colliders, with $M_\Sigma = 500$ GeV and $V_{eN} = 0.05$ [509]; **(B)** Significance of $\Sigma^+\Sigma^-$ production vs. integrated luminosity at $\sqrt{s} = 2$ TeV [509].

operator is not generated at tree-level: For some models, this may be because the particles required to generate tree-level masses, i.e., SM singlet fermions in Type I, triplet scalars in Type II, or triplet leptons in Type III, do not exist in the theory. For others, it may be the case that the required couplings are forbidden by new symmetries. Whatever the case, it is necessary that the new field multiplets run in the loops to generate neutrino masses.

At one-loop, such models were first proposed in Zee [28] and Hall and Suzuki [29], at two-loop in Cheng and Li [16], Zee [30], and Babu [31], and more recently at three-loop order in Krauss et al. [32]. Besides these early works, a plethora of radiative mass models exist due to the relative ease with which unique loop topologies can be constructed at a given loop order, as well as the feasibility to accommodate loop contributions from various exotic particles, including leptoquarks, vector-like leptons and quarks, electrically charged scalars, and EW multiplets. For a recent, comprehensive review, see Cai et al. [510].

However, the diversity of the exotic particles and interactions in radiative neutrino mass models make it neither feasible nor pragmatic to develop a simple and unique strategy to test these theories at colliders. Although some effort has been made to advance approaches to collider tests of radiative neutrino mass models more systematically [511, 512], it remains largely model-dependent. As a comprehensive summary of the literature for radiative neutrino mass models and their collider study is beyond the scope of this review, in this section, we focus on a small number of representative models with distinctive L-violating collider signatures.

It is worth pointing out that some popular radiative neutrino mass models do not predict clear lepton number violation at collider scales. A prime example are the Scotogenic models [513], a class of one-loop radiative neutrino mass scenario with a discrete Z_2 symmetry. Scotogenic models typically contain three SM singlet fermions N_i with Majorana masses and are odd under the Z_2, whereas SM fields are even. The discrete symmetry forbids the mixing between the SM neutrinos and N_i that one needs to trigger the Type I and III Seesaw mechanisms. As a result, collider strategies to search for lepton number violation mediated by heavy Majorana neutrinos as presented in section 3 are not applicable to the Scotogenic model. Instead, collider tests of Scotogenic models include, for example, searches for the additional EW scalars [514–517] that facilitate lepton number conserving processes. Subsequently, we avoid further discussing radiative models without collider-scale lepton number violation.

Like in the previous sections, we first present in section 6.1 an overview of representative radiative models. Then, in section 6.2, we review collider searches for lepton number violation associated with radiative neutrino mass models.

6.1. Selected Radiative Neutrino Mass Models

6.1.1. The Zee-Babu Model

The first radiative scenario we consider is the well-known Zee-Babu model, a two-loop radiative neutrino mass model proposed independently by Zee [30] and Babu [31]. In the model, the SM field content is extended by including one singly-charged scalar ($h^\pm$) and one doubly-charged scalar ($k^{\pm\pm}$). Both scalars are singlets under $SU(3)_c \times SU(2)_L$, leading to the lepton number violating interaction Lagrangian

$$\Delta\mathcal{L} = \bar{L}Y^\dagger e_R H + \bar{\tilde{L}} f L h^+ + \overline{e_R^c} g e_R k^{++} + \mu_{ZB} h^+ h^+ k^{--} + \text{H.c.}, \tag{6.1}$$

where L (H) is the SM LH lepton (Higgs) doublet. The 3×3 Yukawa coupling matrices f and g are anti-symmetric and symmetric, respectively. The trilinear coupling μ_{ZB} contributes to the masses of the charged scalars at the loop level. For large values of $(\mu_{ZB}/m_{h^\pm})$ or $(\mu_{ZB}/m_{k^{\pm\pm}})$, where $m_{h^\pm, k^{\pm\pm}}$ are the masses of $h^\pm$ and $k^{\pm\pm}$, the scalar potential may have QED-breaking minima. This can be avoided by imposing the condition $|\mu_{ZB}| \ll 4\pi \min(m_h, m_k)$.

The combined presence of Y, f, g and μ_{ZB} collectively break lepton number and lead to the generation of a small Majorana neutrino mass. At lowest order, neutrino masses in the Zee-Babu model arise at two-loop order, as depicted in **Figure 39A**. The resulting neutrino mass matrix scales as

$$\mathcal{M}_\nu \simeq \left(\frac{v^2 \mu_{ZB}}{96\pi^2 M^2}\right) f Y g^\dagger Y^T f^T, \tag{6.2}$$

where $M = \max(m_{h^\pm}, m_{k^{\pm\pm}})$ is the heaviest mass in the loop. Since f is antisymmetric, the determinant of the neutrino mass

matrix vanishes, $\det \mathcal{M}_\nu = 0$. Therefore the Zee-Babu models yields at least one exactly massless neutrino. An important consequence is that the heaviest neutrino mass is determined by the atmospheric mass difference, which can be estimated as

$$m_\nu \approx 6.6 \times 10^{-3} f^2 g \left(\frac{m_\tau^2}{M}\right) \approx 0.05 \text{ eV} , \tag{6.3}$$

where $m_\tau \approx 1.778$ GeV is the tau lepton mass. This implies the product $f^2 g$ can not be arbitrarily small, e.g., for $M \sim 100$ GeV, one finds $g^2 f \gtrsim 10^{-7}$. Subsequently, the parameter space of the Zee-Babu model is constrained by both neutrino oscillation data, low-energy experiments such as decays mediated $k^{\pm\pm}$ at tree level, and high-energy searches for direct pair production of $k^{\pm\pm}$.

The study of $h^\pm$ is mostly similar to that of the singly-charged scalar in the Zee model [28], although the lepton number violating effects are not experimentally observable due to the missing information carried away by the light (Majorana) neutrino in the decay product. The doubly-charged scalar $k^{\pm\pm}$ can decay to a pair of same-sign leptons, which manifestly violates lepton number by $\Delta L = \pm 2$, with a partial decay width given by

$$\Gamma(k^{\pm\pm} \to \ell_a^\pm \ell_b^\pm) = \frac{|g_{ab}|^2}{4\pi(1+\delta_{ab})} m_k . \tag{6.4}$$

If $m_{k^{\pm\pm}} > 2m_{h^\pm}$, then the $k^{\pm\pm} \to h^\pm h^\pm$ decay mode opens with a partial decay width of

$$\Gamma(k^{\pm\pm} \to h^\pm h^\pm) = \frac{m_{k^{\pm\pm}}}{8\pi} \left(\frac{\mu_{ZB}}{m_{k^{\pm\pm}}}\right)^2 \sqrt{1 - \frac{4m_{h^\pm}^2}{m_{k^{\pm\pm}}^2}} . \tag{6.5}$$

Doubly-charged scalars, appear in many other radiative neutrino mass models, including the three-loop Cocktail Model [518], whose eponymous mass-generating diagram is shown in the right panel of **Figure 39**. The doubly-charged scalar couples to the SM lepton doublet and a singly-charged scalar in the same manner as in the Zee-Babu model, and thus again is similar to a Type II scenario. Radiative Type II Seesaw model [519] that generates neutrino mass at one-loop order contains an $SU(2)_L$ triplet scalar and thus also has similar LHC phenomenology as the tree-level Type II Seesaw mechanism [520].

6.1.2. The Colored Zee-Babu Model With Leptoquark

In a particularly interesting variant of the Zee-Babu model, proposed in Kohda et al. [521], all particles in the neutrino mass-loop are charged under QCD. As shown in **Figure 40**, the lepton doublet in the loop of the Zee-Babu model is replaced with down-type quark while the singly- and doubly-charged scalars are replaced with a leptoquark $S_{LQ}^{-\frac{1}{3}}$ and a diquark $S_{DQ}^{-\frac{2}{3}}$. Under the SM gauge group, the leptoquark and diquark quantum numbers are

$$S_{LQ}^{-\frac{1}{3}} \;:\; (3,1,-\frac{1}{3}) \quad \text{and} \quad S_{DQ}^{-\frac{2}{3}} \;:\; (6,1,-\frac{2}{3}) . \tag{6.6}$$

The decay of the diquark $S_{DQ}^{-\frac{2}{3}}$ is analogous to that of the doubly-charged scalar $k^{\pm\pm}$ in that it can decay to a pair of same-sign down-type quarks or a pair of same-sign leptoquarks, if kinematically allowed.

For the models mentioned above, we will only review the collider study with the characteristics different from the tree-level Seesaws in the following.

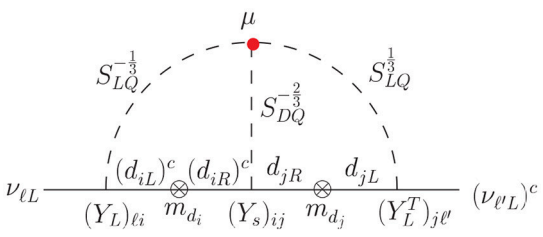

FIGURE 40 | Feynman diagram for the generation of neutrino masses at two-loop order in the colored Zee-Babu model [521].

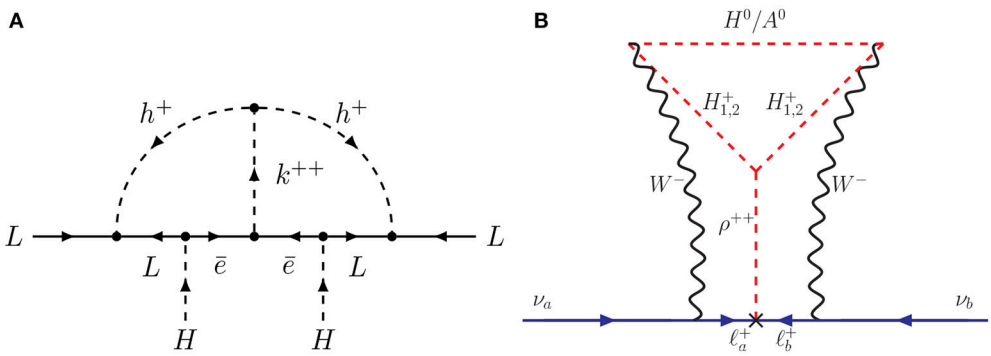

FIGURE 39 | (A) Feynman diagram for the generation of neutrino masses at two-loop order in the Zee-Babu model. **(B)** Feynman diagram at three-loop order in the cocktail model [518].

6.2. Radiative Neutrino Mass Models at Colliders

6.2.1. Doubly-Charged Scalar at the LHC

As mentioned above, the Zee-Babu model contains two singlet charged scalars, $h^{\pm}$ and $k^{\pm\pm}$. Moreover, due to the presence of the doubly-charged scalar decay mode to two same-sign leptons $k^{\pm\pm} \to \ell^{\pm}\ell^{\pm}$ via the coupling μ_{ZB}, collider searches for L-violating effects in the context of the Zee-Babu model are centered on $k^{\pm\pm}$ and its decays.

Like the triplet Higgs in Type II Seesaw, the doubly-charged scalar $k^{\pm\pm}$ can be pair produced via the Drell-Yan process at the LHC if kinematically accessible and is given by

$$pp \to \gamma^*/Z^* \to k^{++}k^{--}. \tag{6.7}$$

This is the same process as shown in **Figure 28A**. However, an important distinction is that while $H^{\pm\pm}$ in the Type II Seesaw is an $SU(2)_L$ triplet, the $k^{\pm\pm}$ here is a singlet. As this quantum-number assignment leads to different Z boson couplings, and hence different production cross section at colliders, it is a differentiating characteristic of the model. Note the $\gamma\gamma$ fusion processes, shown in **Figure 28**, also applies to $k^{++}k^{--}$ pair production and leads to the same production cross section.

Since the collider signal for pair produced $k^{\pm\pm}$ is the same as $H^{\pm\pm}$ in the Type II Seesaw, the search for doubly-charged scalar can be easily performed for both cases as shown in **Figure 31**. Obviously the constraint on the singlet is less stringent due to the absence of weak isospin interactions. With 36.1 fb^{-1} data at 13 TeV, ATLAS has excluded $k^{\pm\pm}$ mass lower than 656-761 GeV for $\mathrm{BR}(k^{\pm\pm} \to e^{\pm}e^{\pm}) + \mathrm{BR}(k^{\pm\pm} \to \mu^{\pm}\mu^{\pm}) = 1$ at 95% CLs [460].

Low energy LFV experiments, especially $\mu \to e\gamma$, impose very stringent constraints on the parameter space of the Zee-Babu model. The MEG experiment [522, 523] has placed an upper bound on the decay branching ratio $\mathrm{BR}(\mu \to e\gamma) < 4.2 \times 10^{-13}$, which can be roughly translated as [524]

$$\left|f_{13}^* f_{23}\right|^2 \frac{m_{k^{\pm\pm}}^2}{m_{h^{\pm}}^2} + 16\left|\sum g_{1i}^* g_{i2}\right|^2 < 1.2 \times 10^{-6}\left(\frac{m_k}{\mathrm{TeV}}\right)^4 . \tag{6.8}$$

To satisfy LFV constraints, the doubly- and singly-charged scalar masses are pushed well above TeV, with $m_{k^{\pm\pm}} > 1.3$ (1.9) TeV and $m_{h^{\pm}} > 1.3$ (2.0) TeV for the NH (IH), assuming $\mu_{ZB} = min(m_{k^{\pm\pm}}, m_{h^{\pm}})$. This can be very easily relaxed, however, by choosing larger μ_{ZB} and balancing smaller Yukawa couplings to generate the right neutrino mass spectrum.

A recent study has projected the sensitivities of the LHC with large luminosities by scaling the cross section bound by $1/\sqrt{\mathcal{L}}$ for two benchmark scenarios: one for NH and one for IH [525]. The projected sensitivities are shown in **Figure 41** for model parameters consistant with neutrino oscillation data. Note that these benchmarks are chosen to have $\mu_{ZB} = 5\,\mathrm{min}(m_{k^{\pm\pm}}, m_{h^{\pm}})$ such that the constraints from flavor experiments such as $\mu \to e\gamma$ are much less stringent at the price of a more fine-tuned the scalar potential. We can see that the NH benchmark is less constrained than the IH one when $m_{k^{\pm\pm}} < 2m_{h^{\pm}}$ because $k^{\pm\pm}$ has a smaller branching ratio to leptons.

6.2.2. Leptoquark at the LHC

In the colored Zee-Babu model, L-violating signals can be observed in events with pair produced leptoquarks $S_{LQ}^{-\frac{1}{3}}$ via s-channel diquark $S_{DQ}^{-\frac{2}{3}}$, shown in **Figure 42**, and given by,

$$pp \to S_{DQ}^{-\frac{2}{3}*} \to S_{LQ}^{-\frac{1}{3}} S_{LQ}^{-\frac{1}{3}} \to u\ell^- u\ell'^-. \tag{6.9}$$

One benchmark has been briefly studied in Kohda et al. [521]. For leptoquark mass of 1 TeV and diquark mass of 4 TeV, a benchmark consistent with neutrino oscillation data and low energy experiments, the L-violating process in Equation (6.9) can proceed with an LHC cross section of 0.18 fb at $\sqrt{s} = 14$ TeV. So far, no dedicated collider study for this model. In general, however, one can recast either ATLAS or CMS search for heavy neutrinos, such as Aad et al. [52] and Khachatryan et al. [363], to derive the limit on the model parameter space.

Lepton number violating collider processes, $pp \to \ell^{\pm}\ell^{\pm} + nj$, involving charged scalars, leptoquarks and diquarks have also been studied for the LHC in Peng et al. [394], Helo et al. [526, 527]. Example diagrams are shown in **Figure 43**. Even though these studies are performed without a concrete neutrino mass model, they possess the most important ingredient of Majorana neutrino mass models: L violation by two units. Therefore radiative neutrino mass models can be constructed from the relevant matter content. Some processes, however, are realized with a SM singlet fermion (for example the left panel of **Figure 43**), which implies the existence of a tree-level Seesaw. Other processes without SM singlet fermions, $\mathrm{SU}(2)_L$ triplet scalars, or triplet fermions, such as the one on the right panel of **Figure 43**, can be realized in a radiative neutrino mass model. Detailed kinematical analyses for resonant mass reconstruction would help to sort out the underlying dynamics.

6.2.3. Correlation With Lepton Flavor Violation

In radiative neutrino mass models the breaking of lepton number generally needs the simultaneous presence of multiple couplings. For example, in the Zee-Babu model, Y, f, g and μ_{ZB} together break lepton number. The observation of pair produced $k^{\pm\pm}$ itself is insufficient to declare L violation. In order to establish L violation in the theory and thus probe the Majorana nature of the neutrinos, the couplings of $h^{\pm}$ to SM leptons and to $k^{\pm\pm}$ have to be studied at the same time. For the colored Zee-Babu model, the L violation process shown in **Figure 42** involves all couplings except the SM Yukawa necessary to break the lepton number. Note, however, the cross section for this process is proportional to the product of couplings and suppressed by the heavy exotic masses which both contributes to the smallness of the neutrino masses. Thus the cross section for this processes must be kinematically suppressed. For radiative neutrino mass models with dark matter candidates, probing lepton number violation at colliders alone is generally much more difficult as the dark matter candidate appears as missing transverse energy just as neutrinos. Overall, the study of L-violation of radiative neutrino mass models can be performed either with the combination of different processes that test different subsets of

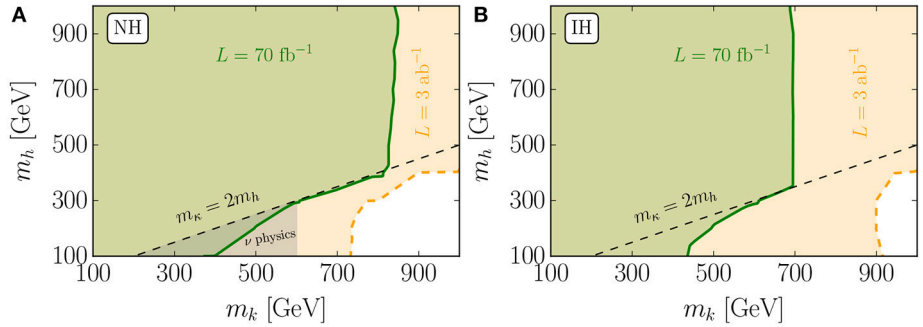

FIGURE 41 | Projection of sensitivities at the LHC in the $m_{k^{\pm\pm}}$-$m_{h^\pm}$ plane: **(A)** the NH benchmark with $g_{11,22} = 0.1$, $g_{12,13,33} = 0.001$, $f_{12,13} = 0.01$ and $f_{23} = 0.02$; **(B)** the IH benchmark with $g_{11,23} = 0.1$, $g_{12,22,13,33} = 0.0001$, $f_{12} = -f_{13} = 0.1$ and $f_{23} = 0.01$. For both benchmarks, the trilinear coupling is chosen to be $\mu_{ZB} = 5\ \min(m_{k^{\pm\pm}}, m_{h^\pm})$. The gray shaded region in the left panel is excluded by low energy experiments. The green and orange regions are excluded by future experiments with an integrated luminosity of 70 fb^{-1} and 3 ab^{-1} respectively [525].

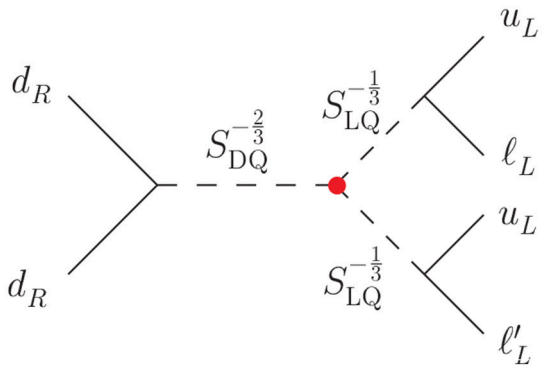

FIGURE 42 | L-violating processes at the LHC in the colored Zee-Babu model [521].

the couplings or in a single process that involves all couplings at once whose production cross section is generally suppressed.

On the contrary, radiative neutrino mass models contain LFV couplings and exotic particles that can be tested much easier than L violation stated above. The search strategies for LFV couplings and new particles vary from model to model. It is definitely impossible to cover all and they are also not the focus of this review. Thus we will take a few simple examples to illustrate the searches.

The leading LFV signals can be produced in a radiative neutrino mass model from the QCD pair production of the leptoquark $S_{LQ}^{-\frac{1}{3}}$ with its suitable subsequent decays such as

$$pp \to S_{LQ}^{+\frac{1}{3}} S_{LQ}^{-\frac{1}{3}} \to \bar{t}\ell^+ t\ell'^- \tag{6.10}$$

where $S_{LQ}^{+\frac{1}{3}} = \left(S_{LQ}^{-\frac{1}{3}}\right)^*$ and the top quarks decay hadronically. Note that the leptoquark pair can also decay to $\bar{b}\nu_\ell\ t\ell'^-$ or $\bar{b}\nu_\ell\ b\bar{\nu}_{\ell'}$, where the LFV effects are not easy to disentangle at colliders due to the invisible neutrinos. However, these decay channels can result in final states $\ell^+\ell'^- X$, inclusive flavour off-diagonal charged lepton pair accompanied by missing transverse energy, jets etc., if the quarks decay to appropriate leptons. The same final states have been used to search for stop in SUSY theories and thus the results for stop searches at the LHC can be translated to that of the leptoquark $S_{LQ}^{-\frac{1}{3}}$, $m(S_{LQ}^{-\frac{1}{3}}) \gtrsim 600$ GeV [511] based on the ATLAS stop search at $\sqrt{s} = 8$ TeV [528] [5]. No recast of stop search has been performed for 13 TeV run yet. Besides leptoquarks, radiative neutrino mass models also comprise exotic particles such as vector-like quarks, vector-like leptons, charged scalar singlets (both singly- and doubly-charged) and higher-dimensional EW multiplets. For example, disappearing tracks can be used to search for higher-dimensional EW multiplet fermions whose mass splitting between the neutral and the singly-charged component is around 100 MeV. The current LHC searches have set a lower mass limit of 430 GeV at 95% CL for a triplet fermion with a lifetime of about 0.2 ns [534–536]. We refer the readers to the section about collider tests of radiative neutrino mass model in Cai et al. [510] and the references therein for details.

We want to stress, however, that even though L violation in the radiative models is more complicated and challenging to search for in collider experiments, their observation is essential and conclusive to establish the Majorana nature of neutrinos. So once we find signals in either LFV processes or new particles searches, we should search for L violation in specific radiative neutrino mass models that give these LFV processes or contain these new particles, in order to ultimately test the generation of neutrino masses.

7. SUMMARY AND CONCLUSIONS

Exploring the origin of neutrinos' tiny masses, their large mixing, and their Dirac or Majorana nature are among the most pressing

[5] There are many dedicated leptoquark searches at the LHC [529–533]. However, the leptoquarks searched only couple to one generation of fermions at a time and thus generate no LFV signals.

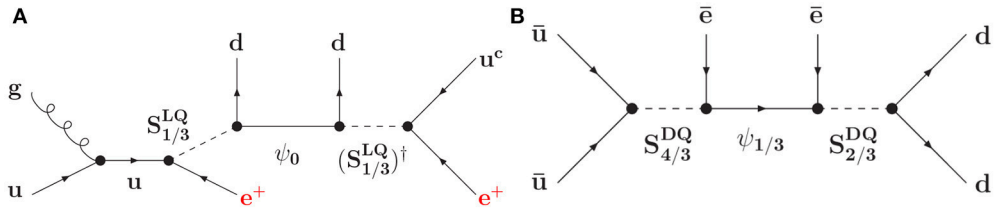

FIGURE 43 | Example diagrams of L violation processes with **(A)** leptoquark $S^{LQ}_{1/3}$ and **(B)** diquarks $S^{DQ}_{4/3,2/3}$ [526, 527]. The singlet fermion ψ_0 in the left panel leads to Type I Seesaw.

issues in particle physics today. If one or more neutrino Seesaw mechanisms are realized in nature, it would be ultimately important to identify the new scales responsible for generating neutrino masses. Neutrino oscillation experiments, however, may not provide such information, and thus complementary pathways, such as collider experiments, are vital to understanding the nature of neutrinos. Observing lepton number violation at collider experiments would be a conclusive verdict for the existence of neutrino Majorana masses, but also direct evidence of a mass scale qualitatively distinct from those in the SM.

In this context, we have reviewed tests of low-scale neutrino mass models at *pp*, *ep*, and *ee* colliders, focusing particularly on searches for lepton number (L) violation: We begin with summarizing present neutrino oscillation and cosmology data and their impact on the light neutrino mass spectra in section 2. We then consider several representative scenarios as phenomenological benchmarks, including the characteristic Type I Seesaw in section 3, the Type II Seesaw in section 4, the Type III in section 5, radiative constructions in section 6, as well as extensions and hybridizations of these scenarios. We summarize the current status of experimental signatures featuring L violation, and present anticipated coverage in the theory parameter space at current and future colliders. We emphasize new production and decay channels, their phenomenological relevance and treatment across different collider facilities. We also summarize available Monte Carlo tools available for studying Seesaw partners in collider environments.

The Type I Seesaw is characterized by new right-handed, SM gauge singlet neutrinos, known also as "sterile neutrinos," which mix with left-handed neutrinos via mass diagonalization. As this mixing scales with light neutrino masses and elements of the PMNS matrix, heavy neutrino decays to charged leptons may exhibit some predictable patterns if one adopts some simplifying assumptions for the mixing matrix, as shown for example in **Figures 3**, **4**, that are correlated with neutrino oscillation data. The canonical high-scale Type I model, however, predicts tiny active-sterile mixing, with $|V_{\ell N}|^2 \sim m_\nu/M_N$, and thus that heavy N decouple from collider experiments. Subsequently, observing lepton number violation in collider experiments, as discussed in section 3.2, implies a much richer neutrino mass-generation scheme than just the canonical, high-scale Type I Seesaw. In exploring the phenomenological parameter space, the 14 TeV LHC (and potential 100 TeV successor) and $\mathcal{L} = 1$ ab^{-1} integrated luminosity could reach at least 2σ sensitivity for heavy neutrino masses of $M_N \lesssim 500$ GeV (1 TeV) with a mixing $|V_{\ell N}|^2 \lesssim 10^{-3}$, as seen in **Figure 9**. If N is charged under another gauge group that also couples to the SM, as in B-L or LR gauge extensions, then the discovery limit may be extended to $M_N \sim M_{Z'}, M_{W_R}$, when kinematically accessible; see sections 3.2.4 and 3.2.5.

The Type II Seesaw is characterized by heavy SU(2)$_L$ triplet scalars, which result in new singly- and doubly-charged Higgs bosons. They can be copiously produced in pairs via SM electroweak gauge interactions if kinematically accessible at collider energies, and search for the doubly-charged Higgs bosons via the same-sign dilepton channel $H^{\pm\pm} \to \ell^\pm\ell^\pm$ is an on-going effort at the LHC. Current direct searches at 13 TeV bound triplet scalar masses to be above (roughly) 800 GeV. With anticipated LHC luminosity and energy upgrades, one can expect for the search to go beyond a TeV. Furthermore, if neutrino masses are dominantly from triplet Yukawa couplings, then the patterns of the neutrino mixing and mass relations from the oscillation experiments will correlate with the decays of the triplet Higgs bosons to charged leptons, as seen from the branching fraction predictions in **Figures 25**, **26** and in **Table 2**. Since a Higgs triplet naturally exists in certain extensions beyond the SM, such as in Little Higgs theory, the LRSM, and GUT theories, the search for such signals may prove beneficial as discussed in section 4.2.2.

The Type III Seesaw is characterized by heavy SU(2)$_L$ triplet leptons, which result in vector-like, charged and neutral leptons. Such multiplets can be realized in realistic GUT theories in hybridization with heavy singlet neutrinos from a Type I Seesaw. Drell-Yan pair production of heavy charged leptons at hadron colliders is sizable as it is governed by the SM gauge interactions. They can decay to the SM leptons plus EW bosons, leading to same-sign dilepton events. Direct searches for promptly decaying triplet leptons at the LHC set a lower bound on the triplet mass scale of around 800 GeV. A future 100 TeV *pp* collider can extend the mass reach to at least several TeV, as seen in **Figure 37**.

Finally, neutrino masses can also be generated radiatively, which provides an attractive explanation for the smallness of neutrino masses with a plausibly low mass scale. Among the large collection of radiative neutrino mass models, the Zee-Babu model contains a doubly-charged SU(2)$_L$ singlet scalar with collider signal akin to the doubly-charged Higgs in the Type II Seesaw. ATLAS has excluded $k^{\pm\pm}$ mass below $660 - 760$ GeV assuming the benchmark decay rate $\sum_{\ell_i=e,\mu} \text{BR}(k^{\pm\pm} \to \ell_1^\pm \ell_2^\pm) = 1$. The high luminosity LHC is sensitive up to about a TeV for both $k^{\pm\pm}$ and its companion scalar $h^\pm$ in the Zee-Babu model with constraints from neutrino oscillation data and other low energy

experiments. For the colored variant of the Zee-Babu model, a pair of same-sign leptoquark can be produced via an *s*-channel diquark at the LHC. Their subsequent decay lead to the lepton number violating same-sign dilepton plus jets final state, which still await dedicated studies.

As a final remark, viable low-scale neutrino mass models often generate a rich flavor structure in the charged lepton sector that predict lepton flavor-violating transitions. Such processes are typically much more easily observable than lepton number violating processes, in part due to their larger production and decay rates, and should be searched for in both high- and low-energy experiments.

AUTHOR CONTRIBUTIONS

The conception and content scope of this review was mainly designed by TH. TL edited the chapter on neutrino masses; TL and RR edited the chapters on the Type I, II, III seesaw models and their collider tests; YC edited the chapter on radiative neutrino mass models. TH drafted the concluding section. TH and RR revised the manuscript critically for important, intellectual content and expressions. Most of the materials compiled in the review came from the early publications from the collective works by the authors.

ACKNOWLEDGMENTS

We thank Michael A. Schmidt for useful discussions. Past and present members of the IPPP are thanked for discussions. The work of TH was supported in part by the U.S. Department of Energy under grant No. DE-FG02-95ER40896 and in part by the PITT PACC. The work of TL was supported in part by the Australian Research Council Centre of Excellence for Particle Physics at the Tera-scale. The work of RR was funded in part by the UK Science and Technology Facilities Council (STFC), the European Union's Horizon 2020 research and innovation programme under the Marie Sklodowska-Curie grant agreements No 690575 (InvisiblesPlus RISE) and No 674896 (InvisiblesPlus RISE). Support for the open accessibility of this work is provided by the Research Councils UK, external grant number ST/G000905/1.

REFERENCES

1. Pontecorvo B. Inverse beta processes and nonconservation of lepton charge. *Sov Phys JETP* (1958) **7**:172–3.
2. Pontecorvo B. Mesonium and anti-mesonium. *Sov Phys JETP* (1957) **6**:429.
3. Maki Z, Nakagawa M, Sakata S. Remarks on the unified model of elementary particles. *Prog Theor Phys.* (1962) **28**:870–80. doi: 10.1143/PTP.28.870
4. Weinberg S. A model of leptons. *Phys Rev Lett.* (1967) **19**:1264–66. doi: 10.1103/PhysRevLett.19.1264
5. Ma E. Pathways to naturally small neutrino masses. *Phys Rev Lett.* (1998) **81**:1171–4. doi: 10.1103/PhysRevLett.81.1171
6. Majorana E. Teoria simmetrica dellelettrone e del positrone. *Nuovo Cim.* (1937) **14**:171–84. doi: 10.1007/BF02961314
7. Weinberg S. Baryon and lepton nonconserving processes. *Phys Rev Lett.* (1979) **43**:1566–70. doi: 10.1103/PhysRevLett.43.1566
8. Minkowski P. $\mu \to e\gamma$ at a rate of one out of 10^9 muon decays? *Phys Lett.* (1977) **67B**:421–8. doi: 10.1016/0370-2693(77)90435-X
9. Yanagida T. Horizontal Symmetry and masses of neutrinos. *Conf Proc.* (1979) **C7902131**:95–9.
10. Gell-Mann M, Ramond P, Slansky R. Complex spinors and unified theories. *Conf Proc.* (1979) **C790927**:315–21.
11. Glashow SL. The future of elementary particle physics. *NATO Sci Ser B* (1980) **61**:687. doi: 10.1007/978-1-4684-7197-7_15
12. Mohapatra RN, Senjanović G. Neutrino mass and spontaneous parity violation. *Phys Rev Lett.* (1980) **44**:912. doi: 10.1103/PhysRevLett.44.912
13. Shrock RE. General theory of weak leptonic and semileptonic decays. 1. Leptonic pseudoscalar meson decays, with associated tests for, and bounds on, neutrino masses and lepton mixing. *Phys Rev.* (1981) **D24**:1232. doi: 10.1103/PhysRevD.24.1232
14. Schechter J, Valle JWF. Neutrino masses in SU(2) ⊗ U(1) theories. *Phys Rev.* (1980) **D22**:2227. doi: 10.1103/PhysRevD.22.2227
15. Konetschny W, Kummer W. Nonconservation of total lepton number with scalar bosons. *Phys Lett.* (1977) **70B**:433–5. doi: 10.1016/0370-2693(77)90407-5
16. Cheng TP, Li LF. Neutrino masses, mixings and oscillations in SU(2) × U(1) models of electroweak interactions. *Phys Rev.* (1980) **D22**:2860. doi: 10.1103/PhysRevD.22.2860
17. Lazarides G, Shafi Q, Wetterich C. Proton lifetime and fermion masses in an SO(10) model. *Nucl Phys.* (1981) **B181**:287–300. doi: 10.1016/0550-3213(81)90354-0
18. Mohapatra RN, Senjanović G. Neutrino masses and mixings in gauge models with spontaneous parity violation. *Phys Rev.* (1981) **D23**:165. doi: 10.1103/PhysRevD.23.165
19. Foot R, Lew H, He XG, Joshi GC. Seesaw neutrino masses induced by a triplet of leptons. *Z Phys.* (1989) **C44**:441.
20. Wyler D, Wolfenstein L. Massless neutrinos in left-right symmetric models. *Nucl Phys.* (1983) **B218**:205–14. doi: 10.1016/0550-3213(83)90482-0
21. Mohapatra RN. Mechanism for understanding small neutrino mass in superstring theories. *Phys Rev Lett.* (1986) **56**:561–3. doi: 10.1103/PhysRevLett.56.561
22. Mohapatra RN, Valle JWF. Neutrino mass and baryon number nonconservation in superstring models. *Phys Rev.* (1986) **D34**:1642. doi: 10.1103/PhysRevD.34.1642
23. Bernabéu J, Santamaria A, Vidal J, Mendez A, Valle JWF. Lepton flavor nonconservation at high-energies in a superstring inspired standard model. *Phys Lett.* (1987) **B187**:303–8. doi: 10.1016/0370-2693(87)91100-2
24. Gavela MB, Hambye T, Hernandez D, Hernandez P. Minimal flavour seesaw models. *J High Energy Phys.* (2009) **9**:38. doi: 10.1088/1126-6708/2009/09/038
25. Akhmedov EK, Lindner M, Schnapka E, Valle JWF. Left-right symmetry breaking in NJL approach. *Phys Lett.* (1996) **B368**:270–80. doi: 10.1016/0370-2693(95)01504-3
26. Akhmedov EK, Lindner M, Schnapka E, Valle JWF. Dynamical left-right symmetry breaking. *Phys Rev.* (1996) **D53**:2752–2780. doi: 10.1103/PhysRevD.53.2752
27. Moffat K, Pascoli S, Weiland C. Equivalence between massless neutrinos and lepton number conservation in fermionic singlet extensions of the Standard Model. (2017) *arXiv:1712.07611*.
28. Zee A. A theory of lepton number violation, neutrino majorana mass, and oscillation. *Phys Lett.* (1980) **93B**:389. doi: 10.1016/0370-2693(80)90349-4
29. Hall LJ, Suzuki M. Explicit R-parity breaking in supersymmetric models. *Nucl Phys.* (1984) **B231**:419–44. doi: 10.1016/0550-3213(84)90513-3

30. Zee A. Quantum numbers of majorana neutrino masses. *Nucl Phys.* (1986) **B264**:99–110. doi: 10.1016/0550-3213(86)90475-X
31. Babu KS. Model of 'calculable' majorana neutrino masses. *Phys Lett.* (1988) **B203**:132–6. doi: 10.1016/0370-2693(88)91584-5
32. Krauss LM, Nasri S, Trodden M. A model for neutrino masses and dark matter. *Phys Rev.* (2003) **D67**:085002. doi: 10.1103/PhysRevD.67.085002
33. Schechter J, Valle JWF. Neutrinoless double-β decay in SU(2) $\times$ U(1) theories. *Phys Rev.* (1982) **D25**:2951.
34. Hirsch M, Kovalenko S, Schmidt I. Extended black box theorem for lepton number and flavor violating processes. *Phys Lett.* (2006) **B642**:106–10. doi: 10.1016/j.physletb.2006.09.012
35. Duerr M, Lindner M, Merle A. On the quantitative impact of the schechter-valle theorem. *J High Energy Phys.* (2011) **6**:91. doi: 10.1007/JHEP06(2011)091
36. Gando A, Gando Y, Hachiya T, Hayashi A, Hayashida S, Ikeda H. Search for majorana neutrinos near the inverted mass hierarchy region with KamLAND-Zen. *Phys Rev Lett.* (2016) **117**:082503. doi: 10.1103/PhysRevLett.117.082503
37. Agostini M, Allardt M, Bakalyarov AM, Balata M, Barabanov I, Baudis L, et al. Background free search for neutrinoless double beta decay with GERDA Phase II. (2017) *Nature* **544**:47. doi: 10.1038/nature21717
38. Alfonso K, Artusa DR, Avignone FT 3rd, Azzolini O, Balata M, Banks TI, et al. Search for neutrinoless double-beta decay of ^{130}Te with CUORE-0. *Phys Rev Lett.* (2015) **115**:102502. doi: 10.1103/PhysRevLett.115.102502
39. Albert JB, Auty DJ, Barbeau PS, Beauchamp E, Beck D, Belov V, et al. Search for Majorana neutrinos with the first two years of EXO-200 data. *Nature* (2014) **510**:229–34. doi: 10.1038/nature13432
40. Arnaboldi C, Avignone FT, Beeman J, Barucci M, Balata M, Brofferio C, et al. CUORE: a Cryogenic underground observatory for rare events. *Nucl Instrum Meth.* (2004) **A518**:775–98. doi: 10.1016/j.nima.2003.07.067
41. Arnold R, Augier C, Baker J, Barabash AS, Basharina-Freshville A, Bongrand M, et al. Probing new physics models of neutrinoless double beta decay with superNEMO. *Eur Phys J.* (2010) **C70**:927–43. doi: 10.1140/epjc/s10052-010-1481-5
42. Alvarez V, Borges FIGM, Cárcel S, Carmona JM, Castel J, Catalá JM, et al. NEXT-100 technical design report (TDR): executive summary. *J Instrum.* (2012) **7**:T06001. doi: 10.1088/1748-0221/7/06/T06001
43. Alekhin S, Altmannshofer W, Asaka T, Batell B, Bezrukov F, Bondarenko K, et al. A facility to Search for Hidden Particles at the CERN SPS: the SHiP physics case. *Rept Prog Phys.* (2016) **79**:124201. doi: 10.1088/0034-4885/79/12/124201
44. Anelli M, Aoki S, Arduini G, Back JJ, Bagulya A, Baldini W. A facility to Search for Hidden Particles (SHiP) at the CERN SPS. (2015) *arXiv:1504.04956*.
45. Liventsev D, Adachi I, Aihara H, Arinstein K, Asner DM, Aulchenko V, et al. Search for heavy neutrinos at Belle. *Phys Rev.* (2013) **D87**:071102. doi: 10.1103/PhysRevD.87.071102
46. Aaij R, Abellan Beteta C, Adeva B, Adinolfi M, Adrover C, Affolder A, et al. Searches for Majorana neutrinos in B^- decays. *Phys Rev.* (2012) **D85**:112004. doi: 10.1103/PhysRevD.85.112004
47. Aaij R, Adeva B, Adinolfi M, Affolder A, Ajaltouni Z, Albrecht J, et al. Search for Majorana neutrinos in $B^- \to \pi^+\mu^-\mu^-$ decays. *Phys Rev Lett.* (2014) **112**:131802. doi: 10.1103/PhysRevLett.112.131802
48. Sirunyan AM, Tumasyan A, Adam W, Aşilar E, Bergauer T, Brandstetter J. Search for third-generation scalar leptoquarks and heavy right-handed neutrinos in final states with two tau leptons and two jets in proton-proton collisions at $\sqrt{s} = 13$ TeV. *J High Energy Phys.* (2017) **7**:121. doi: 10.1007/JHEP07(2017)121
49. Khachatryan V, Sirunyan AM, Tumasyan A, Adam W, Aşilar E, Bergauer T. Search for heavy neutrinos or third-generation leptoquarks in final states with two hadronically decaying τ leptons and two jets in proton-proton collisions at $\sqrt{s} = 13$ TeV. *J High Energy Phys.* (2017) **3**:77. doi: 10.1007/JHEP03(2017)077
50. Khachatryan V, Sirunyan AM, Tumasyan A, Adam W, Aşilar E, Bergauer T. Search for heavy Majorana neutrinos in ee+ jets and e μ+ jets events in proton-proton collisions at $\sqrt{s} = 8$ TeV. *J High Energy Phys.* (2016) **4**:169. doi: 10.1007/JHEP04(2016)169
51. Khachatryan V, Sirunyan AM, Tumasyan A, Adam W, Bergauer T, Dragicevic M. Search for heavy Majorana neutrinos in $\mu^\pm\mu^\pm$+ jets events in proton-proton collisions at $\sqrt{s}$ = 8 TeV. *Phys Lett.* (2015) **B748**:144–66. doi: 10.1016/j.physletb.2015.06.070
52. Aad G, Abbott B, Abdallah J, Abdel Khalek S, Abdinov O, Aben R, et al. Search for heavy Majorana neutrinos with the ATLAS detector in pp collisions at $\sqrt{s} = 8$ TeV. *J High Energy Phys.* (2015) **7**:162. doi: 10.1007/JHEP07(2015)162
53. ATLAS Collaboration. Search for doubly-charged Higgs bosons in same-charge electron pair final states using proton-proton collisions at $\sqrt{s} = 13$ TeV with the ATLAS detector. *ATLAS-CONF-2016-051* (2016).
54. Aad G, Abbott B, Abdallah J, Abdel Khalek S, Abdinov O, Aben R, et al. Search for anomalous production of prompt same-sign lepton pairs and pair-produced doubly charged Higgs bosons with $\sqrt{s} = 8$ TeV *pp* collisions using the ATLAS detector. *J High Energy Phys.* (2015) **3**:041.
55. Chatrchyan S, Khachatryan V, Sirunyan AM, Tumasyan A, Adam W, Bergauer T. A search for a doubly-charged Higgs boson in *pp* collisions at $\sqrt{s} = 7$ TeV. *Eur Phys J.* (2012) **C72**:2189. doi: 10.1140/epjc/s10052-012-2189-5
56. Aad G, Abbott B, Abdallah J, Abdinov O, Aben R, Abolins M. Search for type-III Seesaw heavy leptons in *pp* collisions at $\sqrt{s} = 8$ TeV with the ATLAS Detector. *Phys Rev.* (2015) **D92**:032001. doi: 10.1103/PhysRevD.92.032001
57. Chatrchyan S, Khachatryan V, Sirunyan AM, Tumasyan A. Search for heavy lepton partners of neutrinos in proton-proton collisions in the context of the type III seesaw mechanism. *Phys Lett.* (2012) **B718**:348–68. doi: 10.1016/j.physletb.2012.10.070
58. Sirunyan AM, Tumasyan A, Adam W, Ambrogi F, Asilar E, Bergauer T, et al. Search for evidence of the type-III seesaw mechanism in multilepton final states in proton-proton collisions at sqrt[s] = 13 TeV. *Phys Rev Lett.* (2017) 119:221802. doi: 10.1103/PhysRevLett.119.221802
59. CMS Collaboration. Search for heavy composite Majorana neutrinos produced in association with a lepton and decaying into a same-flavour lepton plus two quarks at $\sqrt{s} = 13$ TeV with the CMS detector. *CMS-PAS-EXO-16-026* (2016).
60. CMS Collaboration. Search for a heavy composite Majorana neutrino in the final state with two leptons and two quarks at $\sqrt{s}$ = 13 TeV. *Phys. Lett. B* (2017) 775:315–37. doi: 10.1016/j.physletb.2017.11.001
61. Gluza J. On teraelectronvolt Majorana neutrinos. *Acta Phys Polon.* (2002) **B33**:1735–46.
62. Barger V, Marfatia D, Whisnant K. Progress in the physics of massive neutrinos. *Int J Mod Phys.* (2003) **E12**:569–647. doi: 10.1142/S0218301303001430
63. Mohapatra RN, Smirnov AY. Neutrino mass and new physics. *Ann Rev Nucl Part Sci.* (2006) **56**:569–628. doi: 10.1146/annurev.nucl.56.080805.140534
64. Rodejohann W. Neutrino-less double beta decay and particle physics. *Int J Mod Phys.* (2011) **E20**:1833–930. doi: 10.1142/S0218301311020186
65. Chen MC, Huang J. TeV scale models of neutrino masses and their phenomenology. *Mod Phys Lett.* (2011) **A26**:1147–67. doi: 10.1142/S0217732311035985
66. Atre A, Han T, Pascoli S, Zhang B. The search for heavy majorana neutrinos. *J High Energy Phys.* (2009) **5**:30. doi: 10.1088/1126-6708/2009/05/030
67. Deppisch FF, Bhupal Dev PS, Pilaftsis A. Neutrinos and collider physics. *New J Phys.* (2015) **17**:075019. doi: 10.1088/1367-2630/17/7/075019
68. An FP, Bai JZ, Balantekin AB, Band HR, Beavis D, Beriguete W, et al. Observation of electron-antineutrino disappearance at Daya Bay. *Phys Rev Lett.* (2012) **108**:171803. doi: 10.1103/PhysRevLett.108.171803
69. Abe Y, Aberle C, Akiri T, dos Anjos JC, Ardellier F, Barbosa AF. Indication of reactor $\bar{\nu}_e$ disappearance in the double chooz experiment. *Phys Rev Lett.* (2012) **108**:131801. doi: 10.1103/PhysRevLett.108.131801
70. Ahn JK, Chebotaryov S, Choi JH, Choi S, Choi W, Choi Y, et al. Observation of reactor electron antineutrino disappearance in the RENO experiment. *Phys Rev Lett.* (2012) **108**:191802. doi: 10.1103/PhysRevLett.108.191802
71. An FP, Balantekin AB, Band HR, Bishai M, Blyth S, Butorov I, et al. New measurement of antineutrino oscillation with the full detector configuration at daya bay. *Phys Rev Lett.* (2015) **115**:111802. doi: 10.1103/PhysRevLett.115.111802

72. Esteban I, Gonzalez-Garcia MC, Maltoni M, Martinez-Soler I, Schwetz T. Updated fit to three neutrino mixing: exploring the accelerator-reactor complementarity. *J High Energy Phys.* (2017) **1**:87. doi: 10.1007/JHEP01(2017)087
73. Abe K, Adam J, Aihara H, Akiri T, Andreopoulos C, Aoki S, et al. Observation of electron neutrino appearance in a muon neutrino beam. *Phys Rev Lett.* (2014) **112**:061802. doi: 10.1103/PhysRevLett.112.061802
74. Adamson P, Ader C, Andrews M, Anfimov N, Anghel I, Arms K, et al. First measurement of electron neutrino appearance in NOvA. *Phys Rev Lett.* (2016) **116**:151806. doi: 10.1103/PhysRevLett.116.151806
75. Abe K, Amey J, Andreopoulos C, Antonova M, Aoki S, Ariga A, et al. Combined analysis of neutrino and antineutrino oscillations at T2K. *Phys Rev Lett.* (2017) **118**:151801. doi: 10.1103/PhysRevLett.118.151801
76. Forero DV, Huber P. Hints for leptonic CP violation or New Physics? *Phys Rev Lett.* (2016) **117**:031801. doi: 10.1103/PhysRevLett.117.031801
77. Ge SF, Smirnov AY. Non-standard interactions and the CP phase measurements in neutrino oscillations at low energies. *J High Energy Phys.* (2016) **10**:138. doi: 10.1007/JHEP10(2016)138
78. de Gouvêa A, Kelly KJ. False signals of CP-invariance violation at DUNE. (2016) *arXiv:1605.09376*.
79. Miranda OG, Tórtola M, Valle JWF. New ambiguity in probing CP violation in neutrino oscillations. *Phys Rev Lett.* (2016) **117**:061804. doi: 10.1103/PhysRevLett.117.061804
80. Ade PAR, Aghanim N, Arnaud M, Ashdown M, Aumont J, Baccigalupi C, et al. Planck 2015 results. XIII. Cosmological parameters. *Astron Astrophys.* (2016) **594**:A13. doi: 10.1051/0004-6361/201525830
81. Lesgourgues J, Pastor S. Neutrino cosmology and planck. *New J Phys.* (2014) **16**:65002. doi: 10.1088/1367-2630/16/6/065002
82. Hamann J, Hannestad S, Wong YYY. Measuring neutrino masses with a future galaxy survey. *J Cosmol Astropart Phys.* (2012) **1211**:52. doi: 10.1088/1475-7516/2012/11/052
83. Acciarri R, Acero MA, Adamowski M, Adams C, Adamson P, Adhikari S. Long-Baseline Neutrino Facility (LBNF) and Deep Underground Neutrino Experiment (DUNE). (2016) *arXiv:1601.05471*.
84. An F, An G, An Q, Antonelli V, Baussan E, Beacom J, et al. Neutrino physics with JUNO. *J Phys.* (2016) **G43**:030401. doi: 10.1088/0954-3899/43/3/030401
85. Abe K, Aihara H, Andreopoulos C, Anghel I, Ariga A, Ariga T, et al. Physics potential of a long-baseline neutrino oscillation experiment using a J-PARC neutrino beam and hyper-kamiokande. *PTEP* (2015) **2015**:053C02. doi: 10.1093/ptep/ptv061
86. Osipowicz A, Blumer H, Drexlin G, Eitel K, Meisel G, Plischke P. KATRIN Collaboration. KATRIN: a next generation tritium beta decay experiment with sub-eV sensitivity for the electron neutrino mass. (2001) *arXiv:hep-ex/0109033*.
87. Han T, Lewis I, Ruiz R, Si Z-g. Lepton number violation and W' chiral couplings at the LHC. *Phys Rev.* (2013) **D87**:035011. doi: 10.1103/PhysRevD.87.035011
88. del Águila F, de Blas J, Pérez-Victoria M. Effects of new leptons in Electroweak Precision Data. *Phys Rev.* (2008) **D78**:013010. doi: 10.1103/PhysRevD.78.013010
89. Antusch S, Fischer O. Non-unitarity of the leptonic mixing matrix: present bounds and future sensitivities. *J High Energy Phys.* (2014) **10**:094. doi: 10.1007/JHEP10(2014)094
90. de Gouvêa A, Kobach A. Global constraints on a heavy neutrino. *Phys Rev.* (2016) **D93**:033005. doi: 10.1103/PhysRevD.93.033005
91. Fernandez-Martinez E, Hernandez-Garcia J, Lopez-Pavon J. Global constraints on heavy neutrino mixing. *J High Energy Phys.* (2016) **8**:33. doi: 10.1007/JHEP08(2016)033
92. Parke S, Ross-Lonergan M. Unitarity and the three flavor neutrino mixing matrix. *Phys Rev.* (2016) **D93**:113009. doi: 10.1103/PhysRevD.93.113009
93. Fileviez Pérez P, Han T, Li T. Testability of type I seesaw at the CERN LHC: revealing the existence of the B-L symmetry. *Phys Rev.* (2009) **D80**:073015. doi: 10.1103/PhysRevD.80.073015
94. Ibarra A, Molinaro E, Petcov ST. Low energy signatures of the TeV scale see-saw mechanism. *Phys Rev.* (2011) **D84**:013005. doi: 10.1103/PhysRevD.84.013005
95. Casas JA, Ibarra A. Oscillating neutrinos and muon → e, gamma. *Nucl Phys.* (2001) **B618**:171–204. doi: 10.1016/S0550-3213(01)00475-8
96. Pilaftsis A. Radiatively induced neutrino masses and large Higgs neutrino couplings in the standard model with Majorana fields. *Z Phys.* (1992) **C55**:275–82. doi: 10.1007/BF01482590
97. Kersten J, Smirnov AY. Right-handed neutrinos at CERN LHC and the mechanism of neutrino mass generation. *Phys Rev.* (2007) **D76**:073005. doi: 10.1103/PhysRevD.76.073005
98. Aristizabal Sierra D, Yaguna CE. On the importance of the 1-loop finite corrections to seesaw neutrino masses. *J High Energy Phys.* (2011) **8**:13. doi: 10.1007/JHEP08(2011)013
99. Lopez-Pavon J, Molinaro E, Petcov ST. Radiative corrections to light neutrino masses in low scale type I seesaw scenarios and neutrinoless double beta decay. *J High Energy Phys.* (2015) **11**:30. doi: 10.1007/JHEP11(2015)030
100. Fernandez-Martinez E, Hernandez-Garcia J, Lopez-Pavon J, Lucente M. Loop level constraints on Seesaw neutrino mixing. *J High Energy Phys.* (2015) **10**:130. doi: 10.1007/JHEP10(2015)130
101. Chen SL, Frigerio M, Ma E. Hybrid seesaw neutrino masses with A(4) family symmetry. *Nucl Phys.* (2005) **B724**:423–31. doi: 10.1016/j.nuclphysb.2005.07.012
102. Akhmedov EK, Frigerio M. Interplay of type I and type II seesaw contributions to neutrino mass. *J High Energy Phys.* (2007) **1**:43. doi: 10.1088/1126-6708/2007/01/043
103. Akhmedov EK, Blennow M, Hallgren T, Konstandin T, Ohlsson T. Stability and leptogenesis in the left-right symmetric seesaw mechanism. *J High Energy Phys.* (2007) **4**:22. doi: 10.1088/1126-6708/2007/04/022
104. Chao W, Luo S, Xing Z-z, Zhou S. A compromise between neutrino masses and collider signatures in the type-II seesaw model. *Phys Rev.* (2008) **D77**:016001. doi: 10.1103/PhysRevD.77.016001
105. Chao W, Si Z-g, Zheng Yj, Zhou S. Testing the realistic seesaw model with two heavy Majorana neutrinos at the CERN large hadron collider. *Phys Lett.* (2010) **B683**:26–32. doi: 10.1016/j.physletb.2009.11.059
106. Gu PH, Hirsch M, Sarkar U, Valle JWF. Neutrino masses, leptogenesis and dark matter in hybrid seesaw. *Phys Rev.* (2009) **D79**:033010. doi: 10.1103/PhysRevD.79.033010
107. Chao W, Si ZG, Xing Z-z, Zhou S. Correlative signatures of heavy Majorana neutrinos and doubly-charged Higgs bosons at the Large Hadron Collider. *Phys Lett.* (2008) **B666**:451–4. doi: 10.1016/j.physletb.2008.08.003
108. Langacker P. Grand unified theories and proton decay. *Phys Rept.* (1981) **72**:185. doi: 10.1016/0370-1573(81)90059-4
109. Hewett JL, Rizzo TG. Low-energy phenomenology of superstring inspired E_6 models. *Phys Rept.* (1989) **183**:193. doi: 10.1016/0370-1573(89)90071-9
110. Faraggi AE, Nanopoulos DV. A SUPERSTRING Z' AT O (1-TeV) ? *Mod Phys Lett.* (1991) **A6**:61–8. doi: 10.1142/S0217732391002621
111. Accomando E, Belyaev A, Fedeli L, King SF, Shepherd-Themistocleous C. Z' physics with early LHC data. *Phys Rev.* (2011) **D83**:075012. doi: 10.1103/PhysRevD.83.075012
112. Faraggi AE, Guzzi M. Extra Z' s and W' s in heterotic-string derived models. *Eur Phys J.* (2015) **C75**:537. doi: 10.1140/epjc/s10052-015-3763-4
113. Salvioni E, Villadoro G, Zwirner F. Minimal Z-prime models: present bounds and early LHC reach. *J High Energy Phys.* (2009) **11**:068. doi: 10.1088/1126-6708/2009/11/068
114. Carlson ED. Limits on a new U(1) coupling. *Nucl Phys.* (1987) **B286**:378–98. doi: 10.1016/0550-3213(87)90446-9
115. Buchmüller W, Greub C, Minkowski P. Neutrino masses, neutral vector bosons and the scale of B-L breaking. *Phys Lett.* (1991) **B267**:395–9. doi: 10.1016/0370-2693(91)90952-M
116. Abbas M, Khalil S. Neutrino masses, mixing and leptogenesis in TeV scale B - L extension of the standard model. *J High Energy Phys.* (2008) **4**:56. doi: 10.1088/1126-6708/2008/04/056
117. Pati JC, Salam A. Lepton number as the fourth color. *Phys Rev.* (1974) **D10**:275–89. doi: 10.1103/PhysRevD.10.275
118. Mohapatra RN, Pati JC. Left-right gauge symmetry and an isoconjugate model of CP violation. *Phys Rev.* (1975) **D11**:566–71.
119. Mohapatra RN, Pati JC. A natural left-right symmetry. *Phys Rev.* (1975) **D11**:2558. doi: 10.1103/PhysRevD.11.2558

120. Senjanović G, Mohapatra RN. Exact left-right symmetry and spontaneous violation of parity. *Phys Rev.* (1975) **D12**:1502. doi: 10.1103/PhysRevD.12.1502
121. Senjanović G. Spontaneous breakdown of parity in a class of Gauge theories. *Nucl Phys.* (1979) **B153**:334–64. doi: 10.1016/0550-3213(79)90604-7
122. Duka P, Gluza J, Zralek M. Quantization and renormalization of the manifest left-right symmetric model of electroweak interactions. *Ann Phys.* (2000) **280**:336–408. doi: 10.1006/aphy.1999.5988
123. Senjanović G. Is left right symmetry the key? *Mod Phys Lett.* (2017) **A32**:1730004. doi: 10.1142/S021773231730004X
124. Maiezza A, Nemevšek M, Nesti F, Senjanović G. Left-right symmetry at LHC. *Phys Rev.* (2010) **D82**:055022. doi: 10.1103/PhysRevD.82.055022
125. Zhang Y, An H, Ji X, Mohapatra RN. Right-handed quark mixings in minimal left-right symmetric model with general CP violation. *Phys Rev.* (2007) **D76**:091301. doi: 10.1103/PhysRevD.76.091301
126. Zhang Y, An H, Ji X, Mohapatra RN. General CP violation in minimal left-right symmetric model and constraints on the right-handed scale. *Nucl Phys.* (2008) **B802**:247–79. doi: 10.1016/j.nuclphysb.2008.05.019
127. Senjanović G, Tello V. Right handed quark mixing in left-right symmetric theory. *Phys Rev Lett.* (2015) **114**:071801. doi: 10.1103/PhysRevLett.114.071801
128. Senjanović G, Tello V. Restoration of parity and the right-handed analog of the CKM matrix. *Phys Rev.* (2016) **D94**:095023. doi: 10.1103/PhysRevD.94.095023
129. Nemevšek M, Senjanović G, Tello V. Connecting dirac and Majorana neutrino mass matrices in the minimal left-right symmetric model. *Phys Rev Lett.* (2013) **110**:151802. doi: 10.1103/PhysRevLett.110.151802
130. Senjanović G, Tello V. Probing seesaw with parity restoration. *Phys Rev Lett.* (2016) 119:201803. doi: 10.1103/PhysRevLett.119.201803
131. Akhmedov EK, Rodejohann W. A Yukawa coupling parameterization for type I + II seesaw formula and applications to lepton flavor violation and leptogenesis. *J High Energy Phys.* (2008) **6**:106. doi: 10.1088/1126-6708/2008/06/106
132. Fileviez Pérez P, Murgui C. Lepton flavour violation in left-right theory. *Phys Rev.* (2017) **D95**:075010. doi: 10.1103/PhysRevD.95.075010
133. Fileviez Pérez P, Murgui C, Ohmer S. Simple left-right theory: lepton number violation at the LHC. *Phys Rev.* (2016) **D94**:051701. doi: 10.1103/PhysRevD.94.051701
134. Fileviez Pérez P. Type III seesaw and left-right symmetry. *J High Energy Phys.* (2009) **3**:142. doi: 10.1088/1126-6708/2009/03/142
135. Duerr M, Fileviez Pérez P, Lindner M. Left-right symmetric theory with light sterile neutrinos. *Phys Rev.* (2013) **D88**:051701. doi: 10.1103/PhysRevD.88.051701
136. Fileviez Pérez P, Spinner S. Spontaneous R-parity breaking and left-right symmetry. *Phys Lett.* (2009) **B673**:251–4. doi: 10.1016/j.physletb.2009.02.047
137. Everett LL, Fileviez Pérez P, Spinner S. The right side of Tev scale spontaneous R-parity violation. *Phys Rev.* (2009) **D80**:055007. doi: 10.1103/PhysRevD.80.055007
138. Deshpande NG, Gunion JF, Kayser B, Olness FI. Left-right symmetric electroweak models with triplet Higgs. *Phys Rev.* (1991) **D44**:837–58. doi: 10.1103/PhysRevD.44.837
139. Basecq J, Liu J, Milutinovic J, Wolfenstein L. Spontaneous *CP* violation in $SU(2)_L \times SU(2)_R \times U(1)_{B-L}$ models. *Nucl Phys.* (1986) **B272**:145–57. doi: 10.1016/0550-3213(86)90345-7
140. Kiers K, Kolb J, Lee J, Soni A, Wu GH. Ubiquitous CP violation in a top inspired left-right model. *Phys Rev.* (2002) **D66**:095002. doi: 10.1103/PhysRevD.66.095002
141. Mitra M, Ruiz R, Scott DJ, Spannowsky M. Neutrino Jets from High-Mass W_R Gauge Bosons in TeV-Scale Left-Right Symmetric Models. *Phys Rev.* (2016) **D94**:095016. doi: 10.1103/PhysRevD.94.095016
142. Xu F, An H, Ji X. Neutron electric dipole moment constraint on scale of minimal left-right symmetric model. *J High Energy Phys.* (2010) **3**:88. doi: 10.1007/JHEP03(2010)088
143. Maiezza A, Nemevšek M. Strong P invariance, neutron electric dipole moment, and minimal left-right parity at LHC. *Phys Rev.* (2014) **D90**:095002. doi: 10.1103/PhysRevD.90.095002
144. Chakrabortty J, Gluza J, Sevillano R, Szafron R. Left-right symmetry at LHC and precise 1-loop low energy data. *J High Energy Phys.* (2012) **7**:38. doi: 10.1007/JHEP07(2012)038
145. Bambhaniya G, Chakrabortty J, Gluza J, Kordiaczyska M, Szafron R. Left-right symmetry and the charged higgs bosons at the LHC. *J High Energy Phys.* (2014) **5**:33. doi: 10.1007/JHEP05(2014)033
146. Maiezza A, Nemevšek M, Nesti F. Perturbativity and mass scales in the minimal left-right symmetric model. *Phys Rev.* (2016) **D94**:035008. doi: 10.1103/PhysRevD.94.035008
147. Bertolini S, Maiezza A, Nesti F. Present and Future K and B meson mixing constraints on TeV scale left-right symmetry. *Phys Rev.* (2014) **D89**:095028. doi: 10.1103/PhysRevD.89.095028
148. Arkani-Hamed N, Han T, Mangano M, Wang LT. Physics opportunities of a 100 TeV proton proton collider. *Phys Rept.* (2016) **652**:1–49. doi: 10.1016/j.physrep.2016.07.004
149. Golling T, Hance M, Harris P, Mangano ML, McCullough M, Moortgat F, et al. Physics at a 100 TeV pp collider: beyond the Standard Model phenomena. *CERN Yellow Rep* (2017) **3**:441–634. doi: 10.23731/CYRM-2017-003.441
150. Bertolini S, Di Luzio L, Malinský M. Intermediate mass scales in the non-supersymmetric SO(10) grand unification: a reappraisal. *Phys Rev.* (2009) **D80**:015013. doi: 10.1103/PhysRevD.80.015013
151. Bertolini S, Di Luzio L, Malinský M. On the vacuum of the minimal nonsupersymmetric SO(10) unification. *Phys Rev.* (2010) **D81**:035015. doi: 10.1103/PhysRevD.81.035015
152. Bertolini S, Di Luzio L, Malinský M. Seesaw scale in the minimal renormalizable SO(10) grand unification. *Phys Rev.* (2012) **D85**:095014. doi: 10.1103/PhysRevD.85.095014
153. Mohapatra RN, Zhang Y. TeV scale universal seesaw, vacuum stability and heavy higgs. *J High Energy Phys.* (2014) **6**:72. doi: 10.1007/JHEP06(2014)072
154. Maiezza A, Senjanović G, Vasquez JC. Higgs sector of the minimal left-right symmetric theory. *Phys Rev.* (2017) **D95**:095004. doi: 10.1103/PhysRevD.95.095004
155. Beall G, Bander M, Soni A. Constraint on the mass scale of a left-right symmetric electroweak theory from the $K_L - K_S$ mass difference. *Phys Rev Lett.* (1982) **48**:848. doi: 10.1103/PhysRevLett.48.848
156. Langacker P, Sankar SU. Bounds on the mass of W_R and the $W_L - W_R$ mixing angle ξ in general $SU(2)_L \times SU(2)_R \times U(1)$ models. *Phys Rev.* (1989) **D40**:1569–85.
157. Bernard V, Descotes-Genon S, Vale Silva L. Short-distance QCD corrections to $K^0\overline{K}^0$ mixing at next-to-leading order in Left-Right models. *J High Energy Phys.* (2016) **8**:128. doi: 10.1007/JHEP08(2016)128
158. Buras AJ, Girrbach J. Towards the identification of new physics through quark flavour violating processes. *Rept Prog Phys.* (2014) **77**:086201. doi: 10.1088/0034-4885/77/8/086201
159. Mescia F, Virto J. Natural SUSY and Kaon Mixing in view of recent results from Lattice QCD. *Phys Rev.* (2012) **D86**:095004. doi: 10.1103/PhysRevD.86.095004
160. Garron N, Hudspith RJ, Lytle AT. Neutral kaon mixing beyond the standard model with $n_f = 2 + 1$ chiral fermions part 1: bare matrix elements and physical results. *J High Energy Phys.* (2016) **11**:1. doi: 10.1007/JHEP11(2016)001
161. Cirigliano V, Dekens W, de Vries J, Mereghetti E. An ϵ' improvement from right-handed currents. *Phys Lett.* (2017) **B767**:1–9. doi: 10.1016/j.physletb.2017.01.037
162. Lindner M, Queiroz FS, Rodejohann W. Dilepton bounds on left right symmetry at the LHC run II and neutrinoless double beta decay. *Phys Lett.* (2016) **B762**:190–5. doi: 10.1016/j.physletb.2016.08.068
163. Ruiz R. Lepton number violation at colliders from kinematically inaccessible gauge bosons. *Eur Phys J.* (2017) **C77**:375. doi: 10.1140/epjc/s10052-017-4950-2
164. del Águila F, Bar-Shalom S, Soni A, Wudka J. Heavy majorana neutrinos in the effective lagrangian description: application to hadron colliders. *Phys Lett.* (2009) **B670**:399–402. doi: 10.1016/j.physletb.2008.11.031
165. Burges CJC, Schnitzer HJ. Virtual effects of excited quarks as probes of a possible new hadronic mass scale. *Nucl Phys.* (1983) **B228**:464–500. doi: 10.1016/0550-3213(83)90555-2

166. Leung CN, Love ST, Rao S. Low-energy manifestations of a new interaction scale: operator analysis. *Z Phys.* (1986) **C31**:433. doi: 10.1007/BF01588041
167. Buchmüller W, Wyler D. Effective lagrangian analysis of new interactions and flavor conservation. *Nucl Phys.* (1986) **B268**:621–53. doi: 10.1016/0550-3213(86)90262-2
168. Grzadkowski B, Iskrzynski M, Misiak M, Rosiek J. Dimension-six terms in the standard model lagrangian. *J High Energy Phys.* (2010) **10**:085. doi: 10.1007/JHEP10(2010)085
169. Aparici A, Kim K, Santamaria A, Wudka J. Right-handed neutrino magnetic moments. *Phys Rev.* (2009) **D80**:013010. doi: 10.1103/PhysRevD.80.013010
170. Elgaard-Clausen G, Trott M. On expansions in neutrino effective field theory. *J High Energ Phys.* (2017) 2017:88. doi: 10.1007/JHEP11(2017)088
171. Bhattacharya S, Wudka J. Dimension-seven operators in the standard model with right handed neutrinos. *Phys Rev.* (2016) **D94**:055022. doi: 10.1103/PhysRevD.94.055022
172. Liao Y, Ma XD. Operators up to dimension seven in standard model effective field theory extended with sterile neutrinos. *Phys Rev.* (2017) **D96**:015012. doi: 10.1103/PhysRevD.96.015012
173. Henning B, Lu X, Melia T, Murayama H. 2, 84, 30, 993, 560, 15456, 11962, 261485, ...: Higher dimension operators in the SM EFT. *J High Energy Phys.* (2017) **8**:16. doi: 10.1007/JHEP08(2017)016
174. Kobach A. Baryon number, lepton number, and operator dimension in the standard model. *Phys Lett.* (2016) **B758**:455–7. doi: 10.1016/j.physletb.2016.05.050
175. Liao Y, Ma X-D. Perturbative power counting, lowest-index operators and their renormalization in standard model effective field theory. *Commun Theor Phys.* (2018) 69:285. doi: 10.1088/0253-6102/69/3/285
176. Abada A, Biggio C, Bonnet F, Gavela MB, Hambye T. Low energy effects of neutrino masses. *J High Energy Phys.* (2007) **12**:61. doi: 10.1088/1126-6708/2007/12/061
177. del Águila F, Aparici A, Bhattacharya S, Santamaria A, Wudka J. Effective lagrangian approach to neutrinoless double beta decay and neutrino masses. *J High Energy Phys.* (2012) **6**:146. doi: 10.1007/JHEP06(2012)146
178. Wolfenstein L. Different varieties of massive dirac neutrinos. *Nucl Phys.* (1981) **B186**:147–52. doi: 10.1016/0550-3213(81)90096-1
179. Petcov ST. On pseudodirac neutrinos, neutrino oscillations and neutrinoless double beta decay. *Phys Lett.* (1982) **110B**:245–9. doi: 10.1016/0370-2693(82)91246-1
180. Leung CN, Petcov ST. A comment on the coexistence of dirac and Majorana massive neutrinos. *Phys Lett.* (1983) **125B**:461–6. doi: 10.1016/0370-2693(83)91326-6
181. Valle JWF, Singer M. Lepton number violation with quasi dirac neutrinos. *Phys Rev.* (1983) **D28**:540. doi: 10.1103/PhysRevD.28.540
182. Weiland C. Effects of fermionic singlet neutrinos on high- and low-energy observables. Orsay, LPT (2013). Available online at: https://inspirehep.net/record/1265676/files/arXiv:1311.5860.pdf
183. Antusch S, Cazzato E, Fischer O. Sterile neutrino searches at future e^-e^+, pp, and e^-p colliders. *Int J Mod Phys.* (2017) **A32**:1750078. doi: 10.1142/S0217751X17500786
184. Littenberg LS, Shrock RE. Upper bounds on lepton number violating meson decays. *Phys Rev Lett.* (1992) **68**:443–6. doi: 10.1103/PhysRevLett.68.443
185. Littenberg LS, Shrock R. Implications of improved upper bounds on $|\Delta L| = 2$ processes. *Phys Lett.* (2000) **B491**:285–90. doi: 10.1016/S0370-2693(00)01041-8
186. Dib C, Gribanov V, Kovalenko S, Schmidt I. K meson neutrinoless double muon decay as a probe of neutrino masses and mixings. *Phys Lett.* (2000) **B493**:82–7. doi: 10.1016/S0370-2693(00)01134-5
187. Atre A, Barger V, Han T. Upper bounds on lepton-number violating processes. *Phys Rev.* (2005) **D71**:113014. doi: 10.1103/PhysRevD.71.113014
188. Cvetič G, Dib C, Kang SK, Kim CS. Probing Majorana neutrinos in rare K and D, D_s, B, B_c meson decays. *Phys Rev.* (2010) **D82**:053010. doi: 10.1103/PhysRevD.82.053010
189. Dib C, Kim CS. Remarks on the lifetime of sterile neutrinos and the effect on detection of rare meson decays $M^+ \to M' - \ell^+\ell^+$. *Phys Rev.* (2014) **D89**:077301. doi: 10.1103/PhysRevD.89.077301
190. Cvetič G, Kim CS, Zamora-Sa J. CP violation in lepton number violating semihadronic decays of K, D, D_s, B, B_c. *Phys Rev.* (2014) **D89**:093012. doi: 10.1103/PhysRevD.89.093012
191. Cvetič G, Kim CS, Kogerler R, Zamora-Saa J. Oscillation of heavy sterile neutrino in decay of $B \to \mu e \pi$. *Phys Rev.* (2015) **D92**:013015. doi: 10.1103/PhysRevD.92.013015
192. Cvetič G, Dib C, Kim CS, Zamora-Saa J. Probing the Majorana neutrinos and their CP violation in decays of charged scalar mesons π, K, D, D_s, B, B_c. *Symmetry* (2015) **7**:726–73. doi: 10.3390/sym7020726
193. Cvetič G, Kim CS. Rare decays of B mesons via on-shell sterile neutrinos. *Phys Rev.* (2016) **D94**:053001. doi: 10.1103/PhysRevD.94.053001
194. Dib CO, Campos M, Kim CS. CP Violation with Majorana neutrinos in K Meson Decays. *J High Energy Phys.* (2015) **2**:108. doi: 10.1007/JHEP02(2015)108
195. Quintero N. Constraints on lepton number violating short-range interactions from $|\Delta L| = 2$ processes. *Phys Lett.* (2017) **B764**:60–5. doi: 10.1016/j.physletb.2016.10.056
196. Milanes D, Quintero N, Vera CE. Sensitivity to Majorana neutrinos in $\Delta L = 2$ decays of B_c meson at LHCb. *Phys Rev.* (2016) **D93**:094026. doi: 10.1103/PhysRevD.93.094026
197. Wang Y, Bao SS, Li ZH, Zhu N, Si ZG. Study Majorana neutrino contribution to B-meson semi-leptonic rare decays. *Phys Lett.* (2014) **B736**:428–32. doi: 10.1016/j.physletb.2014.08.006
198. Dong HR, Feng F, Li HB. Lepton number violation in D meson decay. *Chin Phys.* (2015) **C39**:013101. doi: 10.1088/1674-1137/39/1/013101
199. Asaka T, Ishida H. Lepton number violation by heavy Majorana neutrino in B decays. *Phys Lett.* (2016) **B763**:393–6. doi: 10.1016/j.physletb.2016.10.070
200. Castro GL, Quintero N. Bounding resonant Majorana neutrinos from four-body B and D decays. *Phys Rev.* (2013) **D87**:077901. doi: 10.1103/PhysRevD.87.077901
201. Yuan H, Wang T, Wang GL, Ju WL, Zhang JM. Lepton-number violating four-body decays of heavy mesons. *J High Energy Phys.* (2013) **8**:66. doi: 10.1007/JHEP08(2013)066
202. Cvetič G, Kim CS. Sensitivity limits on heavy-light mixing $|U_{\mu N}|^2$ from lepton number violating B meson decays. *Phys Rev.* (2017) **D96**:35025. doi: 10.1103/PhysRevD.96.035025
203. Cvetič G, Dib C, Kim CS. Probing Majorana neutrinos in rare $\pi^+ \to e^+e^+\mu^-\nu$ decays. *J High Energy Phys.* (2012) **6**:149. doi: 10.1007/JHEP06(2012)149
204. Cvetič G, Kim CS, Zamora-Saá J. CP violations in $\pi^\pm$ Meson Decay. *J Phys.* (2014) **G41**:075004. doi: 10.1088/0954-3899/41/7/075004
205. Mejía-Guisao J, Milanés D, Quintero N, Ruiz-Álvarez JD. Exploring GeV-scale Majorana neutrinos in lepton-number-violating Λ_b^0 baryon decays. *Phys Rev.* (2017) **D96**:015039. doi: 10.1103/PhysRevD.96.015039
206. Kobach A, Dobbs S. Heavy neutrinos and the kinematics of Tau decays. *Phys Rev.* (2015) **D91**:053006. doi: 10.1103/PhysRevD.91.053006
207. Zamora-Saa J. Resonant *CP* violation in rare $\tau^\pm$ decays. *J High Energy Phys.* (2017) **5**:110. doi: 10.1007/JHEP05(2017)110
208. Yuan H, Jiang Y, Wang Th, Li Q, Wang GL. Testing the nature of neutrinos from four-body τ decays. *J Phys.* (2017) **G44**:115002. doi: 10.1088/1361-6471/aa8a1e
209. Lopez Castro G, Quintero N. Lepton number violating four-body tau lepton decays. *Phys Rev.* (2012) **D85**:076006. doi: 10.1103/PhysRevD.85.076006
210. Mandal S, Sinha N. Favoured B_c Decay modes to search for a Majorana neutrino. *Phys Rev.* (2016) **D94**:033001. doi: 10.1103/PhysRevD.94.033001
211. Bar-Shalom S, Deshpande NG, Eilam G, Jiang J, Soni A. Majorana neutrinos and lepton-number-violating signals in top-quark and W-boson rare decays. *Phys Lett.* (2006) **B643**:342–7. doi: 10.1016/j.physletb.2006.10.060
212. Dib CO, Kim CS, Wang K. Signatures of Dirac and Majorana sterile neutrinos in trilepton events at the LHC. *Phys Rev.* (2017) **D95**:115020. doi: 10.1103/PhysRevD.95.115020
213. Dib CO, Kim CS, Wang K. Search for heavy sterile neutrinos in trileptons at the LHC. (2017) *Chin Phys.* **C41**:103103. doi: 10.1088/1674-1137/41/10/103103
214. Dib CO, Kim CS, Wang K, Zhang J. Distinguishing Dirac/Majorana sterile neutrinos at the LHC. *Phys Rev.* (2016) **D94**:013005. doi: 10.1103/PhysRevD.94.013005

215. Dib CO, Kim CS. Discovering sterile Neutrinos ligther than M_W at the LHC. *Phys Rev.* (2015) **D92**:093009. doi: 10.1103/PhysRevD.92.093009
216. Bhupal Dev PS, Franceschini R, Mohapatra RN. Bounds on TeV seesaw models from LHC higgs data. *Phys Rev.* (2012) **D86**:093010. doi: 10.1103/PhysRevD.86.093010
217. Gago AM, Hernández P, Jones-Pérez J, Losada M, Moreno Briceño A. Probing the type I seesaw mechanism with displaced vertices at the LHC. *Eur Phys J.* (2015) **C75**:470. doi: 10.1140/epjc/s10052-015-3693-1
218. Caputo A, Hernández P, López-Pavón J, Salvado J. The seesaw portal in testable models of neutrino masses. *J High Energy Phys.* (2017) **6**:112. doi: 10.1007/JHEP06(2017)112
219. Das A, Dev PSB, Kim CS. Constraining sterile neutrinos from precision higgs data. *Phys Rev.* (2017) **D95**:115013. doi: 10.1103/PhysRevD.95.115013
220. Si Z, Wang K. GeV Majorana neutrinos in top-quark decay at the LHC. *Phys Rev.* (2009) **D79**:014034. doi: 10.1103/PhysRevD.79.014034
221. Quintero N, López Castro G, Delepine D. Lepton number violation in top quark and neutral B meson decays. *Phys Rev.* (2011) **D84**:096011. doi: 10.1103/PhysRevD.84.096011
222. Shuve B, Peskin ME. Revision of the LHCb limit on majorana neutrinos. *Phys Rev.* (2016) **D94**:113007. doi: 10.1103/PhysRevD.94.113007
223. Helo JC, Hirsch M, Kovalenko S. Heavy neutrino searches at the LHC with displaced vertices. *Phys Rev.* (2014) **D89**:073005. doi: 10.1103/PhysRevD.89.073005
224. Blondel A, Graverini E, Serra N, Shaposhnikov M. Search for heavy right handed neutrinos at the FCC-ee. *Nucl Part Phys Proc.* (2016) **273–275**:1883–90. doi: 10.1016/j.nuclphysbps.2015.09.304
225. Izaguirre E, Shuve B. Multilepton and Lepton jet probes of sub-weak-scale right-handed neutrinos. *Phys Rev.* (2015) **D91**:093010. doi: 10.1103/PhysRevD.91.093010
226. Antusch S, Cazzato E, Fischer O. Sterile neutrino searches via displaced vertices at LHCb. *Phys Lett.* (2017) **B774**:114–8. doi: 10.1016/j.physletb.2017.09.057
227. Antusch S, Cazzato E, Fischer O. Displaced vertex searches for sterile neutrinos at future lepton colliders. *J High Energy Phys.* (2016) **12**:7. doi: 10.1007/JHEP12(2016)007
228. Anamiati G, Hirsch M, Nardi E. Quasi-Dirac neutrinos at the LHC. *J High Energy Phys.* (2016) **10**:10. doi: 10.1007/JHEP10(2016)010
229. Antusch S, Cazzato E, Fischer, O. Heavy neutrino-antineutrino oscillations at colliders. (2017) *arXiv:1709.03797*.
230. Das A, Dev PSB, Mohapatra RN. Same sign vs opposite sign dileptons as a probe of low scale seesaw mechanisms. *Phys Rev D* (2017) **97**:015018. doi: 10.1103/PhysRevD.97.015018
231. Antusch S, Cazzato E Drewes M, Fischer O, Garbrecht B, Gueter D. Probing leptogenesis at future colliders. (2017) *arXiv:1710.03744*.
232. Bicer M, Duran Yildiz H, Yildiz I, Coignet G, Delmastro M, Alexopoulos T, et al. First look at the physics case of TLEP. *J High Energy Phys.* (2014) **1**:164. doi: 10.1007/JHEP01(2014)164
233. Antusch S, Fischer O. Testing sterile neutrino extensions of the Standard Model at future lepton colliders. *J High Energy Phys.* (2015) **5**:53. doi: 10.1007/JHEP05(2015)053
234. Baer H, Barklow T, Fujii K, Gao Y, Hoang A, Kanemura S. The international linear collider technical design report - Volume 2: Physics. (2013) *arXiv:1306.6352*.
235. Fujii K, Grojean C, Peskin ME, Barklow T, Gao Y, Kanemura S. Physics case for the international linear collider. *arXiv:1506.05992*.
236. Group CSS. CEPC-SPPC preliminary conceptual design report. 1. Physics and detector. (2015).
237. Schael S, Barate R, Bruneliere R, Buskulic D, De Bonis I, Decamp D. Precision electroweak measurements on the *Z* resonance. *Phys Rept.* (2006) **427**:257–454. doi: 10.1016/j.physrep.2005.12.006
238. Beringer J, Arguin JF, Barnett RM, Copic K, Dahl O, Groom DE. Review of particle physics (RPP). *Phys Rev.* (2012) **D86**:010001. doi: 10.1103/PhysRevD.86.010001
239. Jarlskog C. Neutrino counting at the *Z* peak and right-handed neutrinos. *Phys Lett.* (1990) **B241**:579–83. doi: 10.1016/0370-2693(90)91873-A
240. Keung WY, Senjanović G. Majorana neutrinos and the production of the right-handed charged gauge boson. *Phys Rev Lett.* (1983) **50**:1427. doi: 10.1103/PhysRevLett.50.1427
241. Gronau M, Leung CN, Rosner JL. Extending limits on neutral heavy leptons. *Phys Rev.* (1984) **D29**:2539. doi: 10.1103/PhysRevD.29.2539
242. Willenbrock SSD, Dicus DA. Production of heavy leptons from gluon fusion. *Phys Lett.* (1985) **156B**:429–33. doi: 10.1016/0370-2693(85)91638-7
243. Petcov ST. Possible signature for production of majorana particles in e+ e- and p anti-p collisions. *Phys Lett.* (1984) **139B**:421. doi: 10.1016/0370-2693(84)91844-6
244. Dicus DA, Karatas DD, Roy P. Lepton nonconservation at supercollider energies. *Phys Rev.* (1991) **D44**:2033–7. doi: 10.1103/PhysRevD.44.2033
245. Dicus DA, Roy P. Supercollider signatures and correlations of heavy neutrinos. *Phys Rev.* (1991) **D44**:1593–6. doi: 10.1103/PhysRevD.44.1593
246. Datta A, Pilaftsis A. Revealing the Majorana nature of heavy neutrinos via a heavy Higgs boson. *Phys Lett.* (1992) **B278**:162–6. doi: 10.1016/0370-2693(92)90727-L
247. Datta A, Guchait M, Pilaftsis A. Probing lepton number violation via majorana neutrinos at hadron supercolliders. *Phys Rev.* (1994) **D50**:3195–203. doi: 10.1103/PhysRevD.50.3195
248. Han T, Zhang B. Signatures for Majorana neutrinos at hadron colliders. *Phys Rev Lett.* (2006) **97**:171804. doi: 10.1103/PhysRevLett.97.171804
249. Bray S, Lee JS, Pilaftsis A. Resonant CP violation due to heavy neutrinos at the LHC. *Nucl Phys.* (2007) **B786**:95–118. doi: 10.1016/j.nuclphysb.2007.07.002
250. del Águila F, Aguilar-Saavedra JA, Pittau R. Neutrino physics at large colliders. *J Phys Conf Ser.* (2006) **53**:506–27. doi: 10.1088/1742-6596/53/1/032
251. del Águila F, Aguilar-Saavedra JA, Pittau R. Heavy neutrino signals at large hadron colliders. *J High Energy Phys.* (2007) **10**:47. doi: 10.1088/1126-6708/2007/10/047
252. del Águila F, Aguilar-Saavedra JA. Distinguishing seesaw models at LHC with multi-lepton signals. *Nucl Phys.* (2009) **B813**:22–90. doi: 10.1016/j.nuclphysb.2008.12.029
253. del Águila F, Aguilar-Saavedra JA, de Blas J. Trilepton signals: the golden channel for seesaw searches at LHC. *Acta Phys Polon.* (2009) **B40**:2901–11.
254. Alva D, Han T, Ruiz R. Heavy Majorana neutrinos from $W\gamma$ fusion at hadron colliders. *J High Energy Phys.* (2015) **2**:72. doi: 10.1007/JHEP02(2015)072
255. Degrande C, Mattelaer O, Ruiz R, Turner J. Fully-automated precision predictions for heavy neutrino production mechanisms at hadron colliders. *Phys Rev.* (2016) **D94**:053002. doi: 10.1103/PhysRevD.94.053002
256. Chen CY, Dev PSB. Multi-lepton collider signatures of heavy dirac and majorana neutrinos. *Phys Rev.* (2012) **D85**:093018. doi: 10.1103/PhysRevD.85.093018
257. Dev PSB, Kim D, Mohapatra RN. Disambiguating seesaw models using invariant mass variables at hadron colliders. *J High Energy Phys.* (2016) **1**:118. doi: 10.1007/JHEP01(2016)118
258. Hessler AG, Ibarra A, Molinaro E, Vogl S. Impact of the Higgs boson on the production of exotic particles at the LHC. *Phys Rev.* (2015) **D91**:115004. doi: 10.1103/PhysRevD.91.115004
259. Ruiz R, Spannowsky M, Waite P. Heavy neutrinos from gluon fusion. *Phys Rev.* (2017) **D96**:055042. doi: 10.1103/PhysRevD.96.055042
260. Chanowitz MS, Gaillard MK. The TeV physics of strongly interacting W's and Z's. *Nucl Phys.* (1985) **B261**:379–431. doi: 10.1016/0550-3213(85)90580-2
261. Lee BW, Quigg C, Thacker HB. The strength of weak interactions at very high-energies and the Higgs Boson mass. *Phys Rev Lett.* (1977) **38**:883–5. doi: 10.1103/PhysRevLett.38.883
262. Dev PSB, Pilaftsis A, Yang Uk. New production mechanism for heavy neutrinos at the LHC. *Phys Rev Lett.* (2014) **112**:081801. doi: 10.1103/PhysRevLett.112.081801
263. Bambhaniya G, Khan S, Konar P, Mondal T. Constraints on a seesaw model leading to quasidegenerate neutrinos and signatures at the LHC. *Phys Rev.* (2015) **D91**:095007. doi: 10.1103/PhysRevD.91.095007
264. Ng JN, de la Puente A, Pan BWP. Search for heavy right-handed neutrinos at the LHC and beyond in the same-sign same-flavor leptons final state. *J High Energy Phys.* (2015) **12**:172. doi: 10.1007/JHEP12(2015)172
265. Arganda E, Herrero MJ, Marcano X, Weiland C. Exotic $\mu\tau$jj events from heavy ISS neutrinos at the LHC. *Phys Lett.* (2016) **B752**:46–50. doi: 10.1016/j.physletb.2015.11.013

266. Andrés F, Alfredo G, Kaiwen G, Carlos P, Diego R. Expanding the reach of heavy neutrino searches at the LHC. *Phys Lett.* (2017) **B778**:94–100. doi: 10.1016/j.physletb.2018.01.009
267. Binosi D, Collins J, Kaufhold C, Theussl L. JaxoDraw: a graphical user interface for drawing Feynman diagrams. Version 2.0 release notes. *Comput Phys Commun.* (2009) **180**:1709–15. doi: 10.1016/j.cpc.2009.02.020
268. Martin AD, Ryskin MG. The photon PDF of the proton. *Eur Phys J.* (2014) **C74**:3040. doi: 10.1140/epjc/s10052-014-3040-y
269. Harland-Lang LA, Khoze VA, Ryskin MG. Photon-initiated processes at high mass. *Phys Rev.* (2016) **D94**:074008. doi: 10.1103/PhysRevD.94.074008
270. Bertone V, Carrazza S, Hartland NP, Rojo, J. Illuminating the photon content of the proton within a global PDF analysis. *arXiv:1712.07053*.
271. Manohar AV, Nason P, Salam GP, Zanderighi G. The photon content of the proton. *J High Energ Phys.* (2017) 12:046. doi: 10.1007/JHEP12(2017)046
272. Manohar A, Nason P, Salam GP, Zanderighi G. How bright is the proton? A precise determination of the photon parton distribution function. *Phys Rev Lett.* (2016) **117**:242002. doi: 10.1103/PhysRevLett.117.242002
273. Schmidt C, Pumplin J, Stump D, Yuan CP. CT14QED parton distribution functions from isolated photon production in deep inelastic scattering. *Phys Rev.* (2016) **D93**:114015. doi: 10.1103/PhysRevD.93.114015
274. Das A, Bhupal Dev PS, Okada N. Direct bounds on electroweak scale pseudo-Dirac neutrinos from $\sqrt{s} = 8$ TeV LHC data. *Phys Lett.* (2014) **B735**:364–70. doi: 10.1016/j.physletb.2014.06.058
275. Ruiz R. QCD corrections to pair production of type III seesaw leptons at hadron colliders. *J High Energy Phys.* (2015) **12**:165. doi: 10.1007/JHEP12(2015)165
276. Collins JC, Soper DE, Sterman GF. Transverse momentum distribution in Drell-Yan pair and W and Z Boson production. *Nucl Phys.* (1985) **B250**:199–224. doi: 10.1016/0550-3213(85)90479-1
277. Dreiner HK, Grab S, Kramer M, Trenkel MK. Supersymmetric NLO QCD corrections to resonant slepton production and signals at the Tevatron and the CERN LHC. *Phys Rev.* (2007) **D75**:035003. doi: 10.1103/PhysRevD.75.035003
278. Chen YQ, Han T, Si ZG. QCD corrections to single slepton production at hadron colliders. *J High Energy Phys.* (2007) **5**:68. doi: 10.1088/1126-6708/2007/05/068
279. Fuchs E, Thewes S, Weiglein G. Interference effects in BSM processes with a generalised narrow-width approximation. *Eur Phys J.* (2015) **C75**:254. doi: 10.1140/epjc/s10052-015-3472-z
280. Fuchs E, Weiglein G. Breit-Wigner approximation for propagators of mixed unstable states. *J High Energy Phys.* (2017) **9**:79. doi: 10.1007/JHEP09(2017)079
281. Ruiz RE. *Hadron Collider Tests of Neutrino Mass-Generating Mechanisms*. Pittsburgh: PA (2015). Available online at: https://inspirehep.net/record/1394386/files/arXiv:1509.06375.pdf
282. del Águila F, Aguilar-Saavedra JA, Pittau R. *Heavy Neutrino Production at Hadron Colliders*. Available online at: http://mlm.home.cern.ch/mlm/alpgen/
283. Degrande C, Mattelaer O, Ruiz R, Turner J. *SM + Heavy N at NLO in QCD*. Available online at: http://feynrules.irmp.ucl.ac.be/wiki/HeavyN
284. Degrande C. Automatic evaluation of UV and R2 terms for beyond the Standard Model Lagrangians: a proof-of-principle. *Comput Phys Commun.* (2015) **197**:239–62. doi: 10.1016/j.cpc.2015.08.015
285. Degrande C, Duhr C, Fuks B, Grellscheid D, Mattelaer O, Reiter T. UFO - the universal FeynRules output. *Comput Phys Commun.* (2012) **183**:1201–14. doi: 10.1016/j.cpc.2012.01.022
286. Christensen ND, Duhr C. FeynRules - Feynman rules made easy. *Comput Phys Commun.* (2009) **180**:1614–41. doi: 10.1016/j.cpc.2009.02.018
287. Alloul A, Christensen ND, Degrande C, Duhr C, Fuks B. FeynRules 2.0 - A complete toolbox for tree-level phenomenology. *Comput Phys Commun.* (2014) **185**:2250–300. doi: 10.1016/j.cpc.2014.04.012
288. Denner A, Eck H, Hahn O, Kublbeck J. Compact Feynman rules for Majorana fermions. *Phys Lett.* (1992) **B291**:278–80. doi: 10.1016/0370-2693(92)91045-B
289. Bellm J, Gieseke S, Grellscheid D, Plätzer S, Rauch M, Reuschle C, et al. Herwig 7.0/Herwig++ 3.0 release note. *Eur Phys J.* (2016) **C76**:196. doi: 10.1140/epjc/s10052-016-4018-8
290. Alwall J, Frederix R, Frixione S, Hirschi V, Maltoni F, Mattelaer O, et al. The automated computation of tree-level and next-to-leading order differential cross sections, and their matching to parton shower simulations. *J High Energy Phys.* (2014) **7**:79. doi: 10.1007/JHEP07(2014)079
291. Gleisberg T, Höche S, Krauss F, Schönherr M, Schumann S, Siegert F, et al. Event generation with SHERPA 1.1. *J High Energy Phys.* (2009) **2**:7. doi: 10.1088/1126-6708/2009/02/007
292. Han T, Valencia G, Willenbrock S. Structure function approach to vector boson scattering in p p collisions. *Phys Rev Lett.* (1992) **69**:3274–7. doi: 10.1103/PhysRevLett.69.3274
293. Degrande C, Hartling K, Logan HE, Peterson AD, Zaro M. Automatic predictions in the Georgi-Machacek model at next-to-leading order accuracy. *Phys Rev.* (2016) **D93**:035004. doi: 10.1103/PhysRevD.93.035004
294. Cacciari M, Dreyer FA, Karlberg A, Salam GP, Zanderighi G. Fully differential vector-boson-fusion higgs production at next-to-next-to-leading order. *Phys Rev Lett.* (2015) **115**:082002. doi: 10.1103/PhysRevLett.115.082002
295. Dreyer FA, Karlberg A. Vector-Boson fusion higgs production at three loops in QCD. *Phys Rev Lett.* (2016) **117**:072001. doi: 10.1103/PhysRevLett.117.072001
296. Bonvini M, Forte S, Ridolfi G, Rottoli L. Resummation prescriptions and ambiguities in SCET vs. direct QCD: Higgs production as a case study. *J High Energy Phys.* (2015) **1**:46. doi: 10.1007/JHEP01(2015)046
297. Anastasiou C, Duhr C, Dulat F, Furlan E, Gehrmann T, Herzog F, et al. High precision determination of the gluon fusion Higgs boson cross-section at the LHC. *J High Energy Phys.* (2016) **5**:58. doi: 10.1007/JHEP05(2016)058
298. Anastasiou C, Duhr C, Dulat F, Herzog F, Mistlberger B. Higgs Boson Gluon-fusion production in QCD at three loops. *Phys Rev Lett.* (2015) **114**:212001. doi: 10.1103/PhysRevLett.114.212001
299. Avetisyan A, Campbell JM, Cohen T, Dhingra N, Hirschauer J, Howe K. Methods and results for standard model event generation at $\sqrt{s}$ = 14 TeV, 33 TeV and 100 TeV proton colliders (A snowmass whitepaper). In: *Proceedings, 2013 Community Summer Study on the Future of U.S. Particle Physics: Snowmass on the Mississippi (CSS2013): USA, July 29-August 6, 2013*. Minneapolis, MN (2013). Available online at: http://lss.fnal.gov/archive/test-fn/0000/fermilab-fn-0965-t.pdf
300. Aad G, Abbott B, Abdallah J, Ali Abdelalim A, Abdesselam A, Abdinov O. Search for heavy neutrinos and right-handed W bosons in events with two leptons and jets in pp collisions at $\sqrt{s} = 7$ TeV with the ATLAS detector. *Eur Phys J.* (2012) **C72**:2056. doi: 10.1140/epjc/s10052-012-2056-4
301. Cox P, Han C, Yanagida TT. LHC search for right-handed neutrinos in Z' models. *J High Energ Phys.* (2018) **1**:37. doi: 10.1007/JHEP01(2018)037
302. Buchmüller W, Greub C. Electroproduction of Majorana neutrinos. *Phys Lett.* (1991) **B256**:465–70. doi: 10.1016/0370-2693(91)91792-T
303. Buchmüller W, Greub C. Heavy Majorana neutrinos in electron - positron and electron - proton collisions. *Nucl Phys.* (1991) **B363**:345–68. doi: 10.1016/0550-3213(91)80024-G
304. Blaksley C, Blennow M, Bonnet F, Coloma P, Fernandez-Martinez E. Heavy neutrinos and lepton number violation in lp colliders. *Nucl Phys.* (2011) **B852**:353–65. doi: 10.1016/j.nuclphysb.2011.06.021
305. Duarte L, Gonzlez-Sprinberg GA, Sampayo OA. Majorana neutrinos production at LHeC in an effective approach. *Phys Rev.* (2015) **D91**:053007. doi: 10.1103/PhysRevD.91.053007
306. Banerjee S, Dev PSB, Ibarra A, Mandal T, Mitra M. Prospects of heavy neutrino searches at future lepton colliders. *Phys Rev.* (2015) **D92**:075002. doi: 10.1103/PhysRevD.92.075002
307. Mondal S, Rai SK. Probing the heavy neutrinos of inverse seesaw model at the LHeC. *Phys Rev.* (2016) **D94**:033008. doi: 10.1103/PhysRevD.94.033008
308. Ingelman G, Rathsman J. Heavy Majorana neutrinos at e p colliders. *Z Phys.* (1993) **C60**:243–54.
309. Liang H, He XG, Ma WG, Wang SM, Zhang RY. Seesaw type I and III at the LHeC. *J High Energy Phys.* (2010) **9**:23. doi: 10.1007/JHEP09(2010)023
310. Abelleira Fernandez JL, Adolphsen C, Akay AN, Aksakal H, Albacete JL, Alekhin S, et al. A large hadron electron collider at CERN: report on the physics and design concepts for machine and detector. *J Phys.* (2012) **G39**:075001. doi: 10.1088/0954-3899/39/7/075001

311. Frixione S, Mangano ML, Nason P, Ridolfi G. Improving the Weizsacker-Williams approximation in electron - proton collisions. *Phys Lett.* (1993) **B319**:339–45. doi: 10.1016/0370-2693(93)90823-Z
312. Mattelaer O, Mitra M, Ruiz, R. Automated neutrino jet and top jet predictions at next-to-leading-order with parton shower matching in effective left-right symmetric models. (2016) *arXiv:1610.08985*.
313. Jenkins EE. Searching for a $B-L$ Gauge Boson in $p\bar{p}$ Collisions. *Phys Lett.* (1987) **B192**:219–22. doi: 10.1016/0370-2693(87)91172-5
314. Carena M, Daleo A, Dobrescu BA, Tait TMP. Z' gauge bosons at the Tevatron. *Phys Rev.* (2004) **D70**:093009. doi: 10.1103/PhysRevD.70.093009
315. Emam W, Khalil S. Higgs and Z-prime phenomenology in $B-L$ extension of the standard model at LHC. *Eur Phys J.* (2007) **C52**:625–33. doi: 10.1140/epjc/s10052-007-0411-7
316. Langacker P. The physics of heavy Z' gauge bosons. *Rev Mod Phys.* (2009) **81**:1199–228. doi: 10.1103/RevModPhys.81.1199
317. Iso S, Okada N, Orikasa Y. The minimal B-L model naturally realized at TeV scale. *Phys Rev.* (2009) **D80**:115007. doi: 10.1103/PhysRevD.80.115007
318. Basso L, Belyaev A, Moretti S, Pruna GM, Shepherd-Themistocleous CH. Z' discovery potential at the LHC in the minimal $B-L$ extension of the Standard Model. *Eur Phys J.* (2011) **C71**:1613. doi: 10.1140/epjc/s10052-011-1613-6
319. Deppisch FF, Desai N, Valle JWF. Is charged lepton flavor violation a high energy phenomenon? *Phys Rev.* (2014) **D89**:051302. doi: 10.1103/PhysRevD.89.051302
320. Freitas A. Weakly coupled neutral gauge bosons at future linear colliders. *Phys Rev.* (2004) **D70**:015008. doi: 10.1103/PhysRevD.70.015008
321. Basso L, Belyaev A, Moretti S, Pruna GM. Probing the Z-prime sector of the minimal B-L model at future Linear Colliders in the $e^+e^- \to \mu^+\mu^-$ process. *J High Energy Phys.* (2009) **10**:6. doi: 10.1088/1126-6708/2009/10/006
322. Ramirez-Sánchez F, Gutiérrez-Rodríguez A, Hernández-Ruíz MA. Higgs bosons production and decay at future e^+e^- linear colliders as a probe of the *BL* model. *J Phys.* (2016) **G43**:095003. doi: 10.1088/0954-3899/43/9/095003
323. del Águila F, Aguilar-Saavedra JA. Like-sign dilepton signals from a leptophobic Z' boson. *J High Energy Phys.* (2007) **11**:72. doi: 10.1088/1126-6708/2007/11/072
324. Huitu K, Khalil S, Okada H, Rai SK. Signatures for right-handed neutrinos at the Large Hadron Collider. *Phys Rev Lett.* (2008) **101**:181802. doi: 10.1103/PhysRevLett.101.181802
325. Basso L, Belyaev A, Moretti S, Shepherd-Themistocleous CH. Phenomenology of the minimal B-L extension of the Standard model: Z' and neutrinos. *Phys Rev.* (2009) **D80**:055030. doi: 10.1103/PhysRevD.80.055030
326. Aguilar-Saavedra JA. Heavy lepton pair production at LHC: model discrimination with multi-lepton signals. *Nucl Phys.* (2010) **B828**:289–316. doi: 10.1016/j.nuclphysb.2009.11.021
327. Li T, Chao W. Neutrino masses, dark matter and B-L symmetry at the LHC. *Nucl Phys.* (2011) **B843**:396–412. doi: 10.1016/j.nuclphysb.2010.10.004
328. Aguilar-Saavedra JA, Joaquim FR. Measuring heavy neutrino couplings at the LHC. *Phys Rev.* (2012) **D86**:073005. doi: 10.1103/PhysRevD.86.073005
329. Accomando E, Coriano C, Delle Rose L, Fiaschi J, Marzo C, Moretti S. Z. Higgses and heavy neutrinos in U(1) models: from the LHC to the GUT scale. *J High Energy Phys.* (2016) **7**:86. doi: 10.1007/JHEP07(2016)086
330. Accomando E, Delle Rose L, Moretti S, Olaiya E, Shepherd-Themistocleous CH. Extra higgs boson and Z' as portals to signatures of heavy neutrinos at the LHC. (2017).
331. Kang Z, Ko P, Li J. New avenues to heavy right-handed neutrinos with pair production at hadronic colliders. *Phys Rev.* (2016) **D93**:075037. doi: 10.1103/PhysRevD.93.075037
332. Abdelalim AA, Hammad A, Khalil S. B-L heavy neutrinos and neutral gauge boson Z at the LHC. *Phys Rev.* (2014) **D90**:115015. doi: 10.1103/PhysRevD.90.115015
333. Dube S, Gadkari D, Thalapillil AM. Lepton-jets and low-mass sterile neutrinos at hadron colliders. *Phys Rev.* (2017) **D96**:055031. doi: 10.1103/PhysRevD.96.055031
334. Nemevšek M, Nesti F, Popara G. Keung-Senjanović process at LHC: from LNV to displaced vertices to invisible decays. (2018) *arXiv:1801.05813*.
335. Basso L, Belyaev A, Moretti S, Shepherd-Themistocleous CH. *SM + $B-L$*. Available online at: http://feynrules.irmp.ucl.ac.be/wiki/B-L-SM
336. Basso L, Moretti S, Pruna GM. Theoretical constraints on the couplings of non-exotic minimal Z' bosons. *J High Energy Phys.* (2011) **8**:122. doi: 10.1007/JHEP08(2011)122
337. Mattelaer O, Mitra M, Ruiz R. *Effective Left-Right Symmetric Model at NLO in QCD*. Available online at: http://feynrules.irmp.ucl.ac.be/wiki/EffLRSM
338. Fuks B, Ruiz R. A comprehensive framework for studying W' and Z' bosons at hadron colliders with automated jet veto resummation. *J High Energy Phys.* (2017) **5**:32. doi: 10.1007/JHEP05(2017)032
339. Fuks B, Ruiz R. *SM + W' and Z' at NLO in QCD* . Available online at: http://feynrules.irmp.ucl.ac.be/wiki/WZPrimeAtNLO
340. Basso L, Moretti S, Pruna GM. Phenomenology of the minimal $B-L$ extension of the Standard Model: the Higgs sector. *Phys Rev.* (2011) **D83**:055014. doi: 10.1103/PhysRevD.83.055014
341. Pruna GM. *Phenomenology of the Minimal $B-L$ Model: The Higgs Sector at the Large Hadron Collider and Future Linear Colliders*. Southampton (2011). Available online at: https://inspirehep.net/record/914976/files/arXiv:1106.4691.pdf
342. Accomando E, Delle Rose L, Moretti S, Olaiya E, Shepherd-Themistocleous CH. Novel SM-like Higgs decay into displaced heavy neutrino pairs in U(1) models. *J High Energy Phys.* (2017) **4**:81. doi: 10.1007/JHEP04(2017)081
343. Klasen M, Lyonnet F, Queiroz FS. NLO+NLL collider bounds, Dirac fermion and scalar dark matter in the BL model. *Eur Phys J.* (2017) **C77**:348. doi: 10.1140/epjc/s10052-017-4904-8
344. Aaboud M, Aad G, Abbott B, Abdinov O, Abeloos B, Haider Abidi S. Search for new high-mass phenomena in the dilepton final state using 36.1 fb^{-1} of proton-proton collision data at $\sqrt{s}$ = 13 TeV with the ATLAS detector. (2017). doi: 10.1007/JHEP10(2017)182
345. del Águila F, de Blas J, Perez-Victoria M. Electroweak limits on general new vector bosons. *J High Energy Phys.* (2010) **9**:33. doi: 10.1007/JHEP09(2010)033
346. del Águila F, de Blas J, Langacker P, Perez-Victoria M. Impact of extra particles on indirect Z' limits. *Phys Rev.* (2011) **D84**:015015. doi: 10.1103/PhysRevD.84.015015
347. Aad G, Abbott B, Abdallah J, Abdel Khalek S, Abdinov O, Aben R. Search for high-mass dilepton resonances in pp collisions at $\sqrt{s}$ = 8TeV with the ATLAS detector. *Phys Rev.* (2014) **D90**:052005. doi: 10.1103/PhysRevD.90.052005
348. Khachatryan V, Sirunyan AM, Tumasyan A, Adam W, Bergauer T, Dragicevic M. Search for physics beyond the standard model in dilepton mass spectra in proton-proton collisions at $\sqrt{s} = 8$ TeV. *J High Energy Phys.* (2015) **4**:25. doi: 10.1007/JHEP04(2015)025
349. Sirunyan AM, Tumasyan A, Adam W, Aşilar E, Bergauer T, Brandstetter J. Search for dijet resonances in proton-proton collisions at $\sqrt{s}$ = 13 TeV and constraints on dark matter and other models. *Phys Lett.* (2017) **B769**:520–42. doi: 10.1016/j.physletb.2017.02.012
350. Aaboud M, Aad G, Abbott B, Abdallah J, Abdinov O, Abeloos B. Search for new phenomena in dijet events using 37 fb^{-1} of *pp* collision data collected at $\sqrt{s}$ =13 TeV with the ATLAS detector. *Phys Rev.* (2017) **D96**:052004. doi: 10.1103/PhysRevD.96.052004
351. Chekanov SV, Childers JT, Frizzell D, Proudfoot J, Wang R. Precision searches in dijets at the HL-LHC and HE-LHC. (2017). *arXiv:1710.09484*.
352. Chen CY, Dev PSB, Mohapatra RN. Probing heavy-light neutrino mixing in left-right seesaw models at the LHC. *Phys Rev.* (2013) **D88**:033014. doi: 10.1103/PhysRevD.88.033014
353. Dev PSB, Mohapatra RN, Zhang Y. Probing the higgs sector of the minimal left-right symmetric model at future hadron colliders. *J High Energy Phys.* (2016) **5**:174. doi: 10.1007/JHEP05(2016)174
354. Fuks B, Klasen M, Lamprea DR, Rothering M. Precision predictions for electroweak superpartner production at hadron colliders with Resummino. *Eur Phys J.* (2013) **C73**:2480. doi: 10.1140/epjc/s10052-013-2480-0
355. Jezo T, Klasen M, Lamprea DR, Lyonnet F, Schienbein I. NLO+NLL limits on W' and Z' gauge boson masses in general extensions of the Standard Model. *J High Energy Phys.* (2014) **12**:92. doi: 10.1007/JHEP12(2014)092
356. Gavin R, Li Y, Petriello F, Quackenbush S. FEWZ 2.0: a code for hadronic Z production at next-to-next-to-leading order. *Comput Phys Commun.* (2011) **182**:2388–403. doi: 10.1016/j.cpc.2011.06.008

357. Gavin R, Li Y, Petriello F, Quackenbush S. W physics at the LHC with FEWZ 2.1. *Comput Phys Commun.* (2013) **184**:208–14. doi: 10.1016/j.cpc.2012.09.005
358. Appell D, Sterman GF, Mackenzie PB. Soft Gluons and the Normalization of the Drell-Yan Cross-section. *Nucl Phys.* (1988) **B309**:259–81. doi: 10.1016/0550-3213(88)90082-X
359. Ferrari A, Collot J, Andrieux ML, Belhorma B, de Saintignon P, Hostachy JY, et al. Sensitivity study for new gauge bosons and right-handed Majorana neutrinos in *pp* collisions at $\sqrt{s}$ = 14 TeV. *Phys Rev.* (2000) **D62**:013001. doi: 10.1103/PhysRevD.62.013001
360. Das SP, Deppisch FF, Kittel O, Valle JWF. Heavy neutrinos and lepton flavour violation in left-right symmetric models at the LHC. *Phys Rev.* (2012) **D86**:055006. doi: 10.1103/PhysRevD.86.055006
361. Goh HS, Krenke CA. Lepton number violating signals of the top partners in the left-right twin higgs model. *Phys Rev.* (2010) **D81**:055008. doi: 10.1103/PhysRevD.81.055008
362. The ATLAS Collaboration. Search for new resonances decaying to a charged lepton and a neutrino in pp collisions at $\sqrt{s} = 13$ TeV with the ATLAS detector. *ATLAS-CONF-2016-061* (2016).
363. Khachatryan V, Sirunyan AM, Tumasyan A, Adam W, Bergauer T, Dragicevic M. Search for heavy neutrinos and W bosons with right-handed couplings in proton-proton collisions at $\sqrt{s} = 8$ TeV. *Eur Phys J.* (2014) **C74**:3149. doi: 10.1140/epjc/s10052-014-3149-z
364. Khachatryan V, Sirunyan AM, Tumasyan A, Adam W, Aşilar E, Bergauer T. Search for heavy gauge W' boson in events with an energetic lepton and large missing transverse momentum at $\sqrt{s} = 13$ TeV. *Phys Lett.* (2017) **B770**:278–301. doi: 10.1016/j.physletb.2017.04.043
365. Aguilar-Saavedra JA, Deppisch F, Kittel O, Valle JWF. Flavour in heavy neutrino searches at the LHC. *Phys Rev.* (2012) **D85**:091301. doi: 10.1103/PhysRevD.85.091301
366. Chatrchyan S, Khachatryan V, Sirunyan AM, Tumasyan A, Adam W, Aguilo E, et al. Search for heavy neutrinos and W[R] bosons with right-handed couplings in a left-right symmetric model in pp collisions at sqrt(s) = 7 TeV. *Phys Rev Lett.* (2012) **109**:261802. doi: 10.1103/PhysRevLett.109.261802
367. Quintero N, Diaz-Cruz JL, Lopéz Castro G. Lepton pair emission in the top quark decay $t \to bW^+\ell^-\ell^+$. *Phys Rev.* (2014) **D89**:093014. doi: 10.1103/PhysRevD.89.093014
368. Maiezza A, Nemevšek M, Nesti F. Lepton number violation in higgs decay at LHC. *Phys Rev Lett.* (2015) **115**:081802. doi: 10.1103/PhysRevLett.115.081802
369. Cottin G, Helo JC, Hirsch M. Searches for light sterile neutrinos with multitrack. *Phys Rev. D* (2018) 97:055025. doi: 10.1103/PhysRevD.97.055025
370. Chen CH, Nomura T. Search for $\delta^{\pm\pm}$ with new decay patterns at the LHC. *Phys Rev.* (2015) **D91**:035023. doi: 10.1103/PhysRevD.91.035023
371. Frank M, Hayreter A, Turan I. Production and Decays of W_R bosons at the LHC. *Phys Rev.* (2011) **D83**:035001. doi: 10.1103/PhysRevD.83.035001
372. Dicus DA, Willenbrock S. Higgs boson production from heavy quark fusion. *Phys Rev.* (1989) **D39**:751. doi: 10.1103/PhysRevD.39.751
373. Maltoni F, Ridolfi G, Ubiali M. b-initiated processes at the LHC: a reappraisal. *J High Energy Phys.* (2012) **7**:22. doi: 10.1007/JHEP07(2012)022
374. Dawson S, Ismail A, Low I. Redux on When is the top quark a parton?. *Phys Rev.* (2014) **D90**:014005. doi: 10.1103/PhysRevD.90.014005
375. Han T, Sayre J, Westhoff S. Top-quark initiated processes at high-energy hadron colliders. *J High Energy Phys.* (2015) **4**:145. doi: 10.1007/JHEP04(2015)145
376. Kaya U, Sahin M, Sultansoy, S. Majorana neutrino and W_R at TeV scale *ep* colliders. (2015) *arXiv:1502.04115*.
377. Lindner M, Queiroz FS, Rodejohann W, Yaguna CE. Left-right symmetry and lepton number violation at the large hadron electron collider. *J High Energy Phys.* (2016) **6**:140. doi: 10.1007/JHEP06(2016)140
378. Buchmüller W, Greub C. Right-handed currents and heavy neutrinos in high-energy *ep* and e^+e^- scattering. *Nucl Phys.* (1992) **B381**:109–28. doi: 10.1016/0550-3213(92)90642-O
379. Mondal S, Rai SK. Reply to Comment on Polarized window for left-right symmetry and a right-handed neutrino at the Large Hadron-Electron Collider. *Phys Rev.* (2016) **D93**:118702. doi: 10.1103/PhysRevD.93.118702
380. Mondal S, Rai SK. Polarized window for left-right symmetry and a right-handed neutrino at the Large Hadron-Electron Collider. *Phys Rev.* (2016) **D93**:011702. doi: 10.1103/PhysRevD.93.011702
381. Sarmiento-Alvarado IA, Bouzas AO, Larios F. Analysis of top-quark charged-current coupling at the LHeC. *J Phys.* (2015) **G42**:085001. doi: 10.1088/0954-3899/42/8/085001
382. Bhupal Dev PS, Lee CH, Mohapatra RN. TeV scale lepton number violation and baryogenesis. *J Phys Conf Ser.* (2015) **631**:012007. doi: 10.1088/1742-6596/631/1/012007
383. Gopalakrishna S, Han T, Lewis I, Si Zg, Zhou YF. Chiral couplings of W' and top quark polarization at the LHC. *Phys Rev.* (2010) **D82**:115020. doi: 10.1103/PhysRevD.82.115020
384. Vasquez JC. Right-handed lepton mixings at the LHC. *J High Energy Phys.* (2016) **5**:176. doi: 10.1007/JHEP05(2016)176
385. Tello V, Nemevšek M, Nesti F, Senjanović G, Vissani F. Left-right symmetry: from LHC to neutrinoless double beta decay. *Phys Rev Lett.* (2011) **106**:151801. doi: 10.1103/PhysRevLett.106.151801
386. Gluza J, Jeliński T. Heavy neutrinos and the $pp \to \ell\ell jj$ CMS data. *Phys Lett.* (2015) **B748**:125–31. doi: 10.1016/j.physletb.2015.06.077
387. Gluza J, Jelinski T, Szafron R. Lepton number violation and 'Diracness' of massive neutrinos composed of Majorana states. *Phys Rev.* (2016) **D93**:113017. doi: 10.1103/PhysRevD.93.113017
388. Bajc B, Nemevšek M, Senjanović G. Probing leptonic CP phases in LFV processes. *Phys Lett.* (2010) **B684**:231–5. doi: 10.1016/j.physletb.2010.01.025
389. Frere JM, Hambye T, Vertongen G. Is leptogenesis falsifiable at LHC? *J High Energy Phys.* (2009) **1**:51. doi: 10.1088/1126-6708/2009/01/051
390. Dhuria M, Hati C, Rangarajan R, Sarkar U. Falsifying leptogenesis for a TeV scale $W_R^{\pm}$ at the LHC. *Phys Rev.* (2015) **D92**:031701. doi: 10.1103/PhysRevD.92.031701
391. Deppisch FF, Harz J, Hirsch M. Falsifying high-scale leptogenesis at the LHC. *Phys Rev Lett.* (2014) **112**:221601. doi: 10.1103/PhysRevLett.112.221601
392. Harz J, Huang WC, Ps H. Lepton number violation and the baryon asymmetry of the universe. *Int J Mod Phys.* (2015) **A30**:1530045. doi: 10.1142/S0217751X15300458
393. Barry J, Rodejohann W. Lepton number and flavour violation in TeV-scale left-right symmetric theories with large left-right mixing. *J High Energy Phys.* (2013) **9**:153. doi: 10.1007/JHEP09(2013)153
394. Peng T, Ramsey-Musolf MJ, Winslow P. TeV lepton number violation: from neutrinoless double-β decay to the LHC. *Phys Rev.* (2016) **D93**:093002. doi: 10.1103/PhysRevD.93.093002
395. Frank M, Saif HN. Signals of left-right supersymmetry in e+ e- collisions. *Z Phys.* (1996) **C69**:673–82. doi: 10.1007/s002880050071
396. Demir DA, Frank M, Ghosh DK, Huitu K, Rai SK, Turan I. Doubly charged higgsinos at tevatron. *Phys Rev.* (2009) **D79**:095006. doi: 10.1103/PhysRevD.79.095006
397. Appelquist T, Shrock R. Dynamical symmetry breaking of extended gauge symmetries. *Phys Rev Lett.* (2003) **90**:201801. doi: 10.1103/PhysRevLett.90.201801
398. de Almeida FML, Coutinho YA, Martins Simoes JA, Ramalho AJ, Ribeiro Pinto L, Wulck S, et al. Double seesaw mechanism in a left-right symmetric model with TeV neutrinos. *Phys Rev.* (2010) **D81**:053005. doi: 10.1103/PhysRevD.81.053005
399. Agashe K, Hong S, Vecchi L. Warped seesaw mechanism is physically inverted. *Phys Rev.* (2016) **D94**:013001. doi: 10.1103/PhysRevD.94.013001
400. Agashe K, Du P, and Hong S. LHC signals for singlet neutrinos from a natural warped seesaw (II). *Phys Rev D* (2017) **97**:075032. doi: 10.1103/PhysRevD.97.075033
401. Agashe K, Du P, Hong S. LHC signals for singlet neutrinos from a natural warped seesaw (II). *Phys Rev D* (2017) 97:075033. doi: 10.1103/PhysRevD.97.075033
402. Bhupal Dev PS, Goswami S, Mitra M, Rodejohann W. Constraining neutrino mass from neutrinoless double beta decay. *Phys Rev.* (2013) **D88**:091301. doi: 10.1103/PhysRevD.88.091301
403. Leonardi R, Alunni L, Romeo F, Fan L, Panella O. Hunting for heavy composite Majorana neutrinos at the LHC. *Eur Phys J.* (2016) **C76**:593. doi: 10.1140/epjc/s10052-016-4396-y
404. Duarte L, Romero I, Peressutti J, Sampayo OA. Effective Majorana neutrino decay. *Eur Phys J.* (2016) **C76**:453. doi: 10.1140/epjc/s10052-016-4301-8

405. Duarte L, Peressutti, J, Sampayo OA. Not-that-heavy Majorana neutrino signals at the LHC. *J Phys.* (2018) G45:025001. doi: 10.1088/1361-6471/aa99f5
406. Duarte L, Peressutti J, Sampayo OA. Majorana neutrino decay in an Effective Approach. *Phys Rev.* (2015) **D92**:093002. doi: 10.1103/PhysRevD.92.093002
407. Gelmini GB, Roncadelli M. Left-handed neutrino mass scale and spontaneously broken lepton number. *Phys Lett.* (1981) **99B**:411–5. doi: 10.1016/0370-2693(81)90559-1
408. Fileviez Pérez P, Han T, Huang Gy, Li T, Wang K. Neutrino masses and the CERN LHC: testing type II seesaw. *Phys Rev.* (2008) **D78**:015018. doi: 10.1103/PhysRevD.78.015018
409. Dutta B, Eusebi R, Gao Y, Ghosh T, Kamon T. Exploring the doubly charged Higgs boson of the left-right symmetric model using vector boson fusionlike events at the LHC. *Phys Rev.* (2014) **D90**:055015. doi: 10.1103/PhysRevD.90.055015
410. Han T, Logan HE, Mukhopadhyaya B, Srikanth R. Neutrino masses and lepton-number violation in the littlest Higgs scenario. *Phys Rev.* (2005) **D72**:053007. doi: 10.1103/PhysRevD.72.053007
411. Melfo A, Nemevšek M, Nesti F, Senjanović G, Zhang Y. Type II seesaw at LHC: the roadmap. *Phys Rev.* (2012) **D85**:055018. doi: 10.1103/PhysRevD.85.055018
412. Arhrib A, Benbrik R, Chabab M, Moultaka G, Peyranère MC, Rahili L, et al. The higgs potential in the type II seesaw model. *Phys Rev.* (2011) **D84**:095005. doi: 10.1103/PhysRevD.84.095005
413. Kanemura S, Yagyu K. Radiative corrections to electroweak parameters in the Higgs triplet model and implication with the recent Higgs boson searches. *Phys Rev.* (2012) **D85**:115009. doi: 10.1103/PhysRevD.85.115009
414. Chen MC, Dawson S, Jackson CB. Higgs triplets, decoupling, and precision measurements. *Phys Rev.* (2008) **D78**:093001. doi: 10.1103/PhysRevD.78.093001
415. Chen MC, Dawson S, Krupovnickas T. Constraining new models with precision electroweak data. *Int J Mod Phys.* (2006) **A21**:4045–70. doi: 10.1142/S0217751X0603388X
416. Das D, Santamaria A. Updated scalar sector constraints in the Higgs triplet model. *Phys Rev.* (2016) **D94**:015015. doi: 10.1103/PhysRevD.94.015015
417. Bhupal Dev PS, Ghosh DK, Okada N, Saha I. 125 GeV higgs boson and the type-II seesaw model. *J High Energy Phys.* (2013) **3**:150. doi: 10.1007/JHEP05(2013)04910.1007/JHEP03(2013)150
418. Dev PSB, Vila CM, Rodejohann W. Naturalness in testable type II seesaw scenarios. *Nucl Phys.* (2017) **B921**:436–53. doi: 10.1016/j.nuclphysb.2017.06.007
419. Hooft G. Naturalness, chiral symmetry, and spontaneous chiral symmetry breaking. *NATO Sci Ser B* (1980) **59**:135–57. doi: 10.1007/978-1-4684-7571-5_9
420. Aad G, Abbott B, Abdallah J, Abdinov O, Abeloos B, Aben R. Measurements of the Higgs boson production and decay rates and constraints on its couplings from a combined ATLAS and CMS analysis of the LHC pp collision data at $\sqrt{s} = 7$ and 8 TeV. *J High Energy Phys.* (2016) **8**:45. doi: 10.1007/JHEP08(2016)045
421. Akeroyd AG, Aoki M, Sugiyama H. Probing majorana phases and neutrino mass spectrum in the higgs triplet model at the CERN LHC. *Phys Rev.* (2008) **D77**:075010. doi: 10.1103/PhysRevD.77.075010
422. Garayoa J, Schwetz T. Neutrino mass hierarchy and Majorana CP phases within the Higgs triplet model at the LHC. *J High Energy Phys.* (2008) **3**:9. doi: 10.1088/1126-6708/2008/03/009
423. Cuypers F, Davidson S. Bileptons: present limits and future prospects. *Eur Phys J.* (1998) **C2**:503–28. doi: 10.1007/s100529800705
424. Tully MB, Joshi GC. Generating neutrino mass in the 331 model. *Phys Rev.* (2001) **D64**:011301. doi: 10.1103/PhysRevD.64.011301
425. Fonseca RM, Hirsch M. Lepton number violation in 331 models. *Phys Rev.* (2016) **D94**:115003. doi: 10.1103/PhysRevD.94.115003
426. Cogollo D, Diniz H, de S Pires CA, Rodrigues da Silva PS. The Seesaw mechanism at TeV scale in the 3-3-1 model with right-handed neutrinos. *Eur Phys J.* (2008) **C58**:455–61. doi: 10.1140/epjc/s10052-008-0749-5
427. Georgi H, Glashow SL. Unity of all elementary particle forces. *Phys Rev Lett.* (1974) **32**:438–41. doi: 10.1103/PhysRevLett.32.438
428. Frampton PH. Chiral dilepton model and the flavor question. *Phys Rev Lett.* (1992) **69**:2889–91. doi: 10.1103/PhysRevLett.69.2889
429. Pisano F, Pleitez V. An $SU(3) \times U(1)$ model for electroweak interactions. *Phys Rev.* (1992) **D46**:410–7. doi: 10.1103/PhysRevD.46.410
430. Dorsner I, Fileviez Pérez P. Unification without supersymmetry: neutrino mass, proton decay and light leptoquarks. *Nucl Phys.* (2005) **B723**:53–76. doi: 10.1016/j.nuclphysb.2005.06.016
431. Fileviez Pérez P, Han T, Li T, Ramsey-Musolf MJ. Leptoquarks and Neutrino Masses at the LHC. *Nucl Phys.* (2009) **B819**:139–76. doi: 10.1016/j.nuclphysb.2009.04.009
432. Bahrami S, Frank M. Vector leptons in the higgs triplet model. *Phys Rev.* (2013) **D88**:095002. doi: 10.1103/PhysRevD.88.095002
433. Nepomuceno A, Meirose B, Eccard F. First results on bilepton production based on LHC collision data and predictions for run II. *Phys Rev.* (2016) **D94**:055020. doi: 10.1103/PhysRevD.94.055020
434. Corcella G, Coriano C, Costantini A, Frampton PH. Bilepton signatures at the LHC. *Phys Lett.* (2017) **B773**:544–52. doi: 10.1016/j.physletb.2017.09.015
435. Meirose B, Nepomuceno AA. Searching for doubly-charged vector bileptons in the Golden Channel at the LHC. *Phys Rev.* (2011) **D84**:055002. doi: 10.1103/PhysRevD.84.055002
436. Rizzo TG. Doubly charged higgs bosons and lepton number violating processes. *Phys Rev.* (1982) **D25**:1355–64. doi: 10.1103/PhysRevD.25.1355
437. Akeroyd AG, Aoki M. Single and pair production of doubly charged Higgs bosons at hadron colliders. *Phys Rev.* (2005) **D72**:035011. doi: 10.1103/PhysRevD.72.035011
438. Mühlleitner M, Spira M. A note on doubly charged Higgs pair production at hadron colliders. *Phys Rev.* (2003) **D68**:117701. doi: 10.1103/PhysRevD.68.117701
439. Chen CS, Geng CQ, Zhuridov DV. Same-sign single dilepton productions at the LHC. *Phys Lett.* (2008) **B666**:340–3. doi: 10.1016/j.physletb.2008.07.088
440. Han T, Mukhopadhyaya B, Si Z, Wang K. Pair production of doubly-charged scalars: neutrino mass constraints and signals at the LHC. *Phys Rev.* (2007) **D76**:075013. doi: 10.1103/PhysRevD.76.075013
441. Drees M, Godbole RM, Nowakowski M, Rindani SD. gamma gamma processes at high-energy p p colliders. *Phys Rev.* (1994) **D50**:2335–8.
442. Bambhaniya G, Chakrabortty J, Gluza J, Jelinski T, Szafron R. Search for doubly charged Higgs bosons through vector boson fusion at the LHC and beyond. *Phys Rev.* (2015) **D92**:015016. doi: 10.1103/PhysRevD.92.015016
443. Babu KS, Jana S. Probing doubly charged higgs bosons at the LHC through photon initiated processes. *Phys Rev.* (2017) **D95**:055020. doi: 10.1103/PhysRevD.95.055020
444. Ball RD, Bertone V, Carrazza S, Del Debbio L, Forte S, Guffanti A, et al. Parton distributions with QED corrections. *Nucl Phys.* (2013) **B877**:290–320. doi: 10.1016/j.nuclphysb.2013.10.010
445. Ball RD, Bertone V, Carrazza S, Deans CS, Del Debbio L, Forte S, et al. Parton distributions for the LHC Run II. *J High Energy Phys.* (2015) **4**:40. doi: 10.1007/JHEP04(2015)040
446. Ghosh K, Jana S, Nandi S. Neutrino mass generation at TeV scale and new physics signatures from charged Higgs at the LHC for photon initiated processes. *J High Energ Phys.* (2018) **3**:180. doi: 10.1007/JHEP03(2018)180
447. del Águila F, Ametller L. On the detectability of sleptons at large hadron colliders. *Phys Lett.* (1991) **B261**:326–33. doi: 10.1016/0370-2693(91)90336-O
448. Nemevšek M, Nesti F, Vasquez JC. Majorana Higgses at colliders. *J High Energy Phys.* (2017) **4**:114. doi: 10.1007/JHEP04(2017)114
449. del Águila F, Chala M. LHC bounds on lepton number violation mediated by doubly and singly-charged scalars. *J High Energy Phys.* (2014) **3**:27. doi: 10.1007/JHEP03(2014)027
450. del Águila F, Chala M. *LNV-Scalars*. Available online at: http://cafpe.ugr.es/index.php/pages/other/software
451. Roitgrund A, Eilam G, Bar-Shalom S. Implementation of the left-right symmetric model in FeynRules. *Comput Phys Commun.* (2016) **203**:18–44. doi: 10.1016/j.cpc.2015.12.009
452. Roitgrund A, Eilam G, Bar-Shalom S. *FeynRules Mod-File for the MLRSM/QMLRSM*. Available online at: https://drive.google.com/folderview?id=0BxMAGX_Tlpi9X0RUZW9tS2RaQ0E&usp=sharing
453. Georgi H, Machacek M. Doubly charged higgs bosons. *Nucl Phys.* (1985) **B262**:463–77. doi: 10.1016/0550-3213(85)90325-6

454. Degrande C, Hartling K, Logan HE, Peterson AD, Zaro M. *Georgi-Machacek Model at Next-to-Leading Order Accuracy*. Available online at: http://feynrules.irmp.ucl.ac.be/wiki/GeorgiMachacekModel.
455. Aad G, Abajyan T, Abbott B, Abdallah J, Abdel Khalek S, Ali Abdelalim A. Search for long-lived, multi-charged particles in pp collisions at $\sqrt{s}$=7 TeV using the ATLAS detector. *Phys Lett.* (2013) **B722**:305–23. doi: 10.1016/j.physletb.2013.04.036
456. Aad G, Abbott B, Abdallah J, Abdinov O, Aben R, Abolins M. Search for heavy long-lived multi-charged particles in pp collisions at $\sqrt{s}$ = 8 TeV using the ATLAS detector. *Eur Phys J.* (2015) **C75**:362. doi: 10.1140/epjc/s10052-015-3534-2
457. CMS Collaboration. Search for multi-charged heavy stable charged particles. *CMS-PAS-EXO-11-090* (2012).
458. Barrie ND, Kobakhidze A, Liang S, Talia M, Wu L. Exotic lepton searches via bound state production at the LHC. *Phys Lett.* (2018) **B781**:364–7. doi: 10.1016/j.physletb.2018.03.087
459. del Águila F, Chala M, Santamaria A, Wudka J. Discriminating between lepton number violating scalars using events with four and three charged leptons at the LHC. *Phys Lett.* (2013) **B725**:310–5. doi: 10.1016/j.physletb.2013.07.014
460. Aaboud M, Aad G, Abbott B, Abdinov O, Abeloos B, Abidi SH. Search for doubly charged Higgs boson production in multi-lepton final states with the ATLAS detector using proton-proton collisions at $\sqrt{s} = 13$ TeV. *Eur Phys J.* (2018) **C78**:199. doi: 10.1140/EPJC/S10052-018-5661-Z
461. CMS Collaboration. A search for doubly-charged Higgs boson production in three and four lepton final states at $\sqrt{s} = 13$ TeV. *CMS-PAS-HIG-16-036* (2017).
462. Nomura T, Okada H, Yokoya H. Discriminating leptonic Yukawa interactions with doubly charged scalar at the ILC. *Nucl Phys.* (2018) **B929**:193–206. doi: 10.1016/j.nuclphysb.2018.02.011
463. Hays C, Mitra M, Spannowsky M, Waite P. Prospects for new physics in $\tau \to l\mu\mu$ at current and future colliders. *J High Energy Phys.* (2017) **5**:14. doi: 10.1007/JHEP05(2017)014
464. Frank M, Hamidian H. Higgs pair production in the left-right symmetric extension of the standard model. *Nuovo Cim.* (1995) **A108**:323–34. doi: 10.1007/BF02787059
465. Rizzo TG. Inverse neutrinoless double beta decay. *Phys Lett.* (1982) **116B**:23–8. doi: 10.1016/0370-2693(82)90027-2
466. Rodejohann W. Inverse neutrino-less double beta decay revisited: neutrinos, higgs triplets and a muon collider. *Phys Rev.* (2010) **D81**:114001. doi: 10.1103/PhysRevD.81.114001
467. Barry J, Dorame L, Rodejohann W. Linear collider test of a neutrinoless double beta decay mechanism in left-right symmetric theories. *Eur Phys J.* (2012) **C72**:2023. doi: 10.1140/epjc/s10052-012-2023-0
468. Atwood D, Bar-Shalom S, Soni A. Signature of heavy Majorana neutrinos at a linear collider: enhanced charged Higgs pair production. *Phys Rev.* (2007) **D76**:033004. doi: 10.1103/PhysRevD.76.033004
469. Ren P, Xing Zz. Lepton-number-violating decays of singly-charged Higgs bosons in the minimal type-(I+II) seesaw model at the TeV scale. *Chin Phys.* (2010) **C34**:433–43. doi: 10.1088/1674-1137/34/4/003
470. Yue CX, Feng HL, Ma W. Heavy charged leptons from type-III seesaw and pair production of the Higgs boson H at the International Linear e^+e^- Collider. *Chin Phys Lett.* (2010) **27**:011202. doi: 10.1088/0256-307X/27/1/011202
471. Banks T, Carpenter LM, Fortin JF. Undetected Higgs decays and neutrino masses in gauge mediated, lepton number violating models. *J High Energy Phys.* (2008) **9**:87. doi: 10.1088/1126-6708/2008/09/087
472. Hektor A, Kadastik M, Muntel M, Raidal M, Rebane L. Testing neutrino masses in little Higgs models via discovery of doubly charged Higgs at LHC. *Nucl Phys.* (2007) **B787**:198–210. doi: 10.1016/j.nuclphysb.2007.07.014
473. Kadastik M, Raidal M, Rebane L. Direct determination of neutrino mass parameters at future colliders. *Phys Rev.* (2008) **D77**:115023. doi: 10.1103/PhysRevD.77.115023
474. Chun EJ, Lee KY, Park SC. Testing Higgs triplet model and neutrino mass patterns. *Phys Lett.* (2003) **B566**:142–51. doi: 10.1016/S0370-2693(03)00770-6
475. Abada A, Biggio C, Bonnet F, Gavela MB, Hambye T. mu $\to$ e gamma and tau $\to$ l gamma decays in the fermion triplet seesaw model. *Phys Rev.* (2008) **D78**:033007. doi: 10.1103/PhysRevD.78.033007
476. Eboli OJP, Gonzalez-Fraile J, Gonzalez-Garcia MC. Neutrino masses at LHC: minimal lepton flavour violation in type-III see-saw. *J High Energy Phys.* (2011) **12**:009. doi: 10.1007/JHEP12(2011)009
477. Agostinho NR, Eboli, OJP, Gonzalez-Garcia MC. LHC run I bounds on minimal lepton flavour violation in type-III see-saw: a case study. *J High Energ Phys.* (2017) **11**:118. doi: 10.1007/JHEP11(2017)118
478. Gogoladze I, Okada N, Shafi Q. Higgs boson mass bounds in the standard model with type III and type I seesaw. *Phys Lett.* (2008) **B668**:121–5. doi: 10.1016/j.physletb.2008.08.023
479. He B, Okada N, Shafi Q. 125 GeV Higgs, type III seesaw and gauge Higgs unification. *Phys Lett.* (2012) **B716**:197–202. doi: 10.1016/j.physletb.2012.08.012
480. Gogoladze I, He B, Shafi Q. New fermions at the LHC and mass of the higgs boson. *Phys Lett.* (2010) **B690**:495–500. doi: 10.1016/j.physletb.2010.05.076
481. Li T, He XG. Neutrino masses and heavy triplet leptons at the LHC: testability of type III seesaw. *Phys Rev.* (2009) **D80**:093003. doi: 10.1103/PhysRevD.80.093003
482. Arhrib A, Bajc B, Ghosh DK, Han T, Huang GY, Puljak I, et al. Collider signatures for heavy lepton triplet in type I+III seesaw. *Phys Rev.* (2010) **D82**:053004. doi: 10.1103/PhysRevD.82.053004
483. He XG, Oh S. Lepton FCNC in type III seesaw model. *J High Energy Phys.* (2009) **9**:27. doi: 10.1088/1126-6708/2009/09/027
484. Franceschini R, Hambye T, Strumia A. Type-III see-saw at LHC. *Phys Rev.* (2008) **D78**:033002. doi: 10.1103/PhysRevD.78.033002
485. Bajc B, Senjanović G. Seesaw at LHC. *J High Energy Phys.* (2007) **8**:14. doi: 10.1088/1126-6708/2007/08/014
486. Dorsner I, Fileviez Pérez P. Upper bound on the mass of the type III seesaw triplet in an SU(5) model. *J High Energy Phys.* (2007) **6**:29. doi: 10.1088/1126-6708/2007/06/029
487. Bajc B, Nemevšek M, Senjanović G. Probing seesaw at LHC. *Phys Rev.* (2007) **D76**:055011.
488. Fileviez Pérez P. Renormalizable adjoint SU(5). *Phys Lett.* (2007) **B654**:189–93. doi: 10.1016/j.physletb.2007.07.075
489. Aristizabal Sierra D, Kamenik JF, Nemevšek M. Implications of flavor dynamics for fermion triplet leptogenesis. *J High Energy Phys.* (2010) **10**:36. doi: 10.1007/JHEP10(2010)036
490. Aguilar-Saavedra JA, Boavida PM, Joaquim FR. Flavored searches for type-III seesaw mechanism at the LHC. *Phys Rev.* (2013) **D88**:113008. doi: 10.1103/PhysRevD.88.113008
491. Biggio C, Calibbi L. Phenomenology of SUSY SU(5) with type I+III seesaw. *J High Energy Phys.* (2010) **10**:37. doi: 10.1007/JHEP10(2010)037
492. Chakrabortty J, Goswami S, Raychaudhuri A. An SO(10) model with adjoint fermions for double seesaw neutrino masses. *Phys Lett.* (2011) **B698**:265–70. doi: 10.1016/j.physletb.2011.03.016
493. Gu PH. A left-right symmetric model with SU(2)-triplet fermions. *Phys Rev.* (2011) **D84**:097301. doi: 10.1103/PhysRevD.84.097301
494. Mohapatra RN. Natural suppression of proton decay in supersymmetric type III seesaw models. *Phys Lett.* (2009) **B679**:382–5. doi: 10.1016/j.physletb.2009.07.064
495. Delgado A, Garcia Cely C, Han T, Wang Z. Phenomenology of a lepton triplet. *Phys Rev.* (2011) **D84**:073007. doi: 10.1103/PhysRevD.84.073007
496. Ma T, Zhang B, Cacciapaglia G. Triplet with a doubly-charged lepton at the LHC. *Phys Rev.* (2014) **D89**:015020. doi: 10.1103/PhysRevD.89.015020
497. Yu Y, Yue CX, Yang S. Signatures of the quintuplet leptons at the LHC. *Phys Rev.* (2015) **D91**:093003. doi: 10.1103/PhysRevD.91.093003
498. Nomura T, Okada H. Neutrino mass with large $SU(2)_L$ multiplet fields. *Phys Rev.* (2017) **D96**:095017. doi: 10.1103/PhysRevD.96.095017
499. Biggio C, Bonnet F. Implementation of the type III seesaw model in FeynRules/MadGraph and prospects for discovery with early LHC data. *Eur Phys J.* (2012) **C72**:1899. doi: 10.1140/epjc/s10052-012-1899-z
500. Biggio C, Bonnet F. *Type III Seesaw Model in FeynRules*. Available online at: http://feynrules.irmp.ucl.ac.be/wiki/TypeIIISeeSaw
501. *Minimal Lepton Flavor Violation Type III Seesaw Model*. Available online at: http://feynrules.irmp.ucl.ac.be/wiki/MLFVtIIIseesaw

502. Choubey S, Mitra M. Spontaneous R-parity violating type III seesaw. *J High Energy Phys.* (2010) **5**:21. doi: 10.1007/JHEP05(2010)021
503. Bandyopadhyay P, Choi S, Chun EJ, Min K. Probing Higgs bosons via the type III seesaw mechanism at the LHC. *Phys Rev.* (2012) **D85**:073013. doi: 10.1103/PhysRevD.85.073013
504. He XG, Oh S, Tandean J, Wen CC. Large mixing of light and heavy neutrinos in seesaw models and the LHC. *Phys Rev.* (2009) **D80**:073012. doi: 10.1103/PhysRevD.80.073012
505. Bandyopadhyay P, Chun EJ. Displaced Higgs production in type III seesaw. *J High Energy Phys.* (2010) **11**:006. doi: 10.1007/JHEP11(2010)006
506. Aad G, et al. Search for heavy lepton resonances decaying to a Z boson and a lepton in pp collisions at $\sqrt{s} = 8$ TeV with the ATLAS detector. *J High Energy Phys.* (2015) **9**:108. doi: 10.1007/JHEP09(2015)108
507. CMS Collaboration. Search for Type-III seesaw heavy fermions with multilepton final states using 2.3/fb of 13 TeV proton-proton collision data. *CMS-PAS-EXO-16-002* (2016).
508. CMS Collaboration. Search for evidence of type-III seesaw mechanism in multilepton final states in pp collisions at $\sqrt{s} = 13$ TeV. *Phys Rev Lett.* (2017) **119**:221802. doi: 10.1103/PhysRevLett.119.221802
509. Goswami D, Poulose P. Direct searches of Type III seesaw triplet fermions at high energy e^+e^- collider. *Eur Phys J.* (2018) **C78**:1. doi: 10.1140/epjc/s10052-017-5478-1
510. Cai Y, Herrero García J, Schmidt MA, Vicente A, Volkas RR. From the trees to the forest: a review of radiative neutrino mass models. *Front Phys.* (2017) **5**:63. doi: 10.3389/fphy.2017.00063
511. Cai Y, Clarke JD, Schmidt MA, Volkas RR. Testing radiative neutrino mass models at the LHC. *J High Energy Phys.* (2015) **2**:161. doi: 10.1007/JHEP02(2015)161
512. Aristizabal Sierra D, Hirsch M, Kovalenko SG. Leptoquarks: neutrino masses and accelerator phenomenology. *Phys Rev.* (2008) **D77**:055011. doi: 10.1103/PhysRevD.77.055011
513. Ma E. Verifiable radiative seesaw mechanism of neutrino mass and dark matter. *Phys Rev.* (2006) **D73**:077301. doi: 10.1103/PhysRevD.73.077301
514. Ho SY, Tandean J. Probing scotogenic effects in higgs boson decays. *Phys Rev.* (2013) **D87**:095015. doi: 10.1103/PhysRevD.87.095015
515. Ho SY, Tandean J. Probing scotogenic effects in e^+e^- colliders. *Phys Rev.* (2014) **D89**:114025. doi: 10.1103/PhysRevD.89.114025
516. Hessler AG, Ibarra A, Molinaro E, Vogl S. Probing the scotogenic FIMP at the LHC. *J High Energy Phys.* (2017) **1**:100. doi: 10.1007/JHEP01(2017)100
517. Daz MA, Rojas N, Urrutia-Quiroga S, Valle JWF. Heavy higgs boson production at colliders in the singlet-triplet scotogenic dark matter model. *J High Energy Phys.* (2017) **8**:17. doi: 10.1007/JHEP08(2017)017
518. Gustafsson M, No JM, Rivera MA. Predictive model for radiatively induced neutrino masses and mixings with dark matter. *Phys Rev Lett.* (2013) **110**:211802. doi: 10.1103/PhysRevLett.110.211802
519. Ma E. Derivation of dark matter parity from lepton parity. *Phys Rev Lett.* (2015) **115**:011801. doi: 10.1103/PhysRevLett.115.011801
520. Guo SY, Han ZL, Liao Y. Testing the type II radiative seesaw model: from dark matter detection to LHC signatures. *Phys Rev.* (2016) **D94**:115014. doi: 10.1103/PhysRevD.94.115014
521. Kohda M, Sugiyama H, Tsumura K. Lepton number violation at the LHC with leptoquark and diquark. *Phys Lett.* (2013) **B718**:1436–40. doi: 10.1016/j.physletb.2012.12.048
522. Adam J, Bai X, Baldini AM, Baracchini E, Bemporad C, Boca G, et al. New constraint on the existence of the $\mu^+ \to e^+\gamma$ decay. *Phys Rev Lett.* (2013) **110**:201801. doi: 10.1103/PhysRevLett.110.201801
523. Baldini AM, Bao Y, Baracchini E, Bemporad C, Berg F, Biasotti M. Search for the lepton flavour violating decay $\mu^+ \to e^+\gamma$ with the full dataset of the MEG experiment. *Eur Phys J.* (2016) **C76**:434. doi: 10.1140/epjc/s10052-016-4271-x
524. Herrero-Garcia J, Nebot M, Rius N, Santamaria A. The ZeeBabu model revisited in the light of new data. *Nucl Phys.* (2014) **B885**:542–70. doi: 10.1016/j.nuclphysb.2014.06.001
525. Alcaide J, Chala M, Santamaria, A. LHC signals of radiatively-induced neutrino masses and implications for the Zee-Babu model. *Phys Lett.* **B779**:107–16. doi: 10.1016/j.physletb.2018.02.001
526. Helo JC, Hirsch M, Ps H, Kovalenko SG. Short-range mechanisms of neutrinoless double beta decay at the LHC. *Phys Rev.* (2013) **D88**:073011. doi: 10.1103/PhysRevD.88.073011
527. Helo JC, Hirsch M, Kovalenko SG, Pas H. Neutrinoless double beta decay and lepton number violation at the LHC. *Phys Rev.* (2013) **D88**:011901. doi: 10.1103/PhysRevD.88.011901
528. Aad G, Abajyan T, Abbott B, Abdallah J, Khalek SA, Abdinov O. Search for direct top-squark pair production in final states with two leptons in pp collisions at $\sqrt{s} = 8$TeV with the ATLAS detector. *J High Energy Phys.* (2014) **6**:124. doi: 10.1007/JHEP06(2014)124
529. Aaboud M, Aad G, Abbott B, Abdallah J, Abdinov O, Abeloos B, et al. Search for scalar leptoquarks in pp collisions at $\sqrt{s}$ = 13 TeV with the ATLAS experiment. *New J Phys.* (2016) **18**:093016. doi: 10.1088/1367-2630/18/9/093016
530. Aad G, et al. Searches for scalar leptoquarks in pp collisions at $\sqrt{s}$ = 8 TeV with the ATLAS detector. *Eur Phys J.* (2016) **C76**:5. doi: 10.1140/epjc/s10052-015-3823-9
531. CMS Collaboration. Search for pair-production of first generation scalar leptoquarks in pp collisions at $\sqrt{s} = 13$ TeV with 2.6 fb^{-1}. (2016).
532. CMS Collaboration. Search for pair-production of second-generation scalar leptoquarks in pp collisions at $\sqrt{s} = 13$ TeV with the CMS detector. (2016).
533. Collaboration C. Search for the third-generation scalar leptoquarks and heavy right-handed neutrinos in $\tau_\ell \tau_h$jj final states in pp collisions at 13 TeV. (2016).
534. collaboration TA. Search for long-lived charginos based on a disappearing-track signature in pp collisions at $\sqrt{s} = 13$ TeV with the ATLAS detector. (2017).
535. Aad G, Abajyan T, Abbott B, Abdallah J, Khalek SA, Abdinov O. Search for charginos nearly mass degenerate with the lightest neutralino based on a disappearing-track signature in pp collisions at $\sqrt{s}$=8 TeV with the ATLAS detector. *Phys Rev.* (2013) **D88**:112006. doi: 10.1103/PhysRevD.88.112006
536. Khachatryan V, Sirunyan AM, Tumasyan A, Adam W, Bergauer T, Dragicevic M Search for disappearing tracks in proton-proton collisions at $\sqrt{s} = 8$ TeV. *J High Energy Phys.* (2015) **1**:96. doi: 10.1007/JHEP01(2015)096

Conflict of Interest Statement: The authors declare that the research was conducted in the absence of any commercial or financial relationships that could be construed as a potential conflict of interest.